UNVEILING AND BLOCKING THE INTERACTION BETWEEN *TOMATO SPOTTED WILT VIRUS* AND ITS INSECT VECTOR, *FRANKLINIELLA OCCIDENTALIS*

by

MAURICIO MONTERO ASTÚA

B.Sc., University of Costa Rica, 2000
M.Sc., University of Costa Rica, 2006

AN ABSTRACT OF A DISSERTATION

submitted in partial fulfillment of the requirements for the degree

DOCTOR OF PHILOSOPHY

Department of Plant Pathology
College of Agriculture

KANSAS STATE UNIVERSITY
Manhattan, Kansas

2012

Abstract

Tomato spotted wilt virus (TSWV) is an economically important plant virus dependent on insects (thrips) for transmission to plant hosts. Like many animal-infecting viruses, TSWV replicates in the cells of its insect vector. The virus is an emergent disease threatening food and fiber crops worldwide. The aim of this work was to develop novel control strategies against TSWV through a better understanding of the virus-vector interaction. Previously, the TSWV G_N protein was shown to be the viral attachment protein, a molecule mediating attachment of virus particles to the midgut epithelial cells of vector thrips. The specific goals of my research were to further examine the utility of disrupting the virus-vector interaction for effective virus control by exploiting G_N properties, and to track the route of TSWV in thrips using confocal microscopy. To achieve these goals, I expressed soluble and insoluble forms of G_N fused to green fluorescent protein (GFP) transiently and transgenically and examined their cellular localization *in planta*. G_N::GFP recombinant protein localized to Golgi stacks throughout the cells as indicated by a punctate pattern or co-localization to a Golgi marker. In contrast, the soluble form of G_N, G_N-S::GFP, localized to the ER and apparently also to the cytoplasm. Virus acquisition and transmission assays with G_N-S::GFP transgenic tomato plants demonstrated that transmission of TSWV by *F. occidentalis* was reduced by 35 to 100%. These results indicated that transgenic expression of G_N-S in tomato plants may have the potential to prevent secondary spread of the virus. Novel features of the morphology of principal (PSGs) and tubular salivary glands (TSGs) of the insect vector *F. occidentalis* and of their infection with TSWV were described. The virus colonized different cell types and regions within the PSGs with variable intensity and distribution; and accumulated at the lumen of individual cells. The TSGs of *F. occidentalis* are proposed as a route for TSWV infection into the PSGs. The transgenic plants and the new knowledge of the virus vector interaction are promising tools to control TSWV and a model approach for the control of other vector-borne viruses.

UNVEILING AND BLOCKING THE INTERACTION BETWEEN *TOMATO SPOTTED WILT VIRUS* AND ITS INSECT VECTOR, *FRANKLINIELLA OCCIDENTALIS*

by

MAURICIO MONTERO ASTÚA

B.Sc., University of Costa Rica, 2000
M.Sc., University of Costa Rica, 2006

A DISSERTATION

submitted in partial fulfillment of the requirements for the degree

DOCTOR OF PHILOSOPHY

Department of Plant Pathology
College of Agriculture

KANSAS STATE UNIVERSITY
Manhattan, Kansas

2012

Approved by:

Major Professor
Anna E. Whitfield

Copyright

Abstract

Tomato spotted wilt virus (TSWV) is an economically important plant virus dependent on insects (thrips) for transmission to plant hosts. Like many animal-infecting viruses, TSWV replicates in the cells of its insect vector. The virus is an emergent disease threatening food and fiber crops worldwide. The aim of this work was to develop novel control strategies against TSWV through a better understanding of the virus-vector interaction. Previously, the TSWV G_N protein was shown to be the viral attachment protein, a molecule mediating attachment of virus particles to the midgut epithelial cells of vector thrips. The specific goals of my research were to further examine the utility of disrupting the virus-vector interaction for effective virus control by exploiting G_N properties, and to track the route of TSWV in thrips using confocal microscopy. To achieve these goals, I expressed soluble and insoluble forms of G_N fused to green fluorescent protein (GFP) transiently and transgenically and examined their cellular localization *in planta*. G_N::GFP recombinant protein localized to Golgi stacks throughout the cells as indicated by a punctate pattern or co-localization to a Golgi marker. In contrast, the soluble form of G_N, G_N-S::GFP, localized to the ER and apparently also to the cytoplasm. Virus acquisition and transmission assays with G_N-S::GFP transgenic tomato plants demonstrated that transmission of TSWV by *F. occidentalis* was reduced by 35 to 100%. These results indicated that transgenic expression of G_N-S in tomato plants may have the potential to prevent secondary spread of the virus. Novel features of the morphology of principal (PSGs) and tubular salivary glands (TSGs) of the insect vector *F. occidentalis* and of their infection with TSWV were described. The virus colonized different cell types and regions within the PSGs with variable intensity and distribution; and accumulated at the lumen of individual cells. The TSGs of *F. occidentalis* are proposed as a route for TSWV infection into the PSGs. The transgenic plants and the new knowledge of the virus vector interaction are promising tools to control TSWV and a model approach for the control of other vector-borne viruses.

Table of Contents

List of Figures x
List of Tables xiii
Acknowledgements xv
Dedication xvi
Chapter 1 - Literature review: *Tomato spotted wilt* virus and its thrips vector, *Frankliniella occidentalis* 1
Introduction to *Tomato spotted wilt virus* and *Tospovirus*-thrips-plant pathosystem 1
Molecular biology of the virus 3
Structural protein interactions and particle morphogenesis 4
Non-structural proteins 6
The Thysanoptera and *Frankliniella occidentalis* 7
Thrips midgut and salivary glands morphology 10
Midgut *10*
Salivary glands *11*
Dynamics of virus infection of thrips vectors 12
Virus routes for dissemination in thrips. 13
Molecular biology of virus-vector interaction 16
Association between virus titer and vector competence 17
Resistance to TSWV 18
Natural resistance against TSWV *18*
Transgenic resistance against TSWV *19*
Transmission-stopping technology 20
Chapter 2 - Transient expression and cellular localization of *Tomato spotted wilt virus* glycoprotein G_N, a soluble form (G_N-S), and the nucleocapsid protein (N) in *Nicotiana benthamiana*. 22
Abstract 22
Introduction 22
Results 25
Recombinant Protein Expression in Nicotiana benthamiana *25*

Relative abundance of different TSWV proteins varied in agroinfiltrated *N. benthamiana* depending on the protein type and fusion tag *26*
G_N localizes to the Golgi *26*
G_N-S localizes through the cytoplasm of the cell *27*
N protein has a complex localization pattern *27*
N protein localization pattern changes over time *28*
Interactions between G_N, G_N-S or N, as evidenced by changes in localization patterns *29*
Discussion 31
Materials and Methods 33
Construction of expression clones *33*
Plant and bacterial culture maintenance *34*
Nicotina benthamiana agroinfiltration *34*
Protein extraction *35*
SDS-Page and western blot *36*
DAPI-staining *37*
Microscopy *37*
Image analysis and statistical analysis *38*
Tables and Figures 39
Chapter 3 - Transgenic G_N-S::GFP tomato plants interfere with TSWV acquisition and transmission by *Frankliniella occidentalis* 52
Abstract 52
Introduction 52
Results 55
Generation of T0 transgenic tomato plants *55*
Segregation of recombinant protein expression phenotype in transgenic plants *55*
Vegetative appearance and performance of the transgenic plants *56*
Varying amounts of recombinant protein occurred among the different transgenic lines and generations *56*
Detection of the recombinant protein by western blot *57*
G_N-S::GFP fluorescent signal shows a reticulate subcellular localization pattern in transgenic tomato plants *58*

Reaction of G_N-S::GFP transgenic plants to TSWV inoculation and detection of recombinant protein in TSWV-infected plants *59*
Transgenic G_N-S::GFP tomato plants interfere with TSWV acquisition by *F. occidentalis* *62*
Normalized abundance of TSWV-N RNA in thrips fed on TSWV-infected transgenic tissue is significantly lower than in thrips fed on non-transgenic plants 24h after AAP *63*
F. occidentalis cohorts show reduced transmission of TSWV when acquired from transgenic G_N-S::GFP tomato plants *63*
Discussion 64
Materials and Methods 66
Construction of expression vectors 66
Tomato transformation 67
ELISA screening of transgenic plants 68
Quantification of recombinant protein in transgenic plants 70
SDS-Page and western blot 71
Screening transgenic plants for the presence of green fluorescence by fluorescent microscopy 72
Seed extraction and decontamination 72
Challenge of G_N-S::GFP transgenic plants with TSWV 73
TSWV acquisition test on transgenic tissue 73
Determination of TSWV acquisition by qRT-PCR 74
Inoculation access period (IAP) 74
Statistical analyses 75
Tables and Figures 75
Chapter 4 - Dynamics of TSWV infection and spread in its insect vector *Frankliniella occidentalis* with an emphasis on the principal salivary glands. 94
Abstract 94
Introduction 95
Results 97
Morphology of the principal and tubular salivary glands of *Frankliniella occidentalis* 97
Initial TSWV infection of *Frankliniella occidentalis* 99
TSWV infection of gut and salivary tissues of *F. occidentalis* 100

TSWV infection at four time points of *Frankliniella occidentalis* life cycle 101
Tracking TSWV through F. occidentalis life cycle by ELISA 103
Comparison of adult female and male infection of the salivary glands and its relation to TSWV transmission 104
Discussion 106
Materials and Methods 109
Plant materials and TSWV inoculum 109
Thrips rearing and acquisition access periods (AAP) 109
Sampling points for thrips immunolabeling time course experiment 110
Dissecting and immunolabeling of thrips guts and salivary glands 110
Confocal fluorescent microscopy 112
Time course experiments tracking TSWV by ELISA in *F. occidentalis* 112
Transmission assay 113
Quantitative analysis of PSGs images: fluorescence signal and size parameters 113
Statistical analyses 114
Tables and Figures 115
Chapter 5 - General discussion and future perspectives 136
Summary of results and products 136
General discussion 140
Future research and perspectives 142
Tables and Figures 144
References 147

List of Figures

Figure 2.1. Fluorescent signal from pEarleygate based expression clones complemented with *Tobacco etch virus* gene silencing suppressor, HcPro, was detected up to 12 days after agro-infiltration (daa) in *Nicotiana benthamiana* leaf tissue and throughout the leaf blade cell layers. 42

Figure 2.2. Detection of transiently expressed recombinant proteins in *N. benthamiana* plant tissue. 43

Figure 2.3. Cell localization patterns for G_N and G_N-S fusion proteins to GFP and RFP and their co-localization to a Golgi marker when transiently expressed in *Nicotiana benthamiana* leavess two days after agroinfiltration (2 daa). 44

Figure 2.4. Co-localization of G_N and a Golgi marker, both fused to fluorescent proteins (GFP or RFP) transiently expressed in *N. benthamiana* 2 days after agroinfiltration. 45

Figure 2.5. Co-localization of G_N-S and a Golgi marker, both fused to fluorescent proteins (GFP or RFP) transiently expressed in *N. benthamiana* 2 days after agroinfiltration..... 47

Figure 2.6. N::GFP showed a complex localization pattern two days after agroinfiltration in *Nicotiana benthamiana* leaves. 48

Figure 2.7. Analysis of N::GFP and GFP localization pattern over time (2, 4, 6 and 8 days after agroinfiltration) in absence or presence of TSWV infection when transiently expressed in *N. benthamiana* leaves. 49

Figure 2.8. N::GFP and GFP transient expression in *N. benthamiana* leavesover time (2, 4, 6 and 8 days after agroinfiltration) in absence and presence of TSWV infection. 51

Figure 3.1. General appearance of T0 G_N::GFP transgenic tomato plants. 81

Figure 3.2. General appearance of G_N-S::GFP transgenic tomato plants. 82

Figure 3.3. Percentage of seed germination in transgenic and non-transgenic plants. 83

Figure 3.4. Amount of recombinant protein estimated in a subsample of G_N::GFP tomato transgenic plants, T0 and T1 generations..... 84

Figure 3.5. Amount of recombinant protein estimated in a subsample of G_N-S::GFP tomato transgenic plants, T1, T2 and T3 generations. 84

Figure 3.6. Western blots for G_N::GFP transgenic plants tested with specific antibodies against GFP (a) or G_N (b). 85
Figure 3.7. Western blots for G_N-S::GFP transgenic plants tested with specific antibodies against GFP (a) or G_N (b). 85
Figure 3.8. Confocal microscope images of G_N::GFP transgenic plants. 87
Figure 3.9. Confocal fluorescence images for T0 G_N-S::GFP transgenic tomato plants. 88
Figure 3.10. Confocal fluorescence images for T1, T2 and T3 G_N-S::GFP transgenic tomato plants. 89
Figure 3.11. Images of G_N-S::GFP fluorescence in TSWV-infected tomato transgenic plants. .. 90
Figure 3.12. Detection of TSWV nucleocapsid protein (N) in thrips cohorts given a 24h acquisition access period (AAP) on TSWV-infected, G_N-S::GFP transgenic or non-transgenic tomato leaf tissue. 91
Figure 3.13. Detection of TSWV nucleocapsid protein (N) by DAS-ELISA in tissue used for thrips AAP. 92
Figure 3.14. Normalized abundance (Log_{10} transformed) of *Tomato spotted wilt virus* (TSWV) N RNAs in thrips fed in transgenic and non-transgenic TSWV-infected plants. 92
Figure 3.15. Frequency of transmission of TSWV by adult *Frankliniella occidentalis* individuals fed as larvae on transgenic and non-transgenic TSWV-infected plant tissue. 93
Figure 4.1. Morphology of principal salivary glands (PSGs) of *Frankliniella occidentalis.* 119
Figure 4.2. Size parameters measured for principal salivary glands (PSGs) of adult *Frankliniella occidentalis* individuals 24 and 96 hours after eclosion. 121
Figure 4.3. Morphology of the tubular salivary glands (TSGs) of *Frankliniella occidentalis.* .. 122
Figure 4.4. Initial infection of *Frankliniella occidentalis* by *Tomato spotted wilt virus* (white arrows) is detected as localized fluorescence in the anterior region of midgut 1 (MG1) just after the foregut (FG). 124
Figure 4.5. Background and TSWV-associated signals in *Frankliniella occidentalis* guts and salivary tissues after immunolabeling procedures. 125
Figure 4.6. *Tomato spotted wilt virus* (TSWV) infection of *Frankliniella occidentalis* midgut (MG) and associated tissues at four time points during the thrips life cycle. 127
Figure 4.7. Percentages for the total number of *Tomato spotted wilt virus* (TSWV) positive tissues observed at four time points through *Frankliniella occidentalis* life cycle. 129

Figure 4.8. *Tomato spotted wilt virus* infection of *Frankliniella occidentalis* tubular salivary glands (TSGs). 131
Figure 4.9. *Tomato spotted wilt virus* (TSWV) infection of *Frankliniella occidentalis* principal salivary glands (PSGs). 132
Figure 4.10. Mean intensity (arbitrary units) of TSWV signal in PSGs of female and male *Frankliniella occidentalis* adult thrips. 133
Figure 4.11. Percentage of area of principal salivary glands (PSGs) with TSWV signal. 134
Figure 4.12. Comparison of infection status of the pair of principal salivary glands of adult *Frankliniella occidentalis* female and male thrips. 134
Figure 4.13. *Tomato spotted wilt virus* (TSWV) relative titer at different time points during the life cycle of *Frankliniella occidentalis*. 135
Figure 5.1. Correlation between *Tomato spotted wilt virus* (TSWV) titer and the corresponding percentage of transmission for cohorts of *Frankliniella occidentalis* thrips. 145
Figure 5.2. Comparison of the percentage of *Tomato spotted wilt virus* transmission for female and male *Frankliniella occidentalis* adults 24h after eclosion. 145

List of Tables

Table 2.1. Number of cells (2x3 contingency table) recorded for three fluorescent signal localization patterns: reticulate, punctuate or soluble, when expressing G_N fused to GFP or RFP, 2 days after agroinfiltration..... 39

Table 2.2. Number of cells (2x3 contingency table) recorded for three fluorescent signal localization patterns: reticulate, punctuate or soluble, when expressing G_N-S fused to GFP or RFP, 2 days after agroinfiltration. 39

Table 2.3. Probabilities calculated by Fisher exact test associated to contingency tables comparing G_N-S co-localization to G_N or a Golgi marker (2x2 table) or comparing localization patterns of G_N and G_N-S in the presence and absence of N protein (2x3 tables). 40

Table 2.4. Primers used to generate Gateway entry clones for *Tomato spotted wilt virus* glycoprotein G_N, a soluble form G_N-S, nucleocapsid protein N, and a GFP control. 40

Table 2.5. Primer combinations used for the generation of Gateway entry clones[1] for *Tomato spotted wilt virus* glycoprotein G_N, a soluble form of G_N (G_N-S), nucleocapsid (N) protein, and a GFP control. 41

Table 3.1. Percentage of germination and percentage of T1 G_N::GFP plants with detectable amounts of recombinant protein by ELISA (anti-G_N/GFP). 75

Table 3.2. Percentage of germination and percentage of transgenic tomato T1 plants positive for the presence of recombinant G_N-S::GFP protein and the selection marker NPTII. 76

Table 3.3. Percentage of germination and of transgenic tomato T2 plants positive for the presence of recombinant G_N-S::GFP protein and the selection marker NPTII. 76

Table 3.4. Percentage of germination and of transgenic tomato T3 G_N-S::GFP plants with detectable amounts of recombinant protein. 77

Table 3.5. Contingency table for the detection of *Tomato spotted wilt virus* (TSWV) and G_N-S::GFP by ELISA in inoculated leaf tissue (old leaf tissue). The second true leaf after the cotyledons of transgenic tomato plants expressing G_N-S::GFP was mechanically inoculated with TSWV and was sampled 15 days after virus inoculation. Samples were simultaneously

tested for the presence of virus and recombinant protein. The number of plants positive for both (virus and recombinant protein) for either one or for any are summarized. 78
Table 3.6. Contingency table for the detection of *Tomato spotted wilt virus* (TSWV) and G_N-S::GFP by ELISA in systemic leaf tissue (new leaf tissue). The second leaf from top to bottom from transgenic tomato plants expressing G_N-S::GFP and that were previously mechanically inoculated with TSWV at a different leaf was sampled 15 days after virus inoculation. Samples were simultaneously tested for the presence of virus and recombinant protein. The number of plants positive for both (virus and recombinant protein) for either one or for any are summarized. 78
Table 3.7. Contingency table for the comparison of TSWV detection[1] pattern in local (old) and systemic (new) leaves between transgenic and non-transgenic inoculated plants. 79
Table 3.8. Contingency table for the comparison of G_N-S::GFP detection[1] pattern in local (old) and systemic (new) leaves between transgenic plants non-inoculated or inoculated with TSWV. 79
Table 3.9. Contingency table for the total number of adult thrips (from three independent experiments) that transmitted or not TSWV to leaf discs during an 48h IAP after feeding as larvae on transgenic or non-transgenic TSWV-infected tissue for a 24h AAP. 80
Table 4.1. Size parameters[1] measured for the principal salivary glands of adult *Frankliniella occidentalis* individuals. 115
Table 4.2. Percentage of tissues determined as positive for TSWV presence by immunolabeling with antibodies against G_N glycoprotein for immunolabeling experiment 1. 116
Table 4.3. Percentage of tissues determined as positive for TSWV presence by immunolabeling with antibodies against G_N glycoprotein for immunolabeling experiment 2. 117
Table 4.4. Transmission[1] of *Tomato spotted wilt virus* (TSWV) by individual *Frankliniella occidentalis* adults 24 hours after eclosion (n = 30) for five experimental cohorts. 118

Acknowledgements

I would like to thank my advisor professor, Dr. Anna Whitfield, and supervisory committee members, Dr. Barbara Valent, Dr. Lorena Passarelli, and Dr. Harold Trick, for their guidance, scientific discussions and teachings.

I am also grateful to all the laboratory members, fellow students, faculty and staff from Plant Pathology for their help and support.

I acknowledge a supplementary scholarship received from Universidad de Costa Rica throughout the Ph.D. studies. I am also thankful to the Tillman Family Memorial Agriculture Scholarship I received from KSU.

Finally, I am grateful to my family and friends for their patience, strength and support throughout the Ph.D. process.

Dedication

This work is dedicated to my parents, Deyanira Astúa Montoya and Fernando Montero Umaña.

Chapter 1 - Literature review: *Tomato spotted wilt* virus and its thrips vector, *Frankliniella occidentalis*

Introduction to *Tomato spotted wilt virus* and *Tospovirus*-thrips-plant pathosystem

Tomato spotted wilt is a viral disease of plants first described in tomatoes in Australia in 1919. However, on this report, the author commented on previous reports from the United States of America that described what seems to be a similar disease as early as 1895. At that time the causal agent of tomato spotted wilt was unknown. The disease spread very fast from a relative small area where it was first noticed to all the state of Victoria, Australia, in a period of three years. Ten years later spotted wilt of tomatoes was distributed throughout Australia and limited tomato production; becoming the most important disease of tomatoes in that country (Brittlebank, 1919; Samuel et al., 1930). Reports from Pittman (1927) and Samuel (1930), already mentioned the disease as of viral cause and showed evidence indicating that the viral disease was transmitted by insects, *Thrips tabaci* and *Frankliniella insularis* (Pittman, 1927; Samuel et al., 1930). It is noteworthy that even when the disease was initially reported and named in Australia, recent phylogenetic analyses suggested that *Tomato spotted wilt virus* (TSWV) is originally from the American continent (New World clade of tospoviruses) (Nagata et al., 2007; Nagata et al., 2007; Bertran et al., 2011; de Oliveira et al., 2011; Zhou et al., 2011).

Since those early reports of *Tomato spotted wilt virus*, other viruses with similar physical, chemical and biological properties have been identified. These are classified as members of the *Tospovirus* genus, of which TSWV is the type member. Tospoviruses belong to the viral family *Buyanviridae*, a rather animal infecting family of viruses that are vectored to their hosts by insects (Whitfield et al., 2005b). Tospoviruses are capable of infecting plant and animal cells; the virus replicates in its plant hosts but also in the insect vectors (Ullman et al., 1993; Wijkamp et al., 1993).

Since its beginning the severity and economic impact of the disease was remarkable (Brittlebank, 1919; Samuel et al., 1930), and TSWV has become one of the most economically important plant viruses worldwide. It is included among the top ten most devastating plant

viruses, not only for its damage to tomato plantations, but for yield losses in several different crops and its unique biological properties (Goldbach and Peters, 1994; Scholthof et al., 2011). TSWV is currently distributed worldwide and known to infect hundreds of plants species (Goldbach and Peters, 1994), including crops such as tomato, pepper, lettuce, tobacco and peanuts. In addition, *Tospovirus* species and the associated plant diseases continue to be described from different locations across the world (Ciuffo et al., 2009; Chiemsombat et al., 2010; Hassani-Mehraban et al., 2010; de Oliveira et al., 2011; Zhou et al., 2011). These viruses and the diseases they cause are emerging and gaining in importance since 1980. This is hypothesized due to (i) the fact that these viruses recently evolved from the animal infecting bunyaviruses and thus are "new" to the plant host; and (ii) to changes in insect control, agricultural practices and increased international trade (Goldbach and Peters, 1994; Pappu et al., 2009). TSWV, together with other tospoviruses, cause economic losses estimated in millions of USA dollars per year (Goldbach and Peters, 1994; Culbreath et al., 2003; Pappu et al., 2009).

The thrips-tospovirus-plant host pathosystem is a complex scenario were the environment and biological characteristics of the insect, the virus and the plant host will determine the success with which virus acquisition and transmission by the vector occurs. Several species of thrips are known to transmit tospoviruses with different specificity and efficiency levels. The determinants that confer specificity for virus transmission are not known. Some vectors may transmit several tospoviruses; meanwhile, other thrips species have been reported to transmit only one specific virus species. The most efficient and notorious vector of TSWV is the western flowers thrips *Frankliniella occidentalis*. This species is worldwide distributed, as is the virus, and is an economically important pest for several crops and in greenhouses. Management of the vector is very difficult due, among other reasons, to its high fecundity, wide host range and development of resistance to insecticides (Reitz, 2005; Whitfield et al., 2005b; Reitz, 2009). The complexity of the pathosystem, its economic impact and its emerging and expanding nature justifies the need for a better understanding of the biology of the pathosystem and the development of novel control tools (with emphasis on biotechnological applications) (Goldbach and Peters, 1994).

Molecular biology of the virus

The genome of the *Tospovirus* genus consists of three segments of single stranded, negative sense RNA (ssRNA), named large (L), medium (M) and small (S). The L segment codes for the viral RNA-dependent RNA-polymerase (RdRp or L protein) in the negative sense or viral sense RNA (vRNA, Figure 2)) (de Haan et al., 1991).The vRNA is the template for mRNA transcription and, therefore, the L protein is translated from mRNA in the genome complementary RNA sense (cRNA, also referred as anti-genomic RNA, agRNA, or viral complementary RNA, vcRNA, Figure 1). The M and S segments have an ambisense coding strategy whereby structural proteins are encoded in the negative sense and the non-structural proteins in the agRNA (de Haan et al., 1990; de Haan et al., 1992; Kormelink et al., 1992b). The M segment codes for a polyprotein precursor (G_N and G_C) and a non-structural protein, NSm (Kormelink et al., 1992b; Cortez et al., 2002). The S segment codes for the nucleocapsid (N) and for a non-structural protein, NSs (de Haan et al., 1990; de Haan et al., 1992).

The genome segments of tospoviruses are replicated and transcribed as ribonucleoprotein (RNP) rather than naked RNA molecules. Inverted complementary repeats at the 3' and 5' untranslated regions (UTRs) of all the genome segments are involved in circularization of the ribonucleoprotein and the formation of pan-handle structures that act as signals for L recognition for replication and transcription (De Haan et al., 1989; Kormelink et al., 1992a). An RdRp catalytic domain in a conserved region of tospoviruses L proteins has been suggested to recognize a conserved terminal sequence (5'-AGAGCAAU-3') in 5' and 3' segments (Zheng et al., 2011).

Tospoviruses produce their mRNA by cap snatching (Kormelink et al., 1992a; van Poelwijk et al., 1996; Duijsings et al., 1999; Duijsings et al., 2001; van Knippenberg et al., 2002) and a prime and realign mechanism of transcription (Garcin et al., 1995; Prehaud et al., 1997). The viral mRNA synthesis is primed with capped oligonucleotides that are sequestered from host or other viral mRNAs (Kormelink et al., 1992a; van Poelwijk et al., 1996; Duijsings et al., 1999; Duijsings et al., 2001; van Knippenberg et al., 2002). The 3' terminal region of both the vRNA and agRNA strands contains the signal for transcription initiation. Segments M and S produce two subgenomic mRNAs each, and the termination signal for the mRNAs is present in the secondary structure of the RNA segment, a stable hairpin, in the intergenic region (de Haan et al., 1990; Kormelink et al., 1992b). Additionally, a polyprotein strategy is used to generate the

two viral glycoproteins. A single ORF in the M segment is translated into a polyprotein which upon cleavage by a host factor, likely a signal sequence peptidase, generates the two mature glycoproteins, G_N and G_C, corresponding to the N- and C- terminus of the polyprotein, respectively (Kormelink et al., 1992b; Adkins et al., 1996; Lober et al., 2001; Whitfield et al., 2004; Bergeron et al., 2007).

Structural protein interactions and particle morphogenesis

The current description of particle morphogenesis in plant cells is based on several studies describing the localization and interactions among the three main structural proteins of TSWV: N, G_N and G_C (Kikkert et al., 1999). After expression in baby hamster kidney (BHK21) cells or *Nicotiana tabacum* protoplasts, N protein fused to yellow fluorescent protein (YFP) or a non-fused form of N protein detected by immunolocalization were observed to form aggregates throughout the cytoplasm (Snippe et al., 2005; Ribeiro et al., 2009a). N aggregates (homopolymerization) are formed through homotypic interactions between N monomers as has been determined by yeast two-hybrid system, size-exclusion chromatography and fluorescence resonance energy transfer (FRET) techniques (Uhrig et al., 1999; Kainz et al., 2004; Snippe et al., 2005; Ribeiro et al., 2009a). N proteins in the cytoplasm will bind, by multiple binding domains, to single stranded viral RNA molecules as determined by gel shift assay with N and partial N proteins (Richmond et al., 1998; Uhrig et al., 1999; Kainz et al., 2004; Snippe et al., 2005; Ribeiro et al., 2009a). When expressed in the absence of other viral proteins, G_C is retained at the ER membrane (Ribeiro et al., 2008), and G_N is detected in the early stages of expression at the ER but it eventually accumulates in the Golgi apparatus via motifs in the transmembrane domain (Ribeiro et al., 2008; Ribeiro et al., 2009b). In later stages, when expressed simultaneously from separate expression plasmids or from the polyprotein, both glycoproteins are found in the Golgi. G_N and/or G_C induce membrane deformation in the ER or Golgi membranes to produce pleomorphic vesicle-like structures. In the presence of N, G_C is redistributed to discrete regions within the ER, hypothesized to be ER export sites (ERES). G_N is responsible for targeting of G_C through their interaction, and more probably G_C-N complexes from the ERES, to be transported to the Golgi by a COPII-dependent mechanism. The interaction between G_N and G_C analyzed by fluorescent microscopy techniques in BHK21 cells or *N.*

tabacum protoplasts was shown to require G_N C-terminal 20 amino acids and also, the glycoprotein ectodomains (luminal domains) are suggested as necessary (Snippe et al., 2007b; Ribeiro et al., 2008; Ribeiro et al., 2009a; Ribeiro et al., 2009b).

The presence of G_N/G_C at the Golgi stacks will induce the changes associated with paired parallel membrane (PPM) structures and subsequent folding of the Golgi cisternae to produce double-enveloped virions (DEVs) (Kikkert et al., 1999). The need for G_N/G_C heterodimerization for transport from the ER into the Golgi and its role in PPM formation is in accordance with the G_N/G_C spikes described for other bunyaviruses (Andersson and Pettersson, 1998; Gerrard and Nichol, 2007; Huiskonen et al., 2010). RNPs in the vicinity of the Golgi membrane, through the interaction of N with the glycoproteins (Ribeiro et al., 2009a), are wrapped inside the DEVs. Additional signals present on the UTR of the genome segments may participate in the packing process (Kohl et al., 2006). Few copies of L protein associated to the RNPs are also encapsidated into DEVs in order to produce a functional viral particle. The external membrane of DEVs fuses to each other or to the ER membrane to produce a vesicle-like membrane filled with single enveloped virions (SEVs). The deformed PPM Golgi cisternae and surrounding N protein may constitute a viral factory in a similar fashion to the viral factories of Bunyamwera virus (Fontana et al., 2008).

Studies on animal cell systems suggests that several steps in particle morphogenesis and viral protein interactions are similar in the insect and plant host cells (Ullman et al., 1995; Kikkert et al., 2001; Snippe et al., 2005; Snippe et al., 2007a; Snippe et al., 2007b). N interactions with the glycoproteins and the requirement for G_N to rescue G_C from ER arrest are similar as described for plant protoplasts (Kikkert et al., 2001; Snippe et al., 2005; Snippe et al., 2007a; Snippe et al., 2007b). Contrary to what is expected from other enveloped viruses, TSWV glycoproteins were not detected at the surface of animal cells (Kikkert et al., 2001). As is the case for other bunyaviruses, the particles are likely delivered to the extracellular space by vesicle fusion with the cell membrane. The trafficking of viral particles in and out of cells is suggested to occur on microtubules (Simon et al., 2009a; Shi et al., 2010). The same process may be occurring for tospoviruses since supernatant fluids from *F. occidentalis* cell cultures infected with TSWV were infectious (Nagata et al., 1997) and observation of the different viral proteins by transmission electron microscopy indicated that TSWV proteins in insect cells via intercellular transport pathways and the autophagic system (Ullman et al., 1995). Viral particles

have been reported to bud from midgut epithelial cells into the extracellular space of the basal labyrinth and particles are found in midgut muscle cells of *F. occidentalis* larvae (Nagata et al., 2002). Moreover, TSWV particles are present in vesicles of salivary glands cells and in the salivary ducts (Wijkamp et al., 1993; Ullman et al., 1995).

Non-structural proteins

NSm is the movement protein of tospoviruses, mediating cell-to-cell movement of viral RNPs in plants by a tubule-guided mechanism (Kormelink et al., 1994; Storms et al., 1995; Lewandowski and Adkins, 2005). NSm also participates in long distance movement of the virus through the plant and has been implicated in symptom development (Lewandowski and Adkins, 2005; Li et al., 2009). In accordance with its role in movement, NSm has the capacity to form tubular structures that extend through plasmodesmata (Storms et al., 1995); it alters the plasmodesmata size exclusion limit (SEL) (Storms et al., 1998); it binds in a sequence-nonspecific manner to ssRNA; and it interacts with N protein and plant proteins of the DnaJ family and proteins involved in intra- and intercellular trafficking (i.e. At-4/1). These data describe a model where NSm recognizes the viral RNPs through interactions with N and ssRNA molecules and facilitates their transport through the plasmodesmata by interacting with plant transport elements (Soellick et al., 2000; Paape et al., 2006). Additionally, the capacity of some TSWV isolates to overcome virus resistance mediated by the R gene *Sw-5* in tomato plants was associated with amino acid substitutions in NSm protein (Hoffmann et al., 2001; Lopez et al., 2011). A role for NSm in virus infection of thrips cells has not been documented.

The NSs protein encoded by tospoviruses is a RNA silencing suppressor that is functional in plant and arthropod cell cultures and it is suggested to have enzymatic functions and to be involved in other processes as well (Takeda et al., 2002; Bucher et al., 2003; Lokesh et al., 2010; Oliveira et al., 2011). The NSs proteins from different *Tospovirus* species were shown to vary in their properties as a silencing suppressor (Schnettler et al., 2010). NSs may interfere with gene silencing by preventing Dicer-mediated processing of dsRNA or/and by sequestering siRNAs from being loaded to the RISC complex (Takeda et al., 2002; Bucher et al., 2003; Schnettler et al., 2010). The ability to bind long dsRNA molecules may represent a strategy to deal with antiviral defense mechanisms in insects or it is a remnant characteristic from the mammal-

infecting bunyaviruses. NSs interferes with the miRNA pathway in plants (Schnettler et al., 2010). One study showed that NSs protein acts as an avirulence determinant for the resistance mediated by the R gene *Tsw* in pepper cultivars (Margaria et al., 2007); however, other studies demonstrated this role for the N protein (Jahn et al., 2000; Lovato et al., 2008).

The Thysanoptera and *Frankliniella occidentalis*

In this section general information on the order Thysanoptera and details on the species of interest for this dissertation, *Frankliniella occidentalis*, are mentioned based on the reviews by Morse and Hoddle (2006), Mound (2005), and Reitz (2005, 2009) (Mound, 2005; Reitz, 2005; Morse and Hoddle, 2006; Reitz, 2009).

The order Thysanoptera (class Insecta) includes ca. 5500 described species of small insects, all sharing the structural characteristic that only the left of the two mandibles is fully developed; whereas the other is reabsorbed by the embryo. Thrips are a few millimeters or less in length and generally are black, brown or yellow. All have complex life cycles consisting of one egg stage, two larval stages, one non-feeding prepupal stage, two possible non-feeding pupal stages (remetaboly metamorphosis) and the adult stage. Larvae and adults share the same ecological niche and feed on the same resources. Extensive polymorphism exists within and among species, and also there is great diversity in behavior and physiology. Generally, adults are winged, but some species may show sexual dimorphism with three possible wing morphologies: macropterae, micropterae or apterae (wingless); while few species are totally apterous. About half of all Thysanoptera species feed on fungal spores or hyphae (fungivorous); the remaining species are mainly phytophagous but facultative and obligate predator species exist. The order comprises two suborders: Tubulifera and Terebrantia; and is divided in eight families. Most of the phytaphogous species and all known virus vectors belong to the suborder Terebrantia. The phytophagous larvae and adults feed by sucking the contents of single plant cells.

Thrips are very complex organisms in morphology, behavior and taxonomy; but many of the species seem to share a series of characteristics that render them with high plasticity or adaptability to varying conditions. Indeed, several authors refer to thrips as opportunistic insects and several species have become established as invading species in different regions of the world. However, few species are considered as economically important plant pests (ca. 1%). The

four most economical important species are: *Frankliniella occidentalis*, *Thrips tabaci*, *T palmi* and *Scirtothrips dorsalis*.

The best example of an invasive species, and the most economically important thrips, due to its damage to economically important plants and to the transmission of tospoviruses is *Frankliniella occidentalis*, the western flower thrips. Among the characteristics that enable many thrips to be successful invading species and specifically allow *F. occidentalis* to be an important pest are (i) small size that allow the insects to easily hide in bracts, buds, flowers and other plant tissues; (ii) thigmotactic behavior; a preference to dwell in enclosed spaces that helps to avoid chemical control and natural enemies. (iii) Likewise, the eggs of *F. occidentalis* and all members of the Terebrantia suborder are protected within the plant tissue, making it less exposed to chemical control, predation and human inspection. (iv) The sexual reproduction strategy of the western flower thrips is haplodiploid; males are haploid and arise from unfertilized eggs, meanwhile females are diploid and originate from fertilized eggs. This characteristic allows even very small number of thrips to initiate a population and colonize a new ecosystem. Moreover, the haploid males allow selection of advantageous alleles regardless of their nature (recessive) and contribute to faster fixation of those desired alleles. (v) Polyphagous feeding is common in many species of thrips and *F. occidentalis* is reported to feed in more than 1000 species of plants. This feeding behavior allows thrips to survive in different environments and is considered one of the causes of insecticide resistance in this species. An insect feeding in many plant species of differing taxonomy are exposed to different plant allelochemicals and thus, need metabolic detoxification systems to coupe with them, i.e. cytochrome P-450 monooxygenases, esterases and glutathione S-transferases. In addition to be highly polyphagous, including pollen grains, *F. occidentalis* can predate in spider mite eggs and thrips larvae. (vi) A complex life cycle is also advantageous, eggs are buried under the tissue; larvae and adults disperse through stems, leaves and flowers; and pupae normally go to the soil for metamorphosis. Any control strategy or natural enemy should be able to reach all these niches in order to be effective. Moreover, insects can be moved without being noticed in soil or as eggs in plant tissue. (vii) High fecundity rates and fast development contribute to building up high populations in a short period of time. Thrips development varies with temperature and host, but it can be as fast as nine days from egg to adult. (viii) Finally, as a consequence from the interplay of several of *F. occidentalis*

characteristics and of human agricultural practices, insecticide resistance strains of the species have developed.

In addition to be a plant pest, *F. occidentalis* is the most efficient vector of TSWV and vectors other tospoviruses as well. Few species of thrips transmit tospoviruses, up to 2004, 10 thrips species out of the approximately 7400 species of thrips were known to vector one or several tospoviruses. The vectoring species are: *Frankliniella bispinosa*, *F. fusca*, *F. intosa*, *F. occidentalis*, *F. schultzei*, *F. setosus*, *F. zucchini*, *Scirtothrips dorsalis*, *Thrips palmi*, and *T. tabaci*. *F. occidentalis* appears to transmit the most, five viral species, and TSWV is the virus transmitted by more number of thrips species, seven (reviewed in Whitfield *et al*. 2004). This fact highlights the significance of studying thrips-tospovirus interactions with the system *F. occidentalis*-TSWV. New reports of other thrips species vectoring or associated to known or new tospoviruses continue to appear; suggesting that still more vector species may be described as a reflect of the actual research, economical importance and understanding of the interaction.

Regarding the topics of thrips biology and of *Tospovirus* transmission, it is important to clarify two terms. *F. occidentalis* is able to feed in hundreds of plant species, but it is not able to reproduce or to complete its life cycle in all of them. Therefore, the term "host plant" has been used for both: plant species were a thrips species is able to maintain a population or those were adults may feed sporadically without completing their life cycle. Likewise, transmission of tospoviruses implies a biological close and specific interaction between the thrips and the virus. Nonetheless, thrips can carry pollen grains from one plant to another; and in this manner contribute to the dispersal of pollen-borne plant viruses (in the genera *Carmovirus*, *Ilarvirus*, and *Sobemovirus*). The term "vector" is used to describe thrips in this former scenario; however, from the point of view of studying thrips-tospoviruses interactions I prefer to reserve the term "vector" to describe the complex biological association between thrips and tospoviruses.

As it will be discussed in a following section, the midgut and the salivary gland of thrips are of special interest for Tospovirus-thrips interaction. Infection of these two tissues is a requisite for virus acquisition by thrips (midgut) and transmission (salivary gland). Work done for this dissertation included midgut and salivary tissues dissection and imaging by confocal fluorescence microscopy. Therefore, a morphological description of thrips midgut and salivary glands is included.

Thrips midgut and salivary glands morphology

Midgut

The digestive system of thrips, the gut, is divided in three sections: fore-, mid- and hind-guts. The gut is a tubular structure longer than the thrips body; therefore it is convoluted inside the thrips body cavity. The fore and hindguts are lined with chitin; whereas the midgut has different surface and histology. The foregut also referred as the esophagus is the proximal section after the mouth structures. The walls of the foregut are surrounded by long muscle cells. The cardiac valve delimitates the transition between the foregut and the midgut (Sharga, 1933; Ullman et al., 1989).

The midgut of *F. occidentalis* and of many other thrips species is a relatively long tube composed of three loops, Mg1, Mg2 and Mg3; and it occupies a large proportion of the abdominal cavity. It is formed by a single layer of columnar epithelial cells with a thick microvillar brush border. The cells are rich in endoplasmic reticulum, mitochondria, and lamellated bodies (= spherocrystals). The microvilli are relative long (up to 2µm) and slender (c. 80nm) and have two different types of glycocalyx, a meshwork of delicate filaments covering the microvilli. A myelin-like membrane surrounds the packed microvilli in Mg1 and most of Mg2. The filaments making this glycocalyx are forklike projections, 10 to 15nm in diameter and c. 35nm long, with a helical arrangement along the microvilli length (Kitajima, 1975). The glycocalyx in Mg3 is a discontinuous membrane arranged as a layer of rod like projections around longer microvilli (Kitajima, 1975; Ullman et al., 1989; Del Bene et al., 1991). The particular glycocalyx found in thrips is suggested to be involved in microvilli protection; microvilli stiffness; food attachment and selection for ingestion; and may function as a type of peritrophic matrix (Kitajima, 1975).

Additionally, an extracellular lipoprotein membrane surrounding the microvilli, the perimicrovillar membrane (PPM), was described for the orders Thysanoptera and Hemiptera. The PPM is suggested to function as a peritrophic matrix and the space between the PPM and the microvilli membranes would facilitate a compartmentalization for processes involved in nutrient uptake (Silva et al., 2004). All microvilli have a central core of parallel running microfilaments composed of F-actin (Kitajima, 1975; Ullman et al., 1989; Del Bene et al., 1991). The midgut

epithelium sits in a thin basal lamella and a layer of longitudinal and circular muscle fibers surrounds it (Del Bene et al., 1991).

After the Mg3 section, the pyloric valve defines the boundary between the midgut and the hindgut. Four Malpighian tubules extend from the junction area and open independently into the hindgut at this region. As with the midgut lumen, the lumen of the Malphigian tubules is surrounded by a single cell layered epithelium, rich in spherocrystlas and with a brush border of microvilli. The epithelium has a thin basal lamina and muscle fibers are rarely visible (Ullman et al., 1989; Dallai et al., 1991). The Malphigian epithelium cells near to the junction with the hindgut epithelium have no microvilli and are lined by a thin cuticle. Two of the Malphigian tubules are oriented posteriorly and contact the hindgut tissue near the rectal pads. The cells of the hindgut are covered by a thin cuticle. Muscle and nerve cells are found beyond the basal lamella that encircles the hindgut (Dallai et al., 1991).

The digestive tract shows a considerable different morphology and structure during the prepupae and pupae stages as compared to larvae or adult stage. The epithelium is lost and the middle region of the midgut becomes wider in the prepupal stage. Eventually the whole midgut becomes pear shaped in the pupal stage; whereas the fore and hindguts are very thin (Kritzman et al., 2002).

Salivary glands

Two principal salivary glands (PSGs) are found within the prothoracic segment of *F. occidentalis*. The two glands are connected through a narrow tissue and two fine ligaments anchor them posteriorly to the anterior section of Mg1, near the cardiac valve. These glands consist of large, loosely aggregated cells. The cells are rich in lipid droplets, Golgi stacks, coated vesicles, and numerous membranous lamellar infoldings (Ullman et al., 1989). In the prepupal and pupal stages the salivary glands are differentiated from the larval or adult stages. During these stages, the salivary glands become swollen and spherical and are surrounded by a large fat body (Kritzman et al., 2002).

Additionally, two tubular salivary glands (TSG) run parallel to the each side of Mg1. At their posterior region the TSGs seem to attach to the midgut wall in the transition region between Mg1 and Mg2 (Ullman et al., 1989; Kritzman et al., 2002). However, no fusion between the

epithelial wall of the TSG and that of the midgut was observed by electron microscopy (Del Bene et al., 1991). In their anterior portion, the TSGs connect to paired salivary reservoirs. The salivary glands are also connected to these salivary reservoirs through two deferent salivary canals, one from each salivary gland (Ullman et al., 1989). Thus it appears that each principal salivary gland is connected to the corresponding TSG by two thread-like structures (Kritzman et al., 2002).

Dynamics of virus infection of thrips vectors

Tospoviruses replicate in the cells of their insect hosts and spread through different cell layers in a circulative-propagative manner (Ullman et al., 1993; Wijkamp et al., 1993; Nagata et al., 1997). TSWV infection and replication in thrips shows a consistent pattern suggesting a defined route for virus spread as determined by tracking virus distribution in insects with immunolabeling after feeding on infected tissue (de Assis Filho et al., 2002; Kritzman et al., 2002; Nagata et al., 2002; Moritz et al., 2004). The virus enters epithelial cells of the anterior midgut region 1 (MG1) of larval thrips and replication is detected initially in this region. The virus moves from MG1 into the muscle cells directly on the MG1 region and from there moves laterally into muscle cells associated with the midgut region 2 (MG2) (de Assis Filho et al., 2002; Kritzman et al., 2002; Nagata et al., 2002; Moritz et al., 2004); salivary gland infection has also been reported at this point (de Assis Filho et al., 2002; Kritzman et al., 2002). TSWV appears to distribute from the MG1 and MG2 muscles cells into adjacent tissues, including the MG2 epithelium, midgut region 3 (MG3), the cardiac valve and salivary glands. From the above-mentioned immunolabeling studies, the extent and intensity of virus infection decreases during the pupal stage; being faintly detected primarily in the muscle cells surrounding the midgut. During the larval and pupal stages, cycles of alternating virus accumulation and reduction have been reported. A decrease in the relative amount of virus detected by ELISA with antibodies against N occurred around two to four hours after acquisition, possibly due to digestion of particles in the gut or excretion (Wijkamp et al., 1993). A second subtle drop in virus accumulation was noted in the passage from L1 to L2 (Wijkamp et al., 1993; Nagata et al., 1999); and a third, major decrease on virus titer in the insect occurred at the pre-pupal stage (P1). In this case, the decrease was explained by histolysis of tissues, primarily the midgut epithelium

(de Assis Filho et al., 2002; Kritzman et al., 2002). In young adults, just after eclosion, virus distribution is restricted mainly to the muscle cells of MG1, but one week post adult-eclosion the virus is detected in all midgut muscle cells and foregut, and in salivary glands and ligaments connecting the salivary gland and MG1 anterior region (Ullman et al., 1993; Nagata et al., 1999; de Assis Filho et al., 2002). Signal of virus presence in the renovated epithelium is very difficult to detect or non-detectable indication of no apparent reinfection from the muscle cells toward the renovated epithelia in adult thrips (de Assis Filho et al., 2002; Kritzman et al., 2002). Further analysis of the dynamics of the dissemination of virus in the vector using quantitative RT-PCR will provide additional details of this process and the barriers to transmission by thrips.

The accumulation of the viral proteins follows a similar pattern with the route of infection in thrips. Using ELISA to monitor NSs or N protein during the infection process over time, it has been documented that the concentration of these viral proteins reaches a plateau before P1 and P1 and P2 harbor lower amounts of viral proteins (Wijkamp et al., 1993), a finding in accordance with the faint immunolabeling of the muscle cells mentioned previously (de Assis Filho et al., 2002; Kritzman et al., 2002). The amount of viral proteins increases again during adult stage. The application of more sensitive techniques such as real time qRT-PCR and more fine-scaled, temporal analysis of thrips and tospovirus interactions will further elucidate the dynamics of tospovirus infection of thrips vectors.

Virus routes for dissemination in thrips.

The mechanism of movement through the different thrips tissues is not well defined. The virus may move by budding from one cell and starting a new infection cycle in neighboring cells; alternatively, it has been hypothesized that intercellular movement occurs as RNA-N complexes (Ullman et al., 1995; Ohnishi et al., 2001). Another important process regarding virus spread through the thrips, which is also unknown, is how the virus crosses through cell-free boundaries such as the basal lamina of the gut. Virions may cross directly through the midgut basal lamina into the insect hemocoel, or indirectly, by trachea branches that protrude into the midgut tissue for aeration. The trachea tubes are lined with epithelium that could possible support virus replication and serve as a conduit to other tissue systems. The tracheal epithelium is also surrounded by a basal lamina; hence the virus needs to cross this layer (Passarelli, 2011). The

basal lamina has been suggested to serve as a barrier for virus spread in thrips (Ohnishi et al., 2001) and has been documented to be a barrier for luteovirus invasion of aphid salivary glands (Gray and Gildow, 2003). Recent evidence indicates that viruses may use host mechanisms including matrix metalloproteases, apoptosis and/or reactive oxygen species to induce the remodeling of the basal lamina in order to escape this barrier (Louboutin et al., 2010; Means and Passarelli, 2010; Passarelli, 2011).

It is well established that in order for a thrips to become a virus transmitter two requisites must be met. First, virus acquisition must occur during the first instar larval stage. The number of adult individuals transmitting virus decreases with an increase in the age at which larvae are exposed to a virus source. Virus acquisition and infection in adult thrips can occur but seems to be restricted to the midgut (van de Wetering et al., 1996; Ohnishi et al., 2001; Moritz et al., 2004; Premachandra et al., 2005). Second, virus infection in the thrips body must reach the salivary glands (van de Wetering et al., 1996; Nagata et al., 1999; Nagata et al., 2000; Nagata et al., 2002). The route through which the virus passes from the midgut and associated muscle cells to the salivary glands has not been demonstrated. It is hypothesized that the virus moves through the ligaments that connect the primary salivary glands to the anterior region of the MG1 section (Nagata et al., 1999; de Assis Filho et al., 2002). The connection between the MG1 and primary salivary glands through the ligaments exists during the complete life cycle of the thrips. Moritz *et al*. (Moritz et al., 2004) observed a developmental stage-dependent juxtaposition between gut tissues and salivary glands and hypothesized that this serves as the primary route for virus invasion of salivary glands. During the L1 and early L2 stages, the midgut, visceral muscles and salivary glands are in contact due to a displacement of the brain into the prothoracic region (Moritz et al., 2004), possibly allowing the virus to move from one tissue to the another. Alternatively, virus has been suggested to circulate in the hemocoel (Ullman et al., 1992; Moritz et al., 2004), and from there it may reach other tissues as in the case of some other arbovirus-vector interactions.

Vector competence of a particular species of thrips to harbor and transmit a particular virus species requires infection of multiple tissue systems. These tissue barriers vary among different tospovirus-thrips combinations. For example, some thrips regarded as non-vectors of a tospovirus can support midgut infections and virus isolates described as non-transmissible by a particular thrips species can as well, infect thrips midguts (Nagata et al., 2000; Naidu et al.,

2008). This observation highlights the requisite for salivary gland infection in order for virus transmission to occur and further indicates a species-specific putative midgut escape barrier or a salivary gland entry barrier. For example, *F.tritici*, a non-vector of TSWV, is able to acquire and support TSWV replication at the midgut, although at low frequency (de Assis et al., 2005). In yet another example, temporal analysis of infection by TSWV in a vector competent population of *F. occidentalis* compared to a non-transmitting population of thelytokous *T. tabaci* revealed that TSWV infected and replicated in the midgut of both thrips species, however did not spread outside the guts of the *T. tabaci* individuals (Nagata et al., 2002). In this case, the virus was nearly non-detectable in the MG3 segment of larvae or in the ligament of adults and completely absent from adult salivary glands. Another suggestion of the existence of a midgut escape barrier is found in a study conducted with primary cell cultures derived from *F. occidentalis* and *T. tabaci* populations (Nagata et al., 1997). The *F. occidentalis* population was an efficient transmitter of virus meanwhile the *T. tabaci* population failed to transmit the virus despite the fact that primary cell cultures derived from these same two populations of thrips supported replication of TSWV *in vitro* with comparable efficiency. Based on these results the authors (Nagata et al., 1997) suggested the existence of a midgut barrier in the *T. tabaci* population.

In other tospovirus-thrips vector combinations, studies to determine virus localization have not been conducted; however, the specificity of the virus-thrips interaction has been demonstrated using transmission experiments and ELISA. A recently reported tospovirus, Polygonum ring spot virus, was transmitted by *Dictyothrips betae* but was not transmitted by *Frankliniella occidentalis* or *Thripstabaci* individuals (Ciuffo et al., 2010). Likewise, Peanut yellow spot virus is transmitted by *Scirtothrips* but no transmission was detected by *T. palmei* or *F. schultzei* (Gopal et al., 2010). In these cases, analyses of thrips infection using no immuno-histochemical or nucleic acid based techniques has been reported. In *T. palmi* and *T. hawaiiensis,* a relatively high virus titer was observed in L2 in comparison to larvae of other thrips species. However, the corresponding adults displayed very low absorbance values and no individual thrips transmitted TSWV out of 80 and 115 individuals tested for each species, respectively. These results showed again that virus infection con occur in thrips species even when they are non-vectors of that particular virus species (Inoue et al., 2004). Based on the relationships between thrips vector species and origins of tospovirus species, a co-evolution model for tospovirus-vector interaction was proposed. This model is supported by congruence between

phylogenic analysis of tospoviruses and thrips in the sense that thrips within the same cluster or branch of the phylogeny will transmit related virus species within the same cluster of the viral phylogeny (Inoue and Sakurai, 2007; Ciuffo et al., 2010)(Inoue and Sakurai, 2007). Further research supporting a co-evolution between thrips and tospoviruses and pointing toward virus transmission and geographical distribution as factors determining the co-evolution has resulted in the proposed two major groups of thrips-viruses: the WSMoV-*Thrips*-EuroAsian and the TSWV-*Frankliniella*-American groups (Zheng et al., 2011).

Molecular biology of virus-vector interaction

Tospoviruses are hypothesized to enter cells of their insect hosts by pH-dependent receptor-mediated endocytosis as described for other members of the *Bunyaviridae* (Gonzalez-Scarano et al., 1984; Jin et al., 2002; Simon et al., 2009a; Lozach et al., 2010). Several lines of evidence support this mechanism of entry for tospoviruses, one of which is the role of viral glycoproteins in entry and transmission by thrips vectors. Tospovirus glycoproteins have been identified as the determinants of virus acquisition and transmission by thrips (Bandla et al., 1998; Nagata et al., 2000; Whitfield et al., 2004; Sin et al., 2005) and have been a primary focus for studies of the early events in the virus and vector interaction.

Glycoprotein G_N is proposed as the viral attachment protein, a ligand that interacts with a specific receptor molecule in thrips midgut cells for virus entry (Kikkert et al., 1998; Medeiros et al., 2000; Whitfield et al., 2004). The identity of the corresponding tospoviruses receptor molecules in thrips cells is not known and several candidate proteins have been proposed as putative receptors for TSWV (Bandla et al., 1998; Kikkert et al., 1998; Medeiros et al., 2000). Integrins are good candidates because G_N proteins of several tospoviruses have an RGD domain, this domain is recognized and binds to integrins, and integrins have been identified as receptor for hantaviruses (Gavrilovskaya et al., 1999). However, the RGD domain is present only in the G_N protein of six tospoviruses belonging to the TSWV serogroup or INSV. Another candidate amino acid residue that determines transmission is a proline in the C-terminus of the G_N protein. This residue is associated with virus transmission (Sin et al., 2005) and it is present in G_N proteins from 16 tospoviruses (Zheng et al., 2011). However, this residue is part of the predicted

cytoplasmic tail domain and would likely not interact directly with a receptor during initial virus binding events.

TSWV G_C protein is hypothesized to be the viral fusion protein (Whitfield et al., 2005a; Whitfield et al., 2005b). G_C mediates the release of viral ribonucleoproteins into the cell after fusion of viral envelope and a host vesicle membrane as showed for G_C of other bunyaviruses (Plassmeyer et al., 2005; Plassmeyer et al., 2007). G_C was proposed as a type II fusion protein based on sequence data comparisons and in analogy to La Crosse virus Gc protein (Garry and Garry, 2004; Plassmeyer et al., 2005; Plassmeyer et al., 2007).

Association between virus titer and vector competence

The efficiency of adult thrips to transmit TSWV is related to virus titer supported by the insect. The amount of virus harbored by thrips has been estimated by ELISA (Wijkamp et al., 1995; Wijkamp et al., 1996; Nagata et al., 1997; Nagata et al., 2002; Rotenberg et al., 2009) and real-time qRT-PCR (Rotenberg et al., 2009) to reveal positive associations with vector competency. For example, a vector competent *Frankliniella occidentalis* population supported higher titers (determined by testing groups of five individuals (Nagata et al., 2002) or individual thrips (Nagata et al., 1997) with ELISA targeting N protein) than and a *T. tabaci* population that failed to transmit virus (Nagata et al., 1997; Nagata et al., 2002). Other studies revealed that non-transmitting individual insects obtained from various thrips x virus species combinations were tested positive for TSWV; however, harbored lower titers than efficient transmitters (Wijkamp et al., 1995). Kritzman *et al*. (Kritzman et al., 2002) provided qualitative evidence for a positive association between the extent of salivary gland infection by TSWV (measured by intensity of immunofluorescent signal using antibodies against N and secondary antibodies conjugated to FITC) and transmission efficiency. Another study reported a positive correlation between transmission efficiency of viruliferous thrips and TSWV titer in source plants determined by DAS-ELISA or qRT-PCR (Okazaki et al., 2011). This finding may be due, in part, to the number of virus particles ingested and acquired by the thrips; however, one study found no apparent correlation between relative amount of virus ingested, measured by ELISA to detect N protein, and the ability to acquire the virus (van de Wetering et al., 1996). The capacity of a vector competent thrips to transmit is also linked to virus titer. Rotenberg et al. (Rotenberg et al., 2009)

found that the number of TSWV transmission events by individual female and male thrips of *F. occidentalis* was positively correlated to virus titer estimated by the relative abundance of TSWV N RNA or 'absolute' number of N RNA molecules in the whole insect body. Individual females harbored more copies of N RNA than males. Males, however, transmitted more frequently than females, indicating that other biological differences between male and female thrips (i.e., feeding behaviors,) or extent of salivary gland infection in males compared to females may explain the enhanced frequency of TSWV transmission by males. Collectively, the studies described above highlight the importance of virus accumulation and spread in the vector as quantitative determinants of a successful transmission event.

Resistance to TSWV

Natural resistance against TSWV

One of the best available ways to manage TSWV in the field is using resistant tomato hybrids. These resistant hybrids have the TSWV resistant dominant gene *Sw-5*, a member of the coiled-coil, nucleotide-binding, leucine-reach repeat class of resistant genes (CC-(NB-ARC)-LRR). The *Sw-5* locus was identified and introgressed in commercial tomatoes from *Lycopersicum peruvianum*. *Sw-5* provides resistance to TSWV and other related tospoviruses as *Groundnut ringspot virus* (GRSV) and *Tomato chlorotic spot virus* (TCSV).

Likewise, all TSWV-resistant pepper (*Capsicum* spp.) cultivars carry the dominant resistant gene *Tsw*. This gene shows a similar phenotypic reaction to TSWV as *Sw-5* resistance in tomatoes. In both cases, local necrotic spots (HR) developed in the inoculated leaves and there is no systemic spread of the virus. In few plants, the necrotic spots may become systemic and the plants eventually die. Nevertheless, several lines of evidence demonstrate that *Sw-5* and *Tsw* are different loci and may not be evolutionary related (Jahn et al., 2000).

More sources for resistance to TSWV are required in order to manage TSWV infection in areas where resistance-breaking strains are found or where new strains of the virus develop. Gordillo and collaborators (2008) demonstrated that there is additional *Tospovirus* resistance in *L. peruvianum* germplasm, but it is not known the nature of this resistance (qualitative or

quantitative) nor the outcome of its introgression in cultivated tomato (Gordillo et al., 2008). In accordance, Spassova and collaborators (2001) found ORFs for several other resistant gene candidates in the proximity of *Sw-5* locus. However, further work is required to confirm their putative role in resistance (Spassova et al., 2001). Likewise, screening for resistance and development of resistant cultivars is actively done with peanut (Culbreath et al., 2003).

Transgenic resistance against TSWV

Pathogen-derived resistance has been used to engineer plants resistant to TSWV by inserting the gene coding for the nucleocapsid protein (N) (Pang et al., 1996; Sherman et al., 1998; Schwach et al., 2004; Accotto et al., 2005; Fedorowicz et al., 2005), NSs (Sonoda and Tsumuki, 2004; Sonoda et al., 2005), NSm or coding for the glycoprotein precursor (GP) (Ismayadi and Prins, 1996). Mainly tobacco (*N. tabacum*), *N. benthamiana* and tomato plants have been transformed, but also there are reports on peanut (*Arachis hypogaea*) (Culbreath et al., 2003; Yang et al., 2004), lettuce (*Lactuca sativa*) (Pang et al., 1996) and ornamentals as chrysanthemum (*Dendranthema grandiflora*) (Sherman et al., 1998). Varying degrees of resistance were obtained, and in the case of a N-transgenic plant resistance to a *Tsw*-resistance-breaking strain of the virus was observed (Accotto et al., 2005). The results suggested that transgenic plants against TSWV and other tospoviruses are a promising strategy to include in an integrated pest management program to control viruses and their thrips vectors.

Most of the examples in the literature used the N gene to generate the transgenic plants. The expression of N protein in the transgenic plants was variable and in occasions there is no association between expression levels and resistance phenotype (Schwach et al., 2004; Fedorowicz et al., 2005). However, Pang and collaborators (1996) found a correlation between resistance phenotype to TSWV with the levels of N protein accumulation in lettuce transgenic plants. The resistance phenotypes were explained either by an RNA-mediated or a protein mediated mechanism in several of the reports (Pang et al., 1996; Schwach et al., 2004; Yang et al., 2004; Fedorowicz et al., 2005). Schwach and collaborators (2004) reported a broad resistance phenotype against TSWV and GRSV mediated by a modified N protein. In this case, the replication of the virus was not affected but its systemic movement through the plant was blocked (Schwach *et al*. 2004).

The level of resistance conferred by the N gene sequence seemed stronger than the one conferred by NSs or NSm. Transgenic plants for NSs or a system were NSs or NSm were expressed through a PVX vector in *N. benthamiana* plants challenged with virus showed a delay in the appearance of symptoms but at the end of the experiments a high proportion of the plants were infected with TSWV (Sonoda and Tsumuki, 2004; Sonoda et al., 2005). In the case of NSm and GP transgenic plants, there is no report on the reaction to virus challenge, but only on the regeneration of transgenic calluses with the objective to generate transgenic plants resistant to TSWV (Ismayadi and Prins, 1996).

Transmission-stopping technology

The concept of transmission stopping technology to control the spread of pathogens vectored by insects is growing as an alternative for the control of diseases in humans, animals and plants. This strategy consists in interfering with the interaction of a pathogen and its vector. As a consequence of this interference, the pathogen will not be able to establish successfully in the insect vector and hence its transmission to the human, animal or plant host will be reduced or abolished. Several strategies are used to achieve the transmission stopping effect; i.e. antimicrobial compounds engineer into the insect vector (Kokoza et al., 2010), the use of third organisms that disrupt the pathogen-vector interaction as *Wolbachia* (Walker et al., 2011) or blocking or altering the attachment sites for the pathogen in its vector (Ghosh et al., 2001; Shao et al., 2003; Whitfield et al., 2004; d'Avila-Levy et al., 2006; Whitfield et al., 2008; Liu et al., 2010; Colpitts et al., 2011; Sparks et al., 2011).

The ligand-receptor interactions that allow for a pathogen to attach and enter/cross the cells of its insect vector are of particular interest for transmission stopping technology. Peptides with the ability to block or compete with the pathogen for its vector receptor are being identified and proposed for the management of the disease in several pathogen-vector systems (Zhou et al., 1999; Ghosh et al., 2001; Shao et al., 2003; Whitfield et al., 2004; d'Avila-Levy et al., 2006; Whitfield et al., 2008; Liu et al., 2010; Colpitts et al., 2011; Sparks et al., 2011). In the case of human pathogens, as malaria, it was proposed to engineer transgenic mosquitos expressing the competing peptide. Such insects will be refractory to the transmission of the pathogen (Ghosh et al., 2001). In the case of plant pathogens, the later approach is a possibility, but it has been

proposed to engineer transgenic plants expressing the competing peptide. For example, *Pea enation mosaic virus* entrance into its aphid vectors' hemocoel and transmission to new plants is hypothesized to be reduced or impeded with such approach (Liu et al., 2010). This concept was demonstrated for a plant virus-insect interaction with *Rice ragged stunt virus* (RRSV) and its vector, the planthopper *Nilaparvata lugens*. The S9 protein of RRSV is the viral spike protein or one of its components and was shown to bind to an insect membrane protein (Zhou et al., 1999) suggesting S9 involvement in virus attachment and entry to the insect vector. Planthopper vectors fed on transgenic rice plants expressing the S9 protein of RRSV prior to feeding on virus-infected non-transgenic plants showed lower virus titer and lower ability to transmit the virus than insects fed on non-transgenic plants (Shao et al., 2003).

In summary, TSWV and related tospoviruses are emergent and economically important diseases worldwide and the resistance available is not enough to control virus spread nor to decrease/avoid the economic loses associated to it. Although a good deal of research, summarized previously, has unlocked aspects of the virus biology and interactions with the thrips vector, many questions remain unanswered. Understanding the molecular aspects, the specific time points and mechanisms involved in the virus life cycle and interaction with the vector would allow the recognition of potential targets to control the virus and its transmission. In this dissertation, I explored further aspects of the virus-vector interaction: TSWV movement through the vector body and infection of the principal salivary glands of the thrips *Frankliniella occidentalis*. Second, the expression of a soluble form of the virus attachment protein, G_N, was studied *in planta* and tested as a strategy to block virus acquisition and transmission by thrips.

Chapter 2 - Transient expression and cellular localization of *Tomato spotted wilt virus* glycoprotein G_N, a soluble form (G_N-S), and the nucleocapsid protein (N) in *Nicotiana benthamiana*.

Abstract

Tomato spotted wilt virus (TSWV) is one of the top ten most important plant viruses worldwide. Novel approaches for its control are required since the current control strategies represent high production costs or have not been effective for prevention of virus spread and yield loss. We aim to develop novel control strategies for TSWV by exploiting the understanding and biology of two of its proteins, G_N glycoprotein and the nucleocapsid (N) protein. We also studied a soluble form of G_N, G_N-S, which has been shown to interfere with virus acquisition by its thrips vector. The objective of this work was to gain better understanding of their biology *in planta* by studying their cellular localization. G_N, G_N-S, and N proteins were transiently expressed in *Nicotiana benthamiana* leaves fused to green fluorescent protein (GFP) or red fluorescent protein (RFP). G_N displayed a punctate localization pattern characteristic of Golgi stacks (71.6%) and co-localized with a Golgi marker (95.5%). G_N-S displayed a soluble-like pattern through the cytoplasm (71.5%) and 18.9% of the cells also had a reticulate pattern, indicating the presence of G_N-S at the endoplasmic reticulum. Co-localization of G_N-S and a Golgi marker was seen in 43.8% of cells. N protein fused to GFP showed a complex localization pattern consisting of different size fluorescent foci distributed throughout the cell and some foci displayed apparent associations to nuclei or cell membranes. N localization pattern changed over time showing aggregation of the fluorescent foci in presence or absence of TSWV.

Introduction

Tomato spotted wilt virus (TSWV), the type member of the *Tospovirus* genus in the family *Bunyaviridae*, is a worldwide increasing and economically important limiting factor for crop production of commodities such as peanut, tomato and ornamental plants. Several species

of tospoviruses are transmitted by thrips (order Thysanoptera). The most efficient vector of TSWV is *Frankliniella occidentalis*, the western flower thrips (Whitfield et al., 2005b; Pappu et al., 2009). Thrips are also important pests of plants and their control is very difficult due, among other reasons, to insecticide resistance. Therefore, the development of tools and novel strategies for the control of TSWV and thrips is urgently needed (Pappu et al., 2009; Reitz, 2009).

The TSWV particle has a host-derived membrane, the viral envelope, with molecules of two viral coded glycoproteins embedded in it: G_N and G_C. The glycoproteins are produced from a single ORF by means of a polyprotein that is cleaved by host cell proteases into the two mature glycoproteins. G_N corresponds to the N-terminus side of the polyprotein, and G_C to the C-terminus. Inside the envelope there are three negative sense, single-stranded RNA (-ssRNA) molecules (TSWV genome) covered with nucleocapsid (N) protein and associated with few molecules of viral RNA-dependent RNA-polymerase (L) (Whitfield et al., 2005b).

The viral glycoproteins are the outermost molecules of the virus particle and therefore are the first components to interact with vector host cell factors. Several lines of evidence identified the glycoproteins as the molecules involved in the interaction between TSWV and thrips midgut (Bandla et al., 1998; Kikkert et al., 1998; Whitfield et al., 2004; Sin et al., 2005). Moreover, the information available from other bunyaviruses, suggested that TSWV enters their host insect cells by pH-dependent endocytosis (Gonzalez-Scarano et al., 1984; Jin et al., 2002; Plassmeyer et al., 2005; Simon et al., 2009b). In accordance with this hypothesis, G_N was demonstrated to be the attachment protein mediating the specific attachment of the virions to cells in the midgut of thrips (Whitfield et al., 2004). G_C was hypothesized to be the fusion peptide involved in the internalization of virus particles in thrips cells (Garry and Garry, 2004; Whitfield et al., 2005a).

G_N is a specific determinant for TSWV attachment to thrips midgut cells and thus this interaction can be exploited by using viral protein to block virus acquisition and subsequent transmission by thrips. A soluble recombinant form of G_N molecule (G_N-S), lacking the transmembrane and cytoplasmic tail domains of the glycoprotein, was designed and produced in insect cells. G_N-S reduced the transmission of TSWV by *F. occidentalis* when fed prior or simultaneously with virus particles in a sucrose-buffered solution (Whitfield et al., 2004; Whitfield et al., 2008). We hypothesized that G_N-S protein produced *in planta* likewise will inhibit acquisition and transmission by thrips. As an initial step to test this hypothesis we expressed G_N-S *in planta* and characterized its subcellular localization.

The nucleocapsid proteins of bunyaviruses are a multifunctional proteins involved with several processes during the virus replication and assembly (Walter and Barr, 2011). Historically, capsid proteins from plant viruses have been used to generate virus resistance in transgenic plants and TSWV is no exception (Kim et al., 1994; Nervo et al., 2003; Accotto et al., 2005; Fedorowicz et al., 2005). However, the multifunctional properties of the nucleocapsid protein may be exploited to actively tag specific steps in the virus replication cycle. In order to deploy N protein in novel control strategies it is required a clear understanding of its participation in the virus cycle in host cells. We aim to increase our understanding of the multifunctional nature of this protein by studying the localization of N::GFP *in planta* over time. We documented protein localization, because it is recognized that localization and function of a protein are associated in most cases (Millar et al., 2009).

The cellular localization and interactions of TSWV G_N, G_C and N proteins have been studied in a mammalian cell culture system (Baby Hamster Kidney [BHK] cells) and in *Nicotiana tabacum* or *N. rustica* protoplast systems. G_N glycoprotein localized to the Golgi when expressed alone in BHK cells. Meanwhile, G_C localized to the ER when singly expressed, but localized to the Golgi apparatus when co-expressed with G_N (Kikkert et al., 2001). N protein expressed in the BHK system was observed forming aggregates throughout the cytoplasm and gradually forming clusters close to the nucleus (perinuclear localization) (Snippe et al., 2005; Snippe et al., 2007a). N displayed partial localization with G_N and G_C when co-expressed with the glycoproteins, implying that it interacts with both proteins. Initially the N-G_C interaction was reported to be of greater significance than N-G_N interaction (Snippe et al., 2007a); however, further studies confirmed the interactions but suggested that N interacts preferentially with G_N protein (Ribeiro et al., 2009a). These studies have contributed information on the role of the different molecules in the viral replication cycle in plants and for a greater understanding of virus particle morphogenesis. Nonetheless, these studies have been made in cell culture systems *in vitro* rather than in plant tissue directly. Studies conducted in plant tissue will generate new information on virus biology.

The primary goal of our research is to exploit G_N specific interaction with the thrips midgut to develop tools to block TSWV acquisition by thrips. As a first step we developed plant expression clones to express TSWV proteins: G_N, N and the recombinant form G_N-S with fusions to fluorescent proteins. The objective of this work was to study the cellular localization pattern

and behavior of these recombinant molecules *in planta* with the long term focus of deploying these molecules in strategies for TSWV control.

Results

Recombinant Protein Expression in Nicotiana benthamiana

The transient expression of GN, GN-S, and N proteins fused to GFP or RFP was determined by observing the corresponding fluorescence in N. benthamiana leaf tissue agroinfiltrated with the different pEarleygate and pSITE expression clones. In a first set of experiments using pEarleygate clones, HC-Pro (from Tobacco etch virus) was co-agroinfiltrated as an enhancer of recombinant protein expression. In this case, fluorescence was evaluated and detected up to 12 days after agroinfiltration (daa) (Fig. 2.1). Consistently, the control construct for GFP expression displayed brighter and larger foci of fluorescent signal through the agroinfiltrated tissue. N::GFP was second in brightness and displayed a similar or increased distribution of the fluorescent signal throughout the abaxial leaf surface. Moreover, N::GFP signal was observed across the leaf blade cell layers (Fig. 2.1j to l). Meanwhile, GN::GFP and GN-S::GFP had a less bright signal (evidenced by the need of longer exposure times in order to detect the fluorescent signal by epifluorescence microscopy) and it was restricted to small patches or individual cells within the agroinfiltrated tissue (Fig. 2.1b to c).

In some cases, a slight yellowing/tan was noticed with the HC-Pro control tissue in late date points of evaluation (ca. 6 daa and afterwards) and this decay of the plant tissue was associated with background signal (Fig. 2.1e to i). Therefore, to avoid any effect from HC-Pro in the plant tissue or in TSWV recombinant protein behavior, the assay was standardized without the use of HC-Pro. Two days after agroinfiltration was determined as a time point of high expression for the three recombinant proteins of interest in the absence of HC-Pro (data not shown). Accordingly, 2 daa was set as the evaluation time for experiments afterwards.

Relative abundance of different TSWV proteins varied in agroinfiltrated N. benthamiana depending on the protein type and fusion tag

Recombinant protein expression from pEarleygate expression clones was confirmed by western blot analysis using total protein extracts from agroinfiltrated leaf tissue (Fig. 2.2). G_N-S::GFP::His bands were more intense than G_N::GFP::His bands when loading equal amounts of total protein and testing with either anti-G_N or anti-GFP antibodies. This result suggested that G_N-S::GFP::His was more abundant than G_N::GFP::His in the plant tissue and this result was in accordance with the visual evaluation of fluorescent signal where the signal from G_N::GFP::His appeared fainter and more difficult to detect throughout the agroinfiltrated tissue. Conversely, the western blot band intensity suggested that there were comparable amounts of G_N-S::GFP::His and N::GFP::His in the tissues. G_N::His and G_N-S::His recombinant proteins appeared to be found in much lower amounts than their GFP fused versions. Results for Liu *et al*. (2008) with Rift Valley fever virus (RVFV) suggested that the recombinant glycoprotein expression was lower than the expression of recombinant N protein (Liu et al., 2008).

G_N localizes to the Golgi

G_N fused to GFP or RFP and transiently expressed in *N. benthamiana* plants by agroinfiltration consistently displayed a defined punctuate pattern similar to and co-localizing to the one observed for a Golgi marker (Table 2.1; Fig. 2.3 and 2.4). In two independent experiments using pSITE expression clones and Golgi markers (evaluated 2 daa), a total of 296 cells displaying fluorescence signal (GFP, RFP or both) were recorded. A punctate pattern was observed in 71.6% of 197 cells with G_N signal. Co-infiltration of the pSITE G_N::GFP with a Golgi::RFP marker or the reciprocal combination (G_N::RFP with a Golgi::GFP marker) showed co-localization of both fluorescent signals (95.5% out of 156 cells with both signals); albeit the co-localization was not complete in any given cell, i.e. some Golgi spots lacked any G_N signal and vice versa. Despite the tissue was infiltrated with a 1:1 (v/v) ratio of each bacterial strain (one for Golgi marker and one for G_N), only 156 (52.7%) cells out of 296 evaluated showed the double fluorescence signal. These results obtained from plant tissue samples confirmed the Golgi localization previously reported for G_N protein in BHK cells (Kikkert et al., 2001) or plant cell protoplasts (Ribeiro et al., 2008).

G_N-S localizes through the cytoplasm of the cell

G_N-S protein, a recombinant form of TSWV G_N glycoprotein lacking the transmembrane and cytoplasmic tail domains, displayed a soluble-like localization pattern (distributed throughout the plant cell cytoplasm) as we have hypothesized (Table 2.2, Fig. 2.3 and 2.5). G_N-S fused to GFP or RFP (pSITE expression clones) displayed a pattern comparable with that of GFP protein alone and contrasted with the localization pattern observed for the Golgi marker or G_N protein (Fig. 2.5). A soluble-like pattern was observed in 71.5% of cells out of a total of 281 displaying G_N-S associated fluorescence in two independent assays. A reticulate pattern was observed for 53 cells (18.9%) and a punctuate pattern for 27 cells (9.6%). The reticulate pattern was expected because G_N-S protein has a signal peptide and its initial processing will occur at the ER; moreover, a reticulate pattern was observed for G_N glycoprotein at early stages of expression in plant protoplasts (Ribeiro et al., 2008) or mammalian cultured cells (Kikkert et al., 2001; Snippe et al., 2007b). When comparing the co-localization of G_N-S protein co-infiltrated with a Golgi marker, co-localization was observed in 110 cells (43.8%) out of 251 cells with both signals. The localization pattern for G_N-S was significantly different from the pattern observed for G_N. Localization pattern comparisons using 2x3 contingency tables were done independently for the GFP or RFP fused forms, $P = 3.86\text{x}10^{-38}$ and $P = 1.08\text{x}10^{-18}$, respectively. Likewise, Golgi co-localization was significantly different between G_N and G_N-S, $P = 3.98\text{x}10^{-30}$, reinforcing the hypothesis that G_N-S protein localizes in the cell differently than G_N.

N protein has a complex localization pattern

TSWV N protein (pEarleygate-N::GFP::His) was observed in agroinfiltrated tissue (2daa) as fluorescent spots through the cell periphery and/or boundary between cells, as small spots around the nucleus (perinuclear), or as aggregates of variable size in the cytoplasm associated or not with the nucleus (Fig. 2.6). Some of the smaller spots in the cell periphery seem to be in between the two adjacent cells. In other cases, the two spots appeared as oblong spots, one to each side of the boundary (cell wall) between adjacent cells (Fig. 2.6d). Previous work examining N localization in BHK cells or plant cell protoplasts reported N protein with a perinuclear localization or as cytoplasmic aggregates (Snippe et al., 2005; Snippe et al., 2007a; Ribeiro et al., 2009a). However, the localization patterns apparently associated with the cell

membrane and/or wall have not been previously reported. We hypothesized that this multiple pattern may be a consequence of the functional diversity of N protein and the viral life cycle strategy to replicate in plant cells in contrast to animal cells. This is the first report for N localization within a leaf plant tissue in contrast to *in vitro* systems.

N protein localization pattern changes over time

The localization pattern of N::GFP changed over time. Initially N::GFP fluorescent foci were distributed throughout the cell as spots of variable size with a high proportion of small ones. Some of these foci seemed to be associated with the cell membrane or the nucleus. As time passed, less number of foci was visible and the individual foci seemed to be greater in size. We described this trend as an aggregation behavior and characterized it in terms of the number of foci per fluorescent tissue and the average size of the foci. Nine images were analyzed per time point (2, 4, 6 and 8 or 9 daa) using ImageJ and the results support our observations. As expected when aggregation occurs, there was less number of individual fluorescent foci, but the remaining ones have a greater size in average (Fig. 2.7a and d). Both observations were interpreted as the result of small foci coming together into a common spot (aggregation).

The experiment was repeated in presence and absence of TSWV infection (14 days after inoculation of the virus). We hypothesized that in presence of the virus, N::GFP protein may be able to interact with the other viral proteins, including non-recombinant N from the virus. The occurrence of a similar behavior in presence or absence of TSWV might be indicative that this behavior is part of the biology of N protein during the virus replication cycle in the plant cell host. Regardless of virus infection, N::GFP fluorescent foci number decreased over time; meanwhile, the average size of the foci increased supporting the idea that N::GFP behavior has a biological significance (Fig. 2.7d and e; and 2.8a to h). In contrast, the mean integral density, a measurement of the fluorescent signal, decreased over time in absence of the virus but increased over time (up to 6 daa) in the presence of the virus (Fig. 2.7g and h). This observation showed that the presence of virus did affect the expression of N::GFP (indirectly measured as amount of fluorescent signal) but it did not affect its pattern of localization, again supporting the idea that the observed pattern of aggregation may be of biological significance.

A GFP control was set for this experiment and treated exactly as the N::GFP treatment: presence or absence of TSWV and three images taken per three different infiltration sites, for a total of nine images per treatment per evaluation day (2, 4, 6 and 8 daa). The number of fluorescent areas identified by ImageJ showed some differences in their pattern between absence and presence of TSWV infection; and in both cases it was different from the pattern observed for N::GFP (Fig. 2.7 and 2.8). This observation suggested that N::GFP pattern in presence or absence of TSWV was not an effect of the GFP protein fusion because GFP molecule alone behaves differently. On the other hand, the total fluorescence signal from each image quantified as the integrated density (Image J) had a similar pattern over time for N::GFP or GFP images, but different patterns for the presence or absence of TSWV. In the case of healthy plant tissue, the intensity of N::GFP or GFP fluorescent signal decreased over time but in the presence of TSWV, there was an increase in the intensity of fluorescence signal for both proteins up to 6 daa and a relatively low decrease toward 8 daa. These results suggest that the presence of TSWV in the tissue did affect the transient expression or protein accumulation and its effect probably is due to TSWV gene silencing suppressor (NSs).

Visual counts and classification of foci for the N::GFP images supported the results and interpretations obtained by ImageJ analysis. The images for N::GFP with or without TSWV infection were evaluated also by a person with no prior knowledge of the treatments or the hypothesis. Fluorescent foci per image were counted and classify in five categories: small foci, large foci, doublet spots at opposite sides of the cell boundary, small foci associated with the nucleus and large foci associated to the nucleus. The percentage of each one was calculated and compared. The total number of foci counted was not corrected per fluorescent area per image, nevertheless, it showed a decrease in the absence of virus as observed with the computational analysis. The relative proportion of different foci classes was comparable in absence or presence of TSWV; and the behavior over time suggest, as noted previously, a tendency for the number of small foci to decrease meanwhile the number of large foci increased.

Interactions between G_N, G_N-S or N, as evidenced by changes in localization patterns

In order to further analyze the behavior of G_N, G_N-S or N *in planta*, we aimed to determine any change in the localization patterns when any two recombinant proteins were co-

agroinfiltrated and expressed simultaneously from the same tissue. We hypothesized that the soluble-like localization pattern of G_N-S might be altered if interacting with G_N or N proteins. Overall, the localization pattern of G_N-S (fused to GFP or RFP) was not apparently altered by the presence in the same cell of G_N or N proteins *in planta*; and if affected, the method was not sensitive enough or too variable to detect statistical clear differences (Table 2.3). If only the localization patterns of GFP fused proteins were considered, then the results suggested that an interaction was occurring among G_N-S and G_N and between G_N and N protein. The localization pattern of G_N-S was altered in presence of G_N ($P = 0.0248$) and the localization pattern of G_N was affected by the presence of N protein ($P = 0.0200$).

TSWV G_N glycoprotein and a recombinant soluble form produced in insect cells were able to oligomerize each one as homodimers (Whitfield et al., 2004). Thus we wanted to test if G_N-S *in planta* was capable of hetero-oligomerizing with G_N. We hypothesized that if hetero-oligomerization takes place then a greater percentage of co-localization between G_N-S and G_N will be determined in comparison to the co-localization seen between G_N-S and the Golgi marker. G_N localized to the Golgi as previously showed, and thus acted as a Golgi marker. If no hetero-oligomerization occurred, the percentage of co-localization of G_N-S to G_N would be similar to the percentage of co-localization of G_N-S to a different Golgi marker. Four independent co-agroinfiltration experiments were done. In each case two *N. benthamiana* plants were co-agroinfiltrated with G_N-S and G_N. In two of the experiments, G_N-S was fused to GFP whereas G_N was fused to RFP; in the other two experiments the reciprocal combination was tested. A total of 198 cells displaying both signals were recorded from these experiments and 40% (80 cells) showed co-localization of the signals. There was no statistical difference ($P = 0.5012$) between the frequency of co-localization observed for G_N-S to G_N compared to the frequency of co-localization previously recorded for G_N-S to a Golgi marker. This result suggested that there is no apparent hetero-oligomerization. Additionally, G_N-S localization pattern (reticulate, punctate or soluble) was recorded for these 198 cells and compared to the pattern recorded for the Golgi co-localization assay (previous data). Overall, a decrease in the percentage of cells with a soluble pattern was noticed (from 71.5% to 50.5%); meanwhile there was an increase in punctate pattern (from 9.6% to 30.8%). This observation is in accordance with G_N-S protein forming hetero-oligomers with G_N because it should be retained at the Golgi when associated to G_N. Independent comparison of the GFP or RFP fusions of G_N-S localization

pattern in presence or absence of G_N indicated a significant difference for G_N-S::GFP (P = 0.0248) but not for G_N-S::RFP (P = 0.4347). In conclusion, there was not clear evidence to support hetero-oligomerization between G_N-S and G_N; however, the contradictory results may be indicative of the occurrence of the interaction at a low frequency.

G_N glycoprotein was reported to interact with N protein, but no apparent change in localization pattern was detected in experiments performed with *in vitro* systems (Ribeiro et al., 2009a). An experiment was conducted to compare the localization pattern of G_N-S and G_N in the presence of N protein. G_N-S and G_N were co-infiltrated with N protein (reciprocal GFP and RFP combinations were tested, 2 plants per combination). A 2:1 (v/v) ratio of the corresponding *Agrobacterium* strains was used (2 vol. of G_N::GFP or G_N-S::GFP to 1 vol. of N::RFP or N::GFP) because in a previous assay (data not shown) very few or any cells displayed G_N or G_N-S associated signal in comparison to N when co-infiltrated at a 1:1 ratio. No apparent difference was observed in the localization patterns of G_N when in the presence of N, however the statistical comparison to the patterns recorded in absence of N was not conclusive, P = 0.0200 and 0.5499 for G_N::GFP and G_N::RFP respectively. In the case of G_N-S protein there was no change in the localization pattern when in the presence of N in comparison to the pattern recorded in previous experiments in the absence of N protein, P = 0.1226 and 0.2376 for GFP and RFP fused forms respectively.

Discussion

G_N protein of TSWV fused to GFP or RFP was confirmed to localize to the Golgi apparatus *in planta* as was previously demonstrated for *in vitro* systems: baby hamster kidney cells (BHK) and *N. tobacum* protoplasts (Kikkert et al., 2001; Ribeiro et al., 2008). Moreover, the G_N glycoproteins of other bunyaviruses (animal-infecting) were showed to localize to the Golgi (Bertolotti-Ciarlet et al., 2005). In some cells (26.9%, pSITE experiments) the fluorescence associated to G_N appeared to be continuous and distributed through the cell in contrast to a punctate pattern characteristic of the Golgi in plants. This soluble-like appearance may rather be G_N molecules anchored throughout the plasma membrane and other membrane systems in the cell as vesicles derived from the Golgi cisternae carrying G_N are incorporated into other cellular membranes. This phenomenon was observed for other bunyaviruses and it may

result from increased glycoprotein expression (driven by double 35S promoters) as was noted when overexpressing Rift Valley fever virus glycoproteins (Filone et al., 2006; Shi et al., 2007; Liu et al., 2008; Shi et al., 2010). However, the general accepted model is that the glycoproteins of bunyaviruses are not delivered to the cell membrane (Bertolotti-Ciarlet et al., 2005). Alternatively, the cells with G_N fluorescence appearing with a soluble-like pattern may be artifacts of the technique. The optical section in study may contain several Golgi stacks arranged one after another producing a continuum of fluorescent signal.

G_N-S, a recombinant soluble form of TSWV G_N glycoprotein lacking the transmembrane domain and cytoplasmic tail, showed a pattern of localization soluble-like and similar to the one observed for GFP protein alone. In addition, G_N-S associated fluorescence (GFP or RFP fusions), was also observed in a reticulate pattern, characteristic of the endoplasmic reticulum (ER). This result suggested that any domain for Golgi targeting occurs in the ectodomain of TSWV G_N; contrary to the Golgi targeting of a soluble G_N glycoprotein Crimean-Congo hemorrhagic fever virus (Bertolotti-Ciarlet et al., 2005), another bunyavirus.

The complex localization pattern of N::GFP and its change over time suggested that N protein has an important role and likely multiple functions during the virus replication cycle in plant cells. Of most interest is the possibility that a fraction of N protein in the cell may interact or target the plasmodesmata structure. Future research with different plasmodesmata markers can test this hypothesis. Several questions arise from the hypothetical interaction and may guide research for a better comprehension of TSWV cell-to-cell movement by a tubule guided mechanism.

The occurrence of interactions was not conclusively demonstrated in this work for either G_N-S with G_N or for these proteins with N. The data of GFP fused proteins suggest interactions between G_N-S and G_N ($P = 0.0248$) and between G_N and N ($P = 0.0200$). Previous reports regarding the interaction of G_N and N encountered some difficulties or were contradictory, suggesting that the interaction occurred at a low frequency and it was difficult to detect. If an interaction between G_N-S and G_N occurred, we hypothesize that it may have a detrimental effect on virion assembly and/or stability and constitute another way in which G_N-S protein might be exploited for TSWV control. The truncated G_N protein, G_N-S, may interfere with the conformation and functionality of the glycoprotein hetero-oligomeric complexes or with the interactions with RNPs for packing (Naidu et al., 2008; Hepojoki et al., 2010a; Hepojoki et al.,

2010b). Likewise, no apparent interaction was determined for G_N-S with N protein (P = 0.1226 and 0.2376, for GFP and RFP fusions). This result is explained by the fact that the domains required for G_N interaction with N protein are found in the cytoplasmic tail of the glycoprotein for other bunyaviruses (Naidu et al., 2008; Hepojoki et al., 2010a; Hepojoki et al., 2010b).

Overall, recombinant forms of TSWV G_N, G_N-S and N proteins were successfully expressed in plant leaves and their cellular localization determined. These proteins are excellent tools for dissecting the viral replication cycle *in planta* and the participation of the individual proteins. Aspects of the virus-vector interaction might also be studied with aid of the recombinant proteins reported herein. The future perspectives of this research are to determine if G_N-S protein expressed from transgenic plants might serve as a transmission blocking agent.

Materials and Methods

Construction of expression clones

The sequences corresponding to TSWV glycoprotein G_N and nucleocapsid protein (N) were amplified from plasmids pGF7 (Adkins et al., 1996) and pBS-NC4.5 (Kim et al., 1994), respectively. The primer sequences and primer combinations used for cloning are indicated in tables 2.4 and 2.5, respectively. The expression clones were constructed using the Gateway® cloning technology (Invitrogen). Entry clones were generated by cloning gel purified PCR amplicons of the sequences of interest into pENTR vector. The entry clones were digested with *Mlu*I and the fragment containing the sequence of interest flanked by *att*L sites was gel purified (QIAquick® Gel Extraction Kit, Qiagen). The purified fragments were recombined (LR clonase reaction) into the appropriate destination vectors, pEarleygate 100 or pEarleygate 103 (Earley *et al*. 2006). pEarleygate 100 was used to generate constructs expressing the proteins of interest without any fluorescent protein fusion and pEarleygate103 was used to express the proteins with a C-terminus GFP and six histidine (6xHis) tag fusion. For proteins cloned into pEarlyGate 100, a 6xHis tag was added by means of the reverse primer sequence. Expression clones were confirmed by sequencing and analyzed with restriction enzymes.

Constructs for two forms of the G_N glycoprotein were done. One corresponds to the complete predicted (Whitfield et al., 2004) ORF of G_N; and another, G_N soluble (G_N-S), includes

only the predicted ectodomain of the glycoprotein, excluding the transmembrane and cytoplasmic domains. Each of these forms was produced with either a C-terminal 6xHis tag or C-terminal fusion to GFP and a 6xHis tag. Likewise, two constructs were done for N, one with a C-terminal 6xHis tag and one with a GFP-6xHis tag C-terminal fusion. Finally, the ORF of the GFP and 6xHis tag in pEarleygate 103 was cloned into pEarleygate 100 to generate a control GFP expressing clone.

Additionally, the entry clones were used to generate a second batch of expression clones using pSITE expression vectors (Chakrabarty et al., 2007). The entry clones for G_N fusion, G_N-S fusion and N fusion were directly (without restriction treatment) recombined with pSITE-2NB and pSITE-4NB to generate C-terminal fusions to EGFP or monomeric RFP, respectively. In total, 13 expression clones were generated.

Plant and bacterial culture maintenance

Nicotiana benthamiana wild type and *N. benthamiana* transgenic lines expressing cellular markers fuse to RFP for the endoplasmic reticulum (Martin et al., 2009) and the nucleus (Chakrabarty et al., 2007) were maintained in a growth chamber, 14 h light/10 h dark and 24°C. Three to four weeks old plants were agroinfiltrated in all cases and kept in the growth chambers for the duration of the assay.

All expression clones were introduced into *Agrobacterium tumefaciens* strain LBA4404 by freeze-thaw method. LB-20% glycerol stocks of transformed lines were stored at -80°C. Strain LBA4404 was grown in rifampicin (15µg/ml) as bacterial selection agent and supplemented with kanamycin (50µg/ml) or spectinomycin (50µg/ml) if carrying pEarleygate or pSITE derived plasmids, respectively.

Nicotina benthamiana agroinfiltration

Transient protein expression was done by infiltrating *N. benthamiana* plants with *A. tumefaciens* carrying the appropriate expression clone. *A. tumefaciens* lines were started from glycerol stocks in LB supplemented with 15µg/ml of rifampicin and the plasmid selection antibiotic. After two days of incubation at 28°C, a single colony was used to inoculate a 5ml LB broth (supplemented with the plasmid selection antibiotic) and incubated overnight. Fifty

milliliters LB flasks (supplemented with the plasmid selection antibiotic) were started by inoculating with 1ml from the 5ml overnight culture. The cultures were grown overnight at 28°C and shaking (200rpm). Cells were collected by centrifugation at 3000rpm for 10 min at 4°C and the pelleted cells suspended in MES-agroinfiltration buffer (45 mM MES salt anhydrous [$C_6H_{13}NO_4S$], 10 mM $MgCl_2$, and 1.5 mM acetosyringone [3',5'-dimethoxy-4'-hydroxyacetophenone 97%]; pH 5.6). Bacterial cultures activation was obtained by shaking at 28°C for 3 to 5 hours. After activation, optical density (OD_{600}) of the cultures was measured. Agroinfiltration was done using final OD_{600} of ~0.8 (0.7 to 1.0). The infiltration of the bacterial suspension was done at the abaxial surface of the leaf (underside) with 5 ml syringes. Leaves were rinsed with tap water after agroinfiltration. Several sites per leaf and leafs per plant were agroinfiltrated in any given case. A negative control consisting in MES-buffer infiltrated plants was always set to check for background fluorescence and a positive pEarleygate-GFP control was done to check the infiltration event in every assay.

In the case of co-infiltrations, the bacterial suspensions in MES buffer were mixed at 1:1 (v:v) ratios if not noted otherwise, and the mixture was infiltrated as previously described. Cellular markers were co-infiltrated in several cases together with the expression clone for the viral protein of interest. The cellular markers were all constructed on pSITE expression vectors (Chakrabarty et al., 2007). We used a Golgi marker fused to GFP or RFP, an endoplasmic reticulum marker fused to GFP and a nuclear marker fused to RFP (Goodin et al., 2007). All pSITE expression vectors, pSITE cellular markers and transgenic plants were facilitated by Dr. Michael Goodin, University of Kentucky.

Protein extraction

Plant tissue was collected after confirming the expected fluorescence under an epifluorescence microscope, at 2, 6, 8 or 12 days after agroinfiltration. Following the results from preliminary trails and early experiments tissue collection for protein analysis was standardized to two days after agroinfiltration. Five hundred grams of fresh tissue were flash frozen in liquid nitrogen and pulverized with mortar and pestle. The powder was collected in a 2ml screw cap microcentrifuge tube with eight metal beads (3mm diameter) and 500ml of ice cold protein extraction buffer (0.03M potassium phosphate (pH 7.4), 0.40M NaCl, 10mM β-

mecaptoethanol, and 1% sarcosyl (N-lauroyl sarcosine)). Samples were homogenized on a bead beater for 2min; incubated on ice for 30min and homogenized again for 2min. Samples were centrifuged 10min at 12000g at 4°C. The supernatant was collected in a new ice cold 1.5ml microcentrifuge tube and the centrifugation and collecting steps were repeated once. A 10µl aliquot was dissolved 1:25 in ddH2O and used for protein quantification using the Pierce BCA Protein Assay Kit (Thermo Scientific, Rockford, IL, USA). Two 130 µl aliquots were collected in new 1.5ml tubes, mixed with 32.5µl of SDS-PAGE sample buffer 5X (Laemmli Buffer; 0.3125 M Tris-HCl (pH 6.8), 10% SDS, 0.375M DTT, 50% glycerol, 0.025% bromophenol blue) and incubated at 100°C for 5min. Protein samples were stored at -20°C.

SDS-Page and western blot

Protein expression was confirmed by separation of total protein extracts by sodium dodecyl sulfate-polyacrylamide gel electrophoresis (SDS-PAGE) and specific detection of the recombinant proteins by antibodies (Western blot). Equal amounts of protein were loaded into 10%-resolving - 5%-stacking polyacrylamide gels and run for 1:45min at 100V in SDS-PAGE running buffer (25mM Tris-Base, 250mM glycine and 0.5% SDS). In most cases protein samples were ran in duplicate gels, one was used for visualizing protein bands by Coomassie staining and the second one was used for western blotting. The identity of the protein bands was assayed by Western blot probing with G_N, N or GFP-specific antibodies. Gels were electrophoretically transfer to nitrocellulose membrane (Hybond-C Extra, GE Healthcare, Little Chalfont, BKM, UK) in transfer buffer (48mM Tris-Base, 39mM glycine, 0.0037% SDS, 20% methanol) at 30mA and 4°C, overnight (ca. 15 h). Membranes were blocked with phosphate-buffered saline (PBS) supplemented with 0.05% Tween (PBST) and 5% nonfat dry milk (NFDM) for 1h and then incubated with primary antibodies for 2h. Primary antibodies were monoclonal mouse anti-G_N (Adkins et al., 1996), polyclonal peptide rabbit anti-G_N, polyclonal rabbit anti-N (Ullman et al., 1995) and polyclonal rabbit anti-GFP (Invitrogen, Carlsbad, CA, USA), diluted in PBS-NFDM at 1:2000, 1:2000, 1:2000, and 1:2500 respectively. The polyclonal peptide rabbit anti-G_N was costumed made during this work (GenScript, Piscataway, NJ, USA) against a 14 amino acid peptide (SQTPGTRQIREEES) from the N-terminus region of G_N, starting at residue 78 from the start methionine of the polyprotein which corresponds to position 42 after the signal

peptide sequence is removed. Secondary horseradish peroxidase-conjugated antibodies (Bio-Rad, Hercules, CA, USA) were diluted 1:5000 and incubated for 1h. Three rinses, each 100µl PBST-5% NFDM for 5min, were done between incubations. Western blot were visualized with ECL Plus Western Blotting Detection System (GE Healthcare, Little Chalfont, BKM, UK) using 2ml of reagent mix (A and B) per membrane.

DAPI-staining

To visualize the cell nuclei, leaf tissue (ca. 2x2cm) containing agroinfiltration lesions were infiltrated with MES-buffer supplemented with 15µg/ml DAPI (4',6-diamidino-2-phenylindole, dihydrochloride) two hours before evaluating the tissue under the microscope. The tissue was kept on the dark, and for the microscopic evaluation a 0.5x0.5cm square was cut out of the area doubly infiltrated.

Microscopy

To evaluate protein expression and localization by fluorescence detection (GFP or RFP), squares (0.5x0.5cm) were cut out from the agroinfiltrated tissue two days after agroinfiltration if not noticed otherwise, and mounted on water on glass slides just before evaluation. Epifluorescence microscopy was done with a Zeiss Axioplan 2 IE Mot microscope and images acquired with a Zeiss AxioCam HRc and Zeiss Axiovision image-processing software. Objectives 20X, 40X and a water-immersion objective lens 63X C-Apochromat (numerical aperture 1.2) were used to analyzed the tissue and acquire images. Fluorescence of GFP was observed using a mercury lamp source and excitation and emission filter settings of 480±10nm and 510±10nm, respectively. Confocal microscopy was done with a Zeiss Axiovert 200M microscope equipped with a Zeiss LSM510 META system. The confocal microscope settings were: a 405nm laser diode at 5% transmission for detecting DAPI fluorescence with a bandpass (BP) filter 420-480nm; a 488 Argon laser at 5% transmission for detecting GFP with a BP filter 505-530nm; and a 543nm HeNe laser at 80% transmission for exciting RFP and chloroplast autofluorescence. A BP filter 585-615nm was used to detect RFP fluorescence excluding the chloroplast autofluorescence and a long pass (LP) filter 585nm for detecting the autofluorescence of the chloroplast. To study the tissue and acquired images a 40X oil- immersion objective was

used with scan zoom set to 0.7X (final zoom 280X) for general images and scan zoom set to 4X for details (final 1600X). Differential interference contrast (DIC, also known as Nomarski Interference Contrast, NCI) method was used in both microscopes to visualize the bright field.

Image analysis and statistical analysis

To evaluate localization pattern of G_N-S and G_N proteins, confocal single section images from the corresponding tissue were evaluated. Single cells were identified and the localization pattern of the fluorescent signal was classified as either: 1-reticulate (net-like pattern), 2-punctate (small dot-shaped uniform fluorescent spots) or 3-soluble-like (a continuous fluorescent signal at the cell periphery, the nucleus area and, in occasions, the whole surface of the cell). Single cells may display more than one pattern simultaneously. Partly this is due to the nature of the plant cell with a large vacuole pressing all organelles and cytoplasm toward the cell periphery, creating the appearance of a soluble-like pattern even when other pattern was present. Therefore, punctate pattern was given the priority, followed by reticulate and last soluble. In example, if a punctate or reticulate pattern were partially visible in a cell with sections seemingly soluble-like, the cell was recorded as either punctate or reticulate, but not soluble-like. In the case of co-localization of the signals for GFP and RFP, this was determined from the appearance of a yellow hue in the picture and the evident overlapping of both signals when comparing among the individual channel and merged images. To be consistent always co-localization was record following these criteria. Counts of data were analyzed by constructing contingency tables for the different hypothesis and combinations to test and determining the statistical difference between comparisons by Fisher exact test using the statistical software SAS.

To evaluate N protein localization pattern, confocal single section images or epifluorescence microscopy images were evaluated for the pattern of fluorescence as: 1-particulate (variable size and shape fluorescent foci distributed heterogeneously throughout the cell) or 2-soluble-like (a continuous fluorescent signal at the cell periphery, the nucleus area and, in occasions, the whole surface of the cell). Quantitative evaluation of N images was done with ImageJ software (Abramoff et al., 2004). Individual images of the channel of interest (corresponding to GFP or RFP) were converted to an 8-bite gray scale image and the scale was set with reference to the image scale bar. The function “Measure” was use to analyze the whole

are of the image. Also, a binary image was generated by thresholding each image and the function "Analyze Particles" was used to count the number of fluorescent foci and measure several parameters for each foci. Additionally, in the case of the experiment testing pEarleygate N::GFP over time in the presence and absence of TSWV, an evaluator unaware of the treatments or the hypothesis being tested was given 200x epifluorescent images at 500ms exposure time and asked to classify the different type of foci (regarding shape and size) and count the number of foci per category per image.

Quantitative comparisons on the degree of fluorescent signal or area were evaluated as the Integrated Density or as the Area Fraction of the image or the region of interest (ROI) calculated using ImageJ. For this type of comparisons/analyses the images among a comparison were taken at the same conditions (including objective magnification, exposure time or gain level, laser intensity, filter specifications, etc…) either by confocal or epifluorescence microscopy.

Tables and Figures

Table 2.1. Number of cells (2x3 contingency table) recorded for three fluorescent signal localization patterns: reticulate, punctuate or soluble, when expressing G_N fused to GFP or RFP, 2 days after agroinfiltration.

Fusion Protein	Numberof cells per localization pattern			Total cells
	Reticulate	*Punctate*	*Soluble*	
G_N::GFP	3	94	50	**147**
G_N::RFP	0	47	3	**50**
Total cells	**3**	**141**	**53**	**197**

Table 2.2. Number of cells (2x3 contingency table) recorded for three fluorescent signal localization patterns: reticulate, punctuate or soluble, when expressing G_N-S fused to GFP or RFP, 2 days after agroinfiltration.

Fusion Protein	N° of cells per localization pattern	Total cells

	Reticulate	*Punctate*	*Soluble*	
G_N-S::GFP	50	6	124	**180**
G_N-S::RFP	3	21	77	**101**
Total cells	**53**	**27**	**201**	**281**

Table 2.3. Probabilities calculated by Fisher exact test associated to contingency tables comparing G_N-S co-localization to G_N or a Golgi marker (2x2 table) or comparing localization patterns of G_N and G_N-S in the presence and absence of N protein (2x3 tables).

Comparison	Probability (*P*)
Co-localization of G_N-S (GFP + RFP) with G_N or a Golgi marker[1]	0.5012
Localization pattern of G_N-S::GFP in presence/absence of G_N::RFP[2]	0.0248
Localization pattern of G_N-S::RFP in presence/absence of G_N::GFP[2]	0.4347
Localization pattern of G_N::GFP in presence/absence of N::RFP[3]	0.0200
Localization pattern of G_N::RFP in presence/absence of N::GFP[3]	0.5499
Localization pattern of G_N-S::GFP in presence/absence of N::RFP[3]	0.1226
Localization pattern of G_N-S::RFP in presence/absence of N::GFP[3]	0.2376

[1] Data from four independent experiments.

[2] Data from two independent experiments.

[3] Data from a single experiment.

Table 2.4. Primers used to generate Gateway entry clones for *Tomato spotted wilt virus* glycoprotein G_N, a soluble form G_N-S, nucleocapsid protein N, and a GFP control.

Primer[1]	Sequence[2]
G_N General Wt/S nt1-31 F	CACCATGAGAATTCTAAAACTACTAGAACTAGTCG
G_N (-A) fusion nt 1356-1386 R	CATAGACATGGGCATTTGAGACAAAATGATC
G_N (-A) 6xHis-Stop nt1369-1386 R	TTAATGATGATGATGATGATGCATAGACATGGGCATTTG
G_N-S fusion nt895-930 R	AATGCTTTTTGAATATTTGATTATGCAATCTCTAAC
G_N-S 6xHis-Stop nt910-930 R	TTAATGATGATGATGATGATGAATGCTTTTTGAATATTTGAT
TSWV-N nt1-25 F	CACCATGTCTAAGGTTAAGCTCACTAAGG
TSWV-N fusion nt751-774 R	AGCAAGTTCTGTGAGTTTTGCCTG

TSWV-N 6xHis-Stop nt754-774 R	TTAATGATGATGATGATGATGAGCAAGTTCTGTGAG TTTTGC
GFP pEarley103 nt4375-4403 F	CACCATGGTAGATCTGACTAGTAAAGGAGAAG
GFP pEarley103 nt5110-5130 R	TCACACGTGGTGGTGGTGGTG

[1] nt = nucleotide positions of TSWV glycoprotein precursor ORF contained in the primer. F = forward primer and R = reverse primer.

[2] Gray highlighted sequences correspond to the CACC sequence required for topoisomerase cloning (Invitrogen, Carlsbad, CA, USA) and underlined sequences correspond to a six histidine tag and a stop codon.

Table 2.5. Primer combinations used for the generation of Gateway entry clones[1] for *Tomato spotted wilt virus* glycoprotein G_N, a soluble form of G_N (G_N-S), nucleocapsid (N) protein, and a GFP control.

Entry clone	Forward primer	Reverse primer
G_N::fusion	G_N General Wt/S nt1-31 F	G_N (-A) fusion nt 1356-1386 R
G_N::His	G_N General Wt/S nt1-31 F	G_N (-A) 6xHis-Stop nt1369-1386 R
G_N-S::fusion	G_N General Wt/S nt1-31 F	G_N-S fusion nt895-930 R
G_N-S::His	G_N General Wt/S nt1-31 F	G_N-S 6xHis-Stop nt910-930 R
N::fusion	TSWV-N nt1-25 F	TSWV-N fusion nt751-774 R
N::His	TSWV-N nt1-25 F	TSWV-N 6xHis-Stop nt754-774 R
GFP::His	GFP pEarley103 nt4375-4403 F	GFP pEarley103 nt5110-5130 R

[1] These entry clones lack a stop codon in order to generate C-terminal fusions of the protein of interest with fluorescent proteins or to generate C-terminal 6-His tagged proteins.

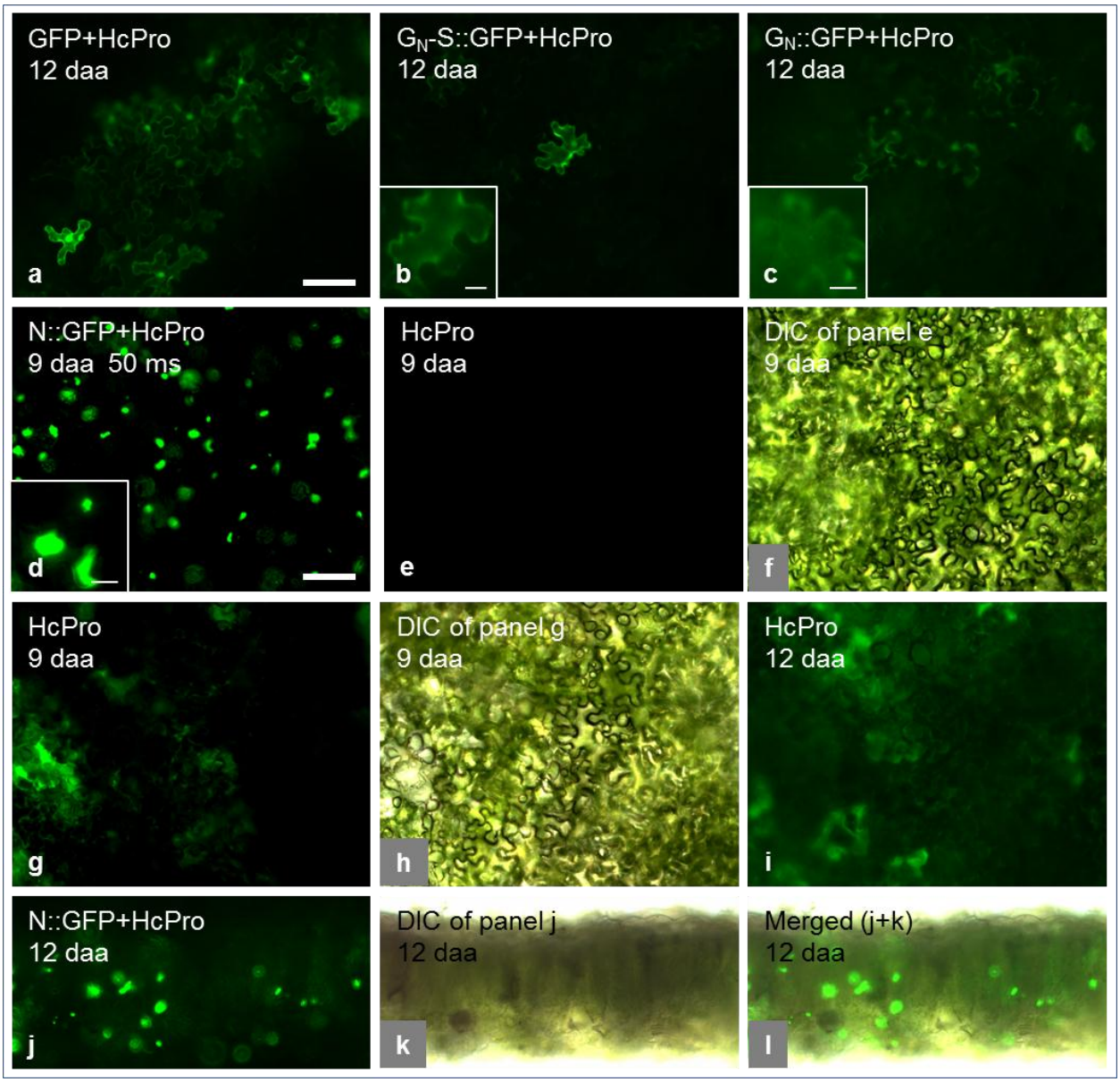

Figure 2.1. Fluorescent signal from pEarleygate based expression clones complemented with *Tobacco etch virus* gene silencing suppressor, HcPro, was detected up to 12 days after agro-infiltration (daa) in *Nicotiana benthamiana* leaf tissue and throughout the leaf blade cell layers.

Epifluorescent images for the signal pattern from GFP, G_N-S::GFP, G_N::GFP and N::GFP pEarleygate expression clones after 12 or 9 daa for N::GFP (a-d). All images are 200x images, scale bar = 100µm. Insets in a-c are zoom images at 400x, scale bars = 20µm. HcPro negative controls nine daa without any apparent signal (e) or with background signal (g). Bright field images (f and h) corresponding to panels e and g respectively. Notice the light

tan/yellowing of the tissue in h. Background signal for HcPro treatment observed 12daa (i). Cross sections of *N. benthamiana* leaf blade showing N::GFP fluorescent signal distributed across mesophyll cell layers in the leaf blade 12 daa (j-l). GFP channel (j), bright field of j (k) and merged image of j and k (l). Exposure times were 150ms for panel a, 2 seconds for panels b, c, e-i; 50ms for panel d and 100ms for panles j-l. Images from panels a-c and i are from one experiment, d-h are from a second experiment and j-l from a third independent experiment.

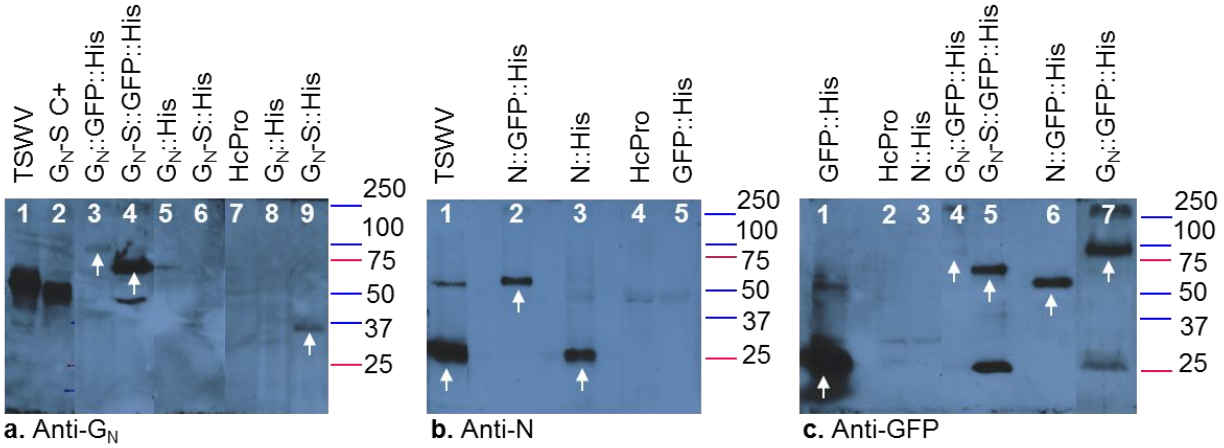

Figure 2.2. Detection of transiently expressed recombinant proteins in *N. benthamiana* plant tissue.

Recombinant protein was detected by western blotting using specific antibodies against G_N (a, monoclonal mouse antibody); N (b, polyclonal rabbit antibody) and GFP (c, polyclonal rabbit antibody). Sixty micrograms of total protein extracted from agro-infiltrated tissue was loaded per sample, except for lanes: a7 = 189; a8 = 270, a9 = 209 and c7 = 288 µg. Sample "G_N-S C+" corresponds to purified G_N-S protein expressed *in vitro* from insect cells (SF21 cell culture). The band positions and mass weight (kD) corresponding to a dual color protein standard (Bio-Rad) are depicted next to each gel image.

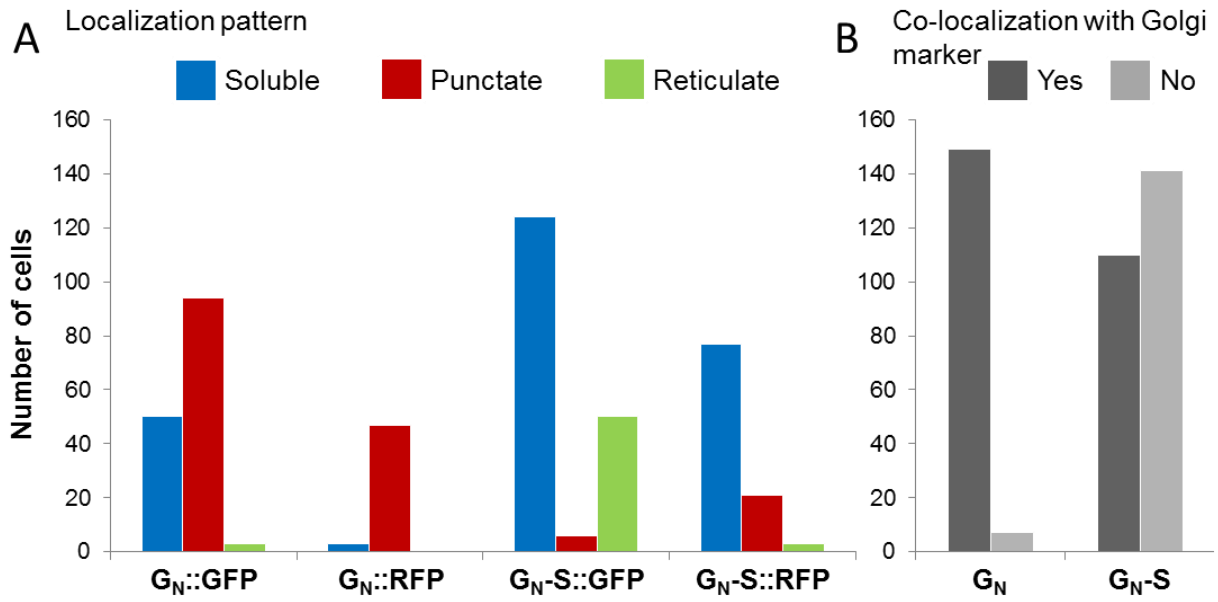

Figure 2.3. Cell localization patterns for G_N and G_N-S fusion proteins to GFP and RFP and their co-localization to a Golgi marker when transiently expressed in *Nicotiana benthamiana* leavess two days after agroinfiltration (2 daa).

Number of cells displaying different fluorescent signal localizations patterns (soluble, punctate and reticulate) when expressing G_N or G_N-S proteins fused to GFP or RFP (A). Each bar represents the total number of cells from two independent experiments. Number of cells showing co-localization between the fusion proteins, G_N or G_N-S, and a Golgi marker (B). Each bar represents the total number of cells coming from two independent experiments and includes cells expressing either GFP or RFP fused protein. The Golgi marker was labeled with either GFP or RFP, and was combined with the opposite labeled G_N or G_N-S.

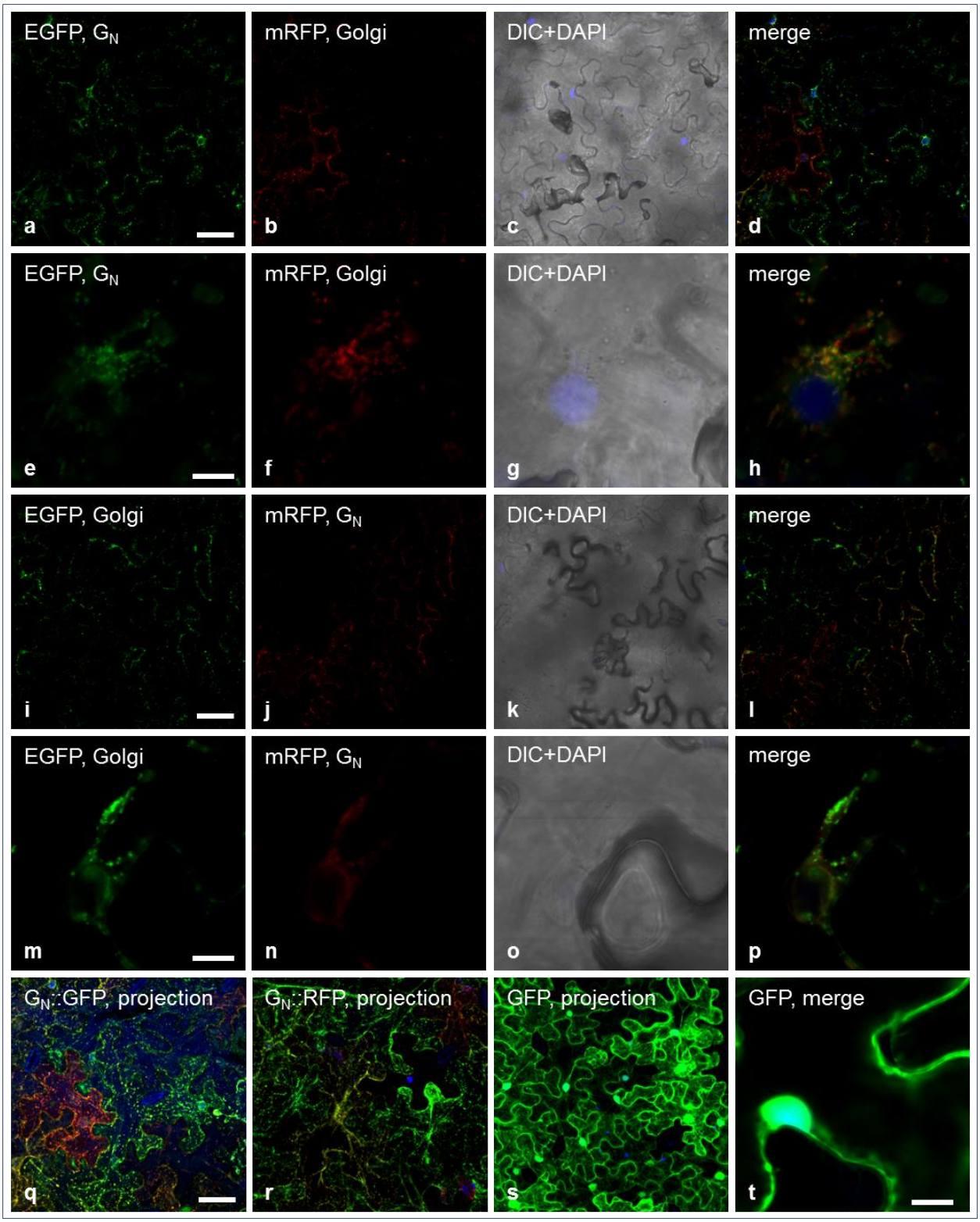

Figure 2.4. Co-localization of G_N and a Golgi marker, both fused to fluorescent proteins (GFP or RFP) transiently expressed in *N. benthamiana* 2 days after agroinfiltration.

G_N::GFP co-localization to a Golgi marker fused to mRFP (a-h) and G_N::RFP co-localization to a Golgi marker fused to EGFP (i-p). Confocal microscopy images (single optical slices) at 280x magnification (a-d and i-l), scale bars = 50µm. Details of the co-localization and signal patterns at 1600x magnification (e-h and m-p), scale bars = 10µm. Green channel images (a, e, i, m); red channel images (b, f, j, n); merged images of bright field (DIC) and blue channel (DAPI, nuclear marker) (c, g, k, o) and merged images of channels green, red and blue (d, h, l, p). Tridimensional reconstruction (optical projection) at 280x of G_N::GFP with Golgi-mRFP (q); G_N::RFP with Golfi-EGFP (r); and GFP (s); images at 280x. Detail of GFP signal pattern (single optical slice, merged image of blue and green channels) at 1600x (t).

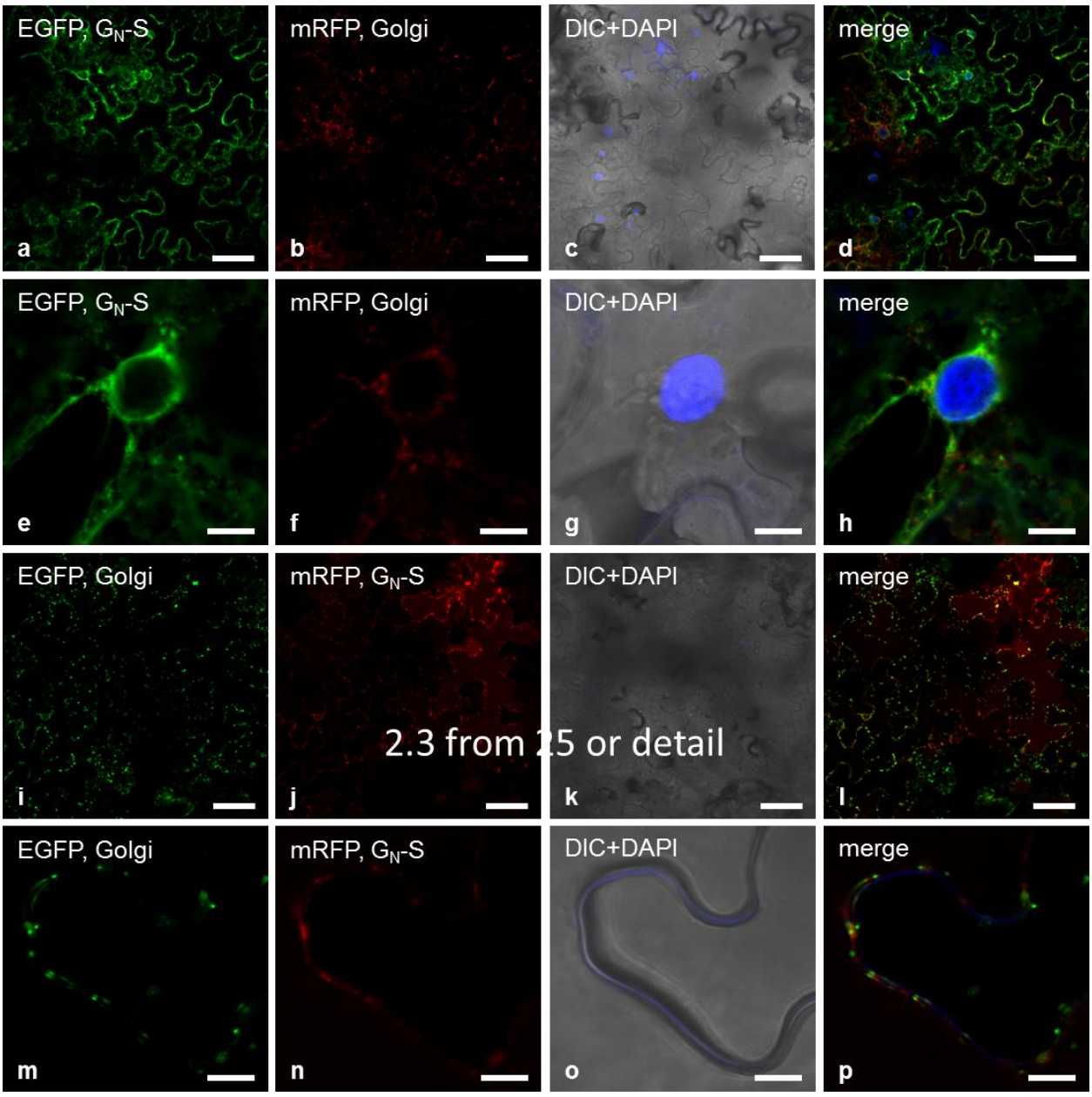

Figure 2.5. Co-localization of G_N-S and a Golgi marker, both fused to fluorescent proteins (GFP or RFP) transiently expressed in *N. benthamiana* 2 days after agroinfiltration. G_N-S::GFP co-localization to a Golgi marker fused to mRFP (a-h) and G_N-S::RFP co-localization to a Golgi marker fused to EGFP (i-p). Confocal microscopy images (single optical slices) at 280x magnification (a-d and i-l), scale bars = 50µm. Details of the co-localization and signal patterns at 1600x magnification (e-h and m-p), scale bars = 10µm. Green channel images (a, e, i, m); red channel images (b, f, j, n); merged images of bright

field (DIC) and blue channel (DAPI, nuclear marker) (c, g, k, o) and merged images of channels green, red and blue (d, h, l, p).

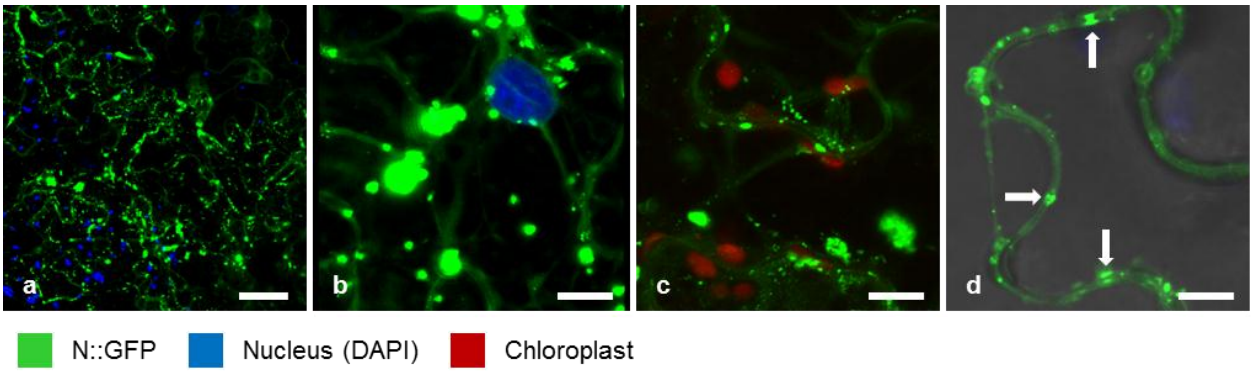

Figure 2.6. N::GFP showed a complex localization pattern two days after agroinfiltration in *Nicotiana benthamiana* leaves.

Confocal microscope projection (280x, scale bar = 50µm) for N::GFP fluorescent signal (a). Magnifications (1600x, scale bar = 10 µm) for N::GFP depicting fluorescent foci of different size and some with perinuclear localization (b); others small foci appeared to be in close proximity to the chloroplast (c); and other small foci appeared associated to the cell membrane or as coupled spots associated with the boundary between two adjacent cells suggesting a possible plasmodesmata localization (white arrows, d). Plant tissue was infiltrated two hours before evaluating with DAPI (4',6-diamidino-2-phenylindole, dihydrochloride) to label the nuclei (blue color). Chloroplasts are shown in red color (autofluorescence of chlorophyll) in c.

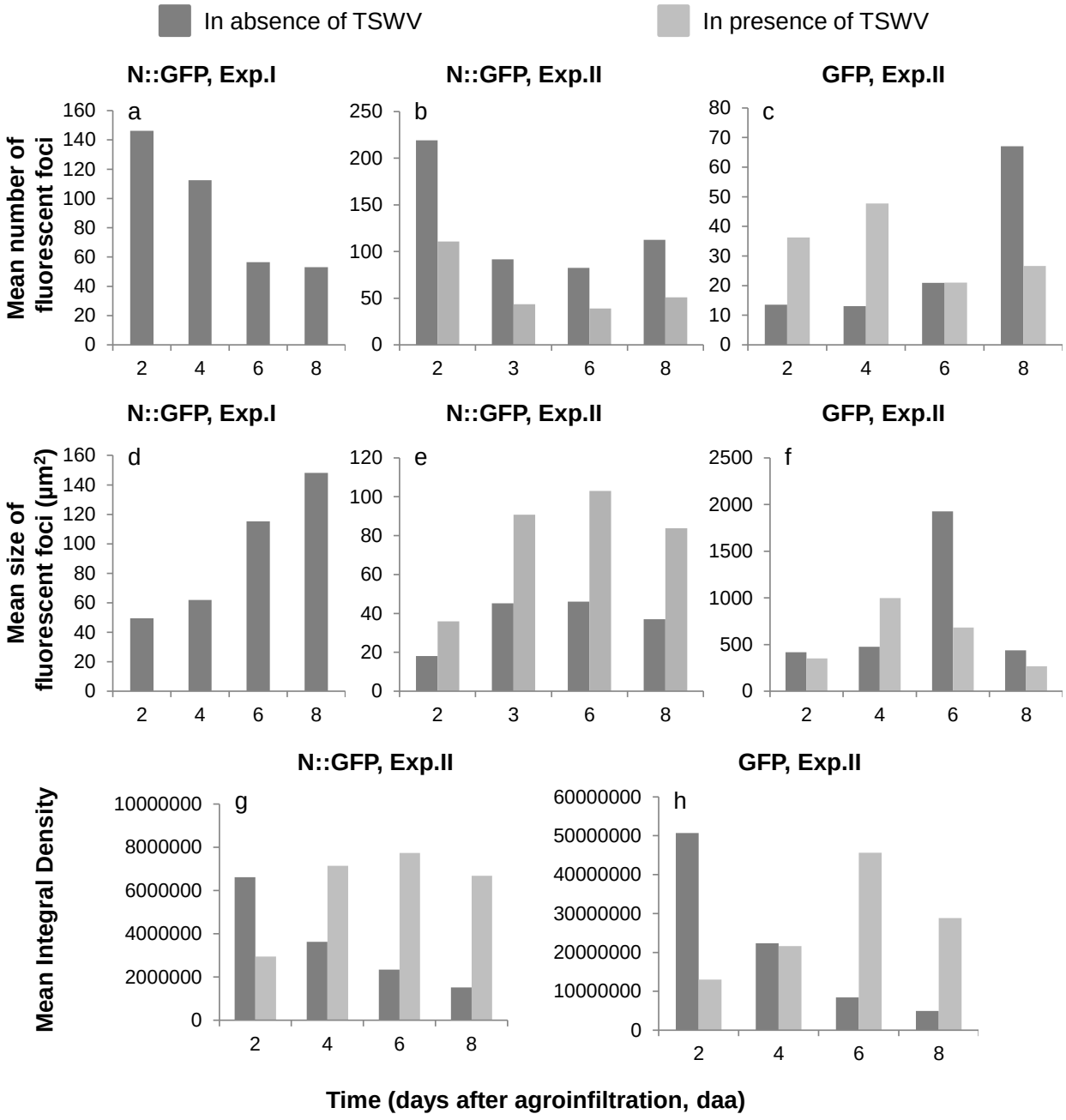

Figure 2.7. Analysis of N::GFP and GFP localization pattern over time (2, 4, 6 and 8 days after agroinfiltration) in absence or presence of TSWV infection when transiently expressed in *N. benthamiana* leaves.

Each bar represents the average value from nine images (samples, n = 9) per treatment per day. Two independent experiments are shown and image analysis was done using the software ImageJ. The localization pattern of N::GFP was described as an aggregation patter characterized by a reduction in the number of fluorescent spots (foci, a-c) and an

increase of size (area) of the remaining spots (d-f). The mean number (counts) of individual fluorescent foci was standardized by fluorescent area fraction to account for differences in the total area displaying a fluorescent signal per image. Graphs (g-h) show the mean integral density (a quantification of fluorescence signal per image, arbitrary units) for N::GFP and GFP.

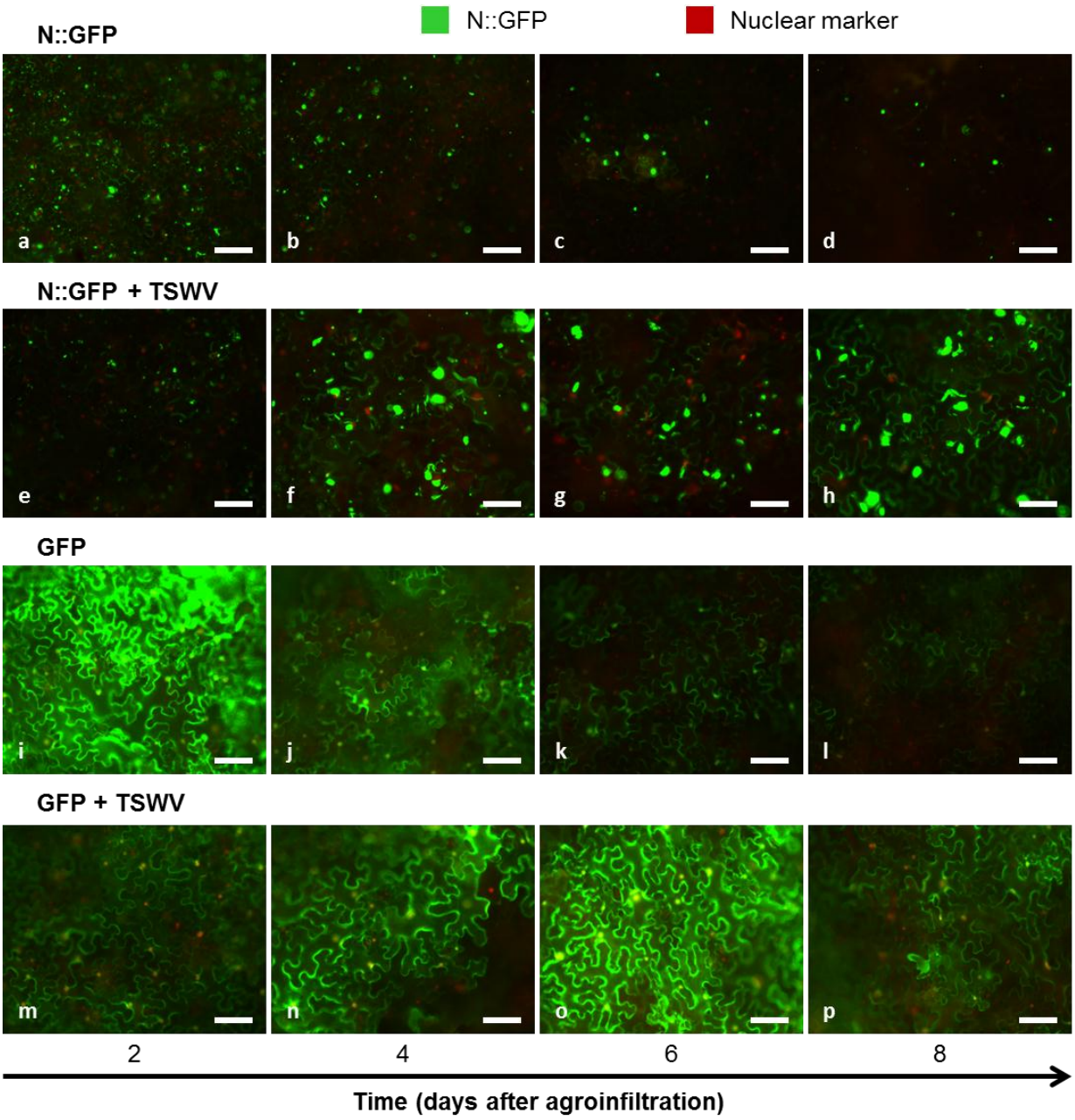

Figure 2.8. N::GFP and GFP transient expression in *N. benthamiana* leavesover time (2, 4, 6 and 8 days after agroinfiltration) in absence and presence of TSWV infection.
Merged images of green and red channels (200x, 250ms exposure time for GFP channel with an epifluorescence microscopy) showing the transient expression of N::GFP and GFP in transgenic *N. benthamiana* leaves (expressing a nuclear marker, NbH2B, fused to RFP). The plants were healthy (virus free) or mechanically inoculated with TSWV 14 days prior to agroinfiltration. Scale bars = 100 µm.

Chapter 3 - Transgenic G_N-S::GFP tomato plants interfere with TSWV acquisition and transmission by *Frankliniella occidentalis*

Abstract

Tomato spotted wilt virus (TSWV) is one of the top ten plant viruses due to the economic losses it causes and together with other tospoviruses is an emerging threat worldwide. TSWV is transmitted by thrips, including the western flower thrips, *Frankliniella occidentalis*. Virus and vector are difficult to control; thrips develop resistance to insecticides and even few thrips may transmit the virus, likewise, TSWV strains are able to overcome the resistant genes deployed commercially. We generated transgenic tomato plants expressing a soluble and GFP-fused form (G_N-S::GFP) of TSWV glycoprotein G_N, the putative virus attachment protein. The transgenic plants had varying amounts of recombinant protein and stable transgenic T3 lines with high levels of protein accumulation were obtained. G_N-S::GFP had a reticulate-like subcellular localization pattern, indicative of the ER. In contrast, G_N::GFP in transgenic plants had a punctate localization, indicative of the Golgi apparatus and the site of virus budding in plant cells. Thrips fed on TSWV-infected transgenic G_N-S::GFP plants showed a significantly lower virus titer 24h after acquisition access period and the resulting adults showed a significant decrease in virus transmission to plant tissue. The results demonstrated that the transgenic plants are interfering with TSWV acquisition and transmission by *F. occidentalis*. Moreover, the results suggested a dose-dependent relationship in virus-vector interaction and highlighted the importance of understanding its molecular determinants. The transgenic G_N-S::GFP plants are a promising new control strategy to include in the integrated management of TSWV and represent new tools to study virus-vector interactions.

Introduction

Tomato spotted wilt virus (TSWV) is one of the top ten plant viruses due to its economic importance (crop damage and the costs resulting from control strategies) and due to its intriguing biology. TSWV is a member of the plant infecting genus *Tospovirus* within the viral family

Bunyaviridae. The virus is distributed worldwide and has a wide host range, infecting hundreds of plant species including important commodities as tomatoes, peppers, lettuce, peanuts, potatoes and many ornamental plants. The losses associated to this virus and other members of the tospoviruses exceed millions of dollars (Goldbach and Peters, 1994; Culbreath et al., 2003; Whitfield et al., 2005b; Pappu et al., 2009; Scholthof et al., 2011; Sevik and Arli-Sokmen, 2012).

Tospoviruses are transmitted by few species of thrips, insects within the order Thysanoptera (Whitfield et al., 2005b); and both viruses and vectors are increasing in importance worldwide. Several thrips species are important as direct plant pests by limiting crop production in fields and greenhouses. Thrips are expanding their geographical range helped, among various factors, by increasing international trade and climate change (Morse and Hoddle, 2006; Reitz, 2009). Tospoviruses are considered emerging diseases because in recent years new species of tospoviruses have being described and tospoviruses species are found infecting new hosts or in geographical areas where they have previously not been reported (Pappu et al., 2009; Seepiban et al., 2011; Mandal et al., 2012; Torres et al., 2012)(Pappu et al., 2009; Seepiban et al., 2011; Mandal et al., 2012; Torres et al., 2012).

The control of TSWV and other tospoviruses relies heavily on control of vector thrips. The management of thrips pests has proved very difficult, and even when reaching levels below an economical threshold for plant damage, few thrips are enough to transmit viruses to plants(Culbreath et al., 2003; Morse and Hoddle, 2006; Reitz, 2009; Mandal et al., 2012). Likewise, chemical control of thrips does not imply a reduction in tospovirus transmission. {{124 Culbreath,A.K. 2003; 90 Mandal,B. 2012; 316 Morse,JG 2006; 317 Reitz,Stuart R. 2009}}. *Frankliniella occidentalis*, is the most efficient TSWV vector and it is an economically important pest in greenhouses and field crops (Reitz, 2009). Populations of *F. occidentalis* have developed high levels of resistance to different insecticides used to control thrips; hence the available insecticides are not efficient to control thrips pests or the tospoviruses they can transmit. New control strategies against thrips and tospoviruses are required; and transgenic plants are recognized as promising options for *Tospovirus* management (Pappu et al., 2009; Mandal et al., 2012).

Natural resistance against TSWV is conferred by the *Sw-5* and *Tsw* genes that are deployed in tomato and pepper plants respectively (Jahn et al., 2000). However, resistance-breaking strains of the virus have been described (Lopez et al., 2011). Additionally, tomato

plants have been transformed previously using TSWV nucleocapsid gene with the objective of obtaining pathogen-derived resistance, where expression of a viral gene in the plant renders a resistance phenotype against the corresponding plant virus. The transgenic tomato plants displayed a range of resistance phenotypes and transgene expression levels (Kim et al., 1994; Ultzen et al., 1995; Gubba et al., 2002; Nervo et al., 2003; Accotto et al., 2005; Accotto et al., 2005; Fedorowicz et al., 2005). However, the high mutation rates of RNA viruses and the possibility of reassortment among tospoviruses (Webster et al., 2011) makes the appearance of virus strains capable of breaking the genetic engineered resistance highly probable. Hence, it is necessary to develop and integrate different strategies to control tospoviruses in order to achieve long term crop protection.

The understanding of the molecular determinants of plant virus–vector interactions has allowed the development of novel ways of virus control by interfering with the acquisition of viruses by their insect vectors: the transmission blocking strategy (Ghosh et al., 2001; Shao et al., 2003; Liu et al., 2010; Sparks et al., 2011). Interfering with the acquisition process renders insects incapable of transmitting the virus or greatly reduces their occurrence and thus, stops the transmission cycle. In the case of TSWV, it was shown that one of the virus glycoproteins, G_N, serves as the attachment protein of the virus (Whitfield et al., 2004). In accordance, a soluble form of G_N produced *in vitro* (G_N-S) was able to interfere with the acquisition and transmission of TSWV by *F. occidentalis* when feed exogenously to thrips prior or simultaneously with TSWV (Whitfield et al., 2004; Whitfield et al., 2008). These results suggest that G_N-S is a good candidate to deploy in transmission blocking strategies against TSWV. Moreover, this approach may be used against other tospoviruses by using the corresponding G_N glycoproteins.

The objective of this work was to generate and characterize transgenic tomato plants expressing a soluble form of TSWV glycoprotein G_N fused to GFP: G_N-S::GFP. We are creating the fusion to GFP in order to ease with the characterization of the plants and tracking the recombinant protein. Transgenic plants carrying G_N-S::GFP will constitute a novel tool to control TSWV spread by means of the transmission blocking strategy. We hypothesize that the recombinant protein (G_N-S::GFP) in the transgenic plants will interfere with TSWV acquisition by thrips; and as a consequence, the transgenic plants will decrease or block the rates of virus transmission by the corresponding adult thrips.

Results

Generation of T0 transgenic tomato plants

Tomato plant tissue (var. Moneymaker) was transformed by means of *Agrobacterium tumefaciens* carrying the plasmids of interest. Putative transgenic plantlets were regenerated *in vitro* under kanamycin selection. A total of 3 and 10 independent putative transgenic plants, for G_N::GFP or G_N-S::GFP respectively, were obtained and transferred to a greenhouse. Two G_N::GFP (66.7%) and six G_N-S::GFP plants (60%) were confirmed as transgenic plants by ELISA test with specific antibodies to detect the recombinant proteins, G_N::GFP or G_N-S::GFP. In the case of G_N::GFP plants, it was very difficult to regenerate the plants *in vitro*; out of more than 300 calli only four plantlets were regenerated and three were successfully grown into viable plants in the greenhouse. Due to the difficulty to obtain plants for G_N::GFP protein, these plantlets were tested for the presence of G_N::GFP or *nptII* transgenes by PCR of genomic DNA. All four plantlets tested positive for the presence of both sequences confirming their transgenic nature.

Segregation of recombinant protein expression phenotype in transgenic plants

Seeds were harvested from the three T0 G_N::GFP plants and from T0 G_N-S::GFP plants confirmed to accumulate the recombinant protein and seeds from selected lines were planted in order to obtain T1 lines. The percentage of seed germination varied among the different transgenic lines. The segregation of the transgenic phenotype (presence of recombinant protein) was evaluated by ELISA with antibodies against G_N and/or GFP proteins. T1 plants with detectable amounts of G_N::GFP were detected from plants T0 G_N::GFP#1 and #2. No T1 plants from T0 G_N::GFP#6 tested positive for the recombinant protein (Table 3.1).

For all five T0 G_N-S::GFP events for which seeds were planted; more than 50% of the T1 seedlings tested positive for the recombinant protein (Table 3.2). Additionally, a commercial DAS-ELISA that detects the protein product of the *nptII* gene (kanamycin resistance marker) was used to evaluate T1 and T2 G_N-S::GFP plants. The transgenic nature of the plants was confirmed by the presence of the selection marker. In most cases, the number of plants

determined to be producing the neomycin phosphotransferase II enzyme are relatively in accordance to the numbers of plants accumulating G_N-S::GFP protein (Table 3.2 and 3.3).

Analysis of T2 progenies from relatively high expressing T1 G_N-S::GFP lines suggested that the transgenic phenotype (presence of recombinant protein) is not segregating for these plants (Table 3.3). Six of these T2 lines were selected to obtain the T3 generation. In accordance with the T2 results, all the progeny from each line was positive for the presence of recombinant protein (Table 3.4). In summary, these results indicate that those T3 transgenic plants are stable transgenic lines for the expression of G_N-S::GFP.

Vegetative appearance and performance of the transgenic plants

The transgenic tomato plants showed similar growth and appearance than non-transgenic plants growing under similar conditions (Fig. 3.1 and 3.2). The only vegetative characteristic that we noticed to be different between transgenic and non-transgenic plants was seed germination; transgenic plants showed consistently lower germination rates in comparison to non-transgenic seeds (Fisher exact test for total number of germinated transgenic vs. non-transgenic seeds, $P < 0.0001$; Tables 3.1 to 3.4 and Fig.3.3). Moreover, the seedlings look initially smaller and/or weaker than the non-transgenic counterparts (Fig.3.2a to e), but after few weeks the plants showed similar growth and vigor than non-transgenic controls (Fig.3.2g to j). Overall, plant morphology and performance was similar for G_N::GFP and G_N-S::GFP plants in comparison to non-transgenic plants. The only morphological alteration was observed in plant T0 G_N::GFP#2, which presented enation-like patterns in few veins of each leaf (Fig.3.1). However, the progeny plants (T1s) from G_N::GFP#2 had no apparent morphological alterations. Moreover, the tomato fruit for the different T0 G_N::GFP plants have similar appearance (Fig.3.1).

Varying amounts of recombinant protein occurred among the different transgenic lines and generations

The relative amount of recombinant protein accumulating in different transgenic lines was indirectly determined by quantifying the amount of GFP protein on those plants. Because the GFP and G_N-S sequences are fused, it is expected that there is a 1:1 molar ratio between G_N

or G_N-S and GFP molecules. Therefore, the amount of GFP protein detected in each plant (500 mg of tissue) by a quantitative DAS-ELISA with a GFP standard curve was used to calculate (see materials and methods) the amount of G_N::GFP or G_N-S::GFP.

The amount of recombinant protein accumulating in the transgenic tissue varies greatly among the different tomato lines. The transgenic G_N::GFP T0 and T1 plants presented a range between 2.6 to 741.5 nanograms of G_N::GFP per milligram of total soluble protein in the sample (Fig. 3.4); and the transgenic G_N-S::GFP T1, T2 and T3 plants have quantities ranging from 1.1 to 4718.1 ng of G_N-S::GFP/mg of total soluble protein (Fig. 3.5). An overall increase in the quantity of G_N-S::GFP protein in plants was observed for the T3 generation in comparison to T2 and T1 generations ($P < 0.05$).

Detection of the recombinant protein by western blot

The presence of recombinant protein and its identity was confirmed by western blot analysis using specific antibodies against G_N and GFP protein with total soluble protein extracts from selected T0, T1, T2 and T3 lines (Fig. 3.6 and 3.7). A band of the expected size for G_N::GFP, approximately 84 kDa, was detected for transgenic plant T1 G_N::GFP#1.13 with antibodies against GFP and G_N (Fig. 3.6). A higher molecular band, around 250 kDa, was observed for this same plant with both antibodies and it was interpreted as oligomers of the recombinant protein. Using the antibody against GFP, a smear was observed for T0 G_N::GFP#2 around the expected band size and a band of higher molecular weight, above 100 kDa was observed for T1 G_N::GFP#1.10 (Fig. 3.6).

Bands corresponding to G_N-S::GFP, approximately 63 kDa, were detected in several transgenic lines and generations (T0 to T3) by western blot (Fig. 3.7). The relative intensity of the bands varied among samples suggesting varying levels of recombinant protein content among different transgenic lines and generations. Moreover, almost no band was detectable for a T2 sample (G_N-S::GFP#9.10.11) suggesting that at the time of sampling for protein extraction this plant may have silenced expression of the recombinant protein. Plant G_N-S::GFP#9.10.11 was estimated to have 1993 ng of recombinant protein per milligram of total protein, in comparison to the other T2 plant included in the western blot (G_N-S::GFP#9.207.7) that contained 838 ng/mg of total soluble protein. In support of this possible explanation to the discrepancy in band

detection and intensity, the progenitor plant for G_N-S::GFP#9.10.11, plant G_N-S::GFP#9.10 was initially detected as a plant with high contents of recombinant protein but after circa three months in the greenhouse, no recombinant protein was detectable in this plant.

Using antibodies against GFP two bands were observed in most cases, one corresponding to G_N-S::GFP (ca. 63 kDa) and another one for GFP alone (ca. 23 kDa). Meanwhile, using antibodies against G_N (peptide polyclonal rabbit antibody) the corresponding band to G_N-S::GFP was observed and also a much higher molecular weight band, that may represent oligomers of the recombinant protein. Dimerization was previously observed for a G_N-S protein produced *in vitro* (Sf9 cells) and it was suggested that the domains involved in dimerization are found in the ectodomain of G_N glycoprotein (Whitfield et al., 2004).

In the TSWV positive control sample and in several of the transgenic samples a double band was observed, suggesting that the wild type G_N and also, the recombinant G_N-S::GFP protein, occurred as two different forms *in planta*. These two different forms may represent different levels of glycosylation as was suggested by Naidu *et al*. (2004) who reported two molecular sizes for G_N, a 58 and a 53 kDa protein sizes. The 58 kDa size protein did not react with the specific anti-G_N monoclonal antibody used in that research (Naidu et al., 2004). In contrast, the two bands observed in this research reacted with a peptide polyclonal rabbit anti-G_N antibody. In the control TSWV-infected plant both bands appear relatively of the same intensity; however, in the tomato transgenic plants, the higher molecular weight band seems much more abundant either tested with anti-GFP or anti-G_N antibodies (Fig. 3.7).

G_N-S::GFP fluorescent signal shows a reticulate subcellular localization pattern in transgenic tomato plants

Leaf tissue from several transgenic lines was evaluated by confocal fluorescent microscopy in order to visualize the fluorescent signal of the recombinant proteins, G_N::GFP and G_N-S::GFP. In the case of G_N::GFP a punctate pattern was observed for the fluorescent signal (Fig. 3.8) in accordance with Golgi subcellular localization of the glycoprotein in plants (Ribeiro et al., 2008). Conversely, G_N-S::GFP signal had a reticulate pattern throughout the cell. Moreover, the fluorescent signal highlights the boundary of the cell, as a dashed line, and a ring of fluorescence is observed inside many cells (Fig. 3.9 and 3.10). The size, localization, general

appearance and comparison with cellular markers (Fig. 3.10, s and t), suggests that this ring is the nuclear envelope. Overall, the fluorescence pattern observed for G_N-S::GFP suggests a localization within the endoplasmic reticulum (ER) of cells. The wild type form of G_N during its translation and glycosylation goes through the ER. Moreover, at early stages of expression G_N localized within the ER in studies done in mammalian cultured cells (baby hamster kidney cells, BHK21) or in plant protoplasts (*Nicotiana tabacum*) (Kikkert et al., 2001; Ribeiro et al., 2008). Therefore, it is possible that a form of G_N, G_N-S, without the transmembrane domain which contains the signal for Golgi localization is retained at the ER.

The intensity of the fluorescent signal varied among transgenic plants in accordance with the GFP quantification data that suggests different amounts of recombinant protein accumulating among plants. In several plants the fluorescence signal was more intense in the guard cells of stomata, and in some of the plants the fluorescent signal seems to be restricted only to the stomata (Fig. 3.10).

Reaction of G_N-S::GFP transgenic plants to TSWV inoculation and detection of recombinant protein in TSWV-infected plants

As requisite to use G_N-S::GFP transgenic plants as a transmission blocking strategy, the recombinant protein must be present during viral infection of the plant, so that when thrips feed on the plant there will be competition between G_N-S protein and virus particles for the receptors in the thrips gut. Alternatively, we hypothesize that presence of the transgene in the plants may trigger resistance mediated by RNAi that will target for degradation the G_N-S::GFP mRNAs and viral M and subgenomic M segments alike. In order to evaluate the reaction of G_N-S::GFP transgenic plants to virus infection and the detection of G_N-S::GFP protein in those plants after virus infection, transgenic T1 and T2 plants were challenged with TSWV. Overall, no resistance to TSWV was detected in the transgenic plants at the level of detection of TSWV nucleocapsid protein by ELISA and G_N-S::GFP protein is apparently stably expressed in the presence of the virus in those plants.

A total of 75 plants (18 T1 and 57 T2) that had previously tested positive for the presence of G_N-S::GFP were mechanically inoculated with TSWV. Plants were evaluated by ELISA methods for TSWV infection and presence of recombinant protein 15 days after inoculation. For

each plant a sample was taken from the old leaves (second true leaf after the cotyledons mechanically inoculated with TSWV, local infection) and a second sample was taken from the second newest leaf (systemic infection). Seventy three plants (97.3%) were positive for TSWV infection (either in local and/or systemic tissue) and 61 plants (81.3%) had detectable amounts of G_N-S::GFP, suggesting that recombinant protein is still produced after virus infection. Viral symptoms were observed in all 73 plants and were comparable to the symptoms displayed by non-transgenic plants inoculated with virus.

The only two plants that were TSWV negative (2.7%) in both local and systemic tissue were positive for G_N-S::GFP presence in both old and new leafs (plants T2 G_N-S::GFP#9.207.6 and #9.10.10). Therefore, the detection of recombinant protein indirectly suggests that no RNAi mechanism triggered by the transgene is responsible for the non-detection of TSWV in those two plants. Forty non-transgenic plants were inoculated as controls of TSWV infection, because we have noticed a varying proportion of tomato plants escape virus infection after mechanical inoculation and this provides data on the efficiency of inoculation. One non-transgenic plant (2.5%) tested negative for TSWV in both old and young tissue. The frequency of negative plants in the non-transgenic plants is similar to the frequency in the transgenic plants ($P = 1.0$), suggesting that those plants may be random escapes to TSWV.

To further test if the presence of TSWV affects the expression of G_N-S::GFP in the transgenic plants, we analyzed the association (co-occurrence) between detection of the virus and recombinant protein in the same leaf tissue per plant. We hypothesized that a high frequency of samples negative for virus and G_N-S::GFP and conversely, a low frequency of samples positive for both will indicate that infection with TSWV triggers an RNAi mechanism causing resistance to TSWV and silencing G_N-S::GFP expression. TSWV inoculated leaf tissue (old leaf) was analyzed independently from systemic leaf (new leaf) because (i) in old tissue G_N-S::GFP protein that accumulated before virus infection may be detected even when its expression was silenced after virus infection and likewise TSWV may have been able to accumulate before the resistance mechanism becomes active. (ii) Second, it is expected that the systemic silencing signal will prime the new tissue to degrade G_N-like sequences prior to virus arrival (recovery phenotype) silencing G_N-S::GFP at early stages of tissue development and rendering resistance to the virus even when the older mechanically inoculated leaf has detectable amounts of virus (recovery phenotype) (Lindbo et al., 1993). Contingency tables were constructed and analyzed by Fisher

exact statistic to compare the pattern of TSWV and G_N-S::GFP detection in the same leaf sample per plant. The analysis was done for old (Table 3.5) and new tissue (Table 3.6) separately. The number of plants recorded for each category is not different (P = 0.3 and 1.0 for old or new tissue respectively) to the frequency expected randomly. The results suggest that TSWV presence is not affecting the expression of GN-S::GFP because a high frequency of samples were positive for both indicating that virus and recombinant protein may occur simultaneously in the same leaf tissue 15 days after TSWV inoculation without any apparent effect on virus accumulation or G_N-S::GFP expression.

In accordance with the former rationale, the pattern of detection (presence "+" or absence "-") of TSWV in old and new leaf tissue was compared between the transgenic plants and non-transgenic inoculated plants (n = 40) (Table 3.7). There is no statistical difference (P = 1.0) between TSWV pattern of detection in old and corresponding new leafs from each plant between transgenic and non-transgenic plants further suggesting that the virus infection is similar between these two groups of plants. Likewise, the pattern of G_N-S::GFP detection in old and new leafs between transgenic plants infected and non-infected (n = 19) with TSWV was compared (Table 3.8). Throughout this work we have noticed that the recombinant protein is no longer detectable in the new tissue of some plants after certain variable period of time; meanwhile for other plants we detected protein after more than a year of age of the plant (the tomato variety we are using is of indeterminate growth). No difference (P = 0.3) in the pattern of expression of G_N-S::GFP in old and new leaf tissue was detected between inoculated or non-inoculated transgenic plants, suggesting that in the cases were the recombinant protein was no longer detected either on old or new leaf tissue or both was not a consequence of virus infection.

To verify the presence of G_N-S::GFP protein in the TSWV infected plants, eight plants that were randomly selected from the ones testing positive for both TSWV and G_N-S::GFP were observed at the confocal microscope. The fluorescence signal pattern in the tissue was not different from the one observed for TSWV non-infected transgenic plants; indicating that TSWV infection and the presence of the native viral proteins did not alter G_N-S::GFP localization. Fluorescent signal was observed throughout the leaf abaxial epidermis or detectable only at the guard cells of stomata as noticed before for non-inoculated plants. In all cases, the subcellular localization pattern appears to be the endoplasmic reticulum of the cell (Fig. 3.11).

Transgenic G_N-S::GFP tomato plants interfere with TSWV acquisition by F. occidentalis

TSWV acquisition assays on TSWV-infected transgenic plants were conducted with the objective of testing the hypothesis that G_N-S::GFP expression *in planta* will interfere with virus acquisition by thrips. The results obtained supported this hypothesis because thrips fed on TSWV-infected transgenic G_N-S::GFP tomato plants had a lower virus titer than thrips fed on TSWV-infected non-transgenic plants ($P < 0.0001$, Fig. 3.12). TSWV-infected tissue confirmed to express the recombinant protein 15 days after virus infection and non-transgenic, TSWV-infected plants (see previous section) were used as virus sources to feed 0-18 hours old first instar (L1) *F. occidentalis*. The L1 thrips were exposed to an acquisition access period (AAP) of 24h on tomato leaflets in water agar plates (three replicates for each treatment: transgenic and non-transgenic) and then moved to green beans for another 24h to allow for virus replication in the insect body. A pooled sample of 15 thrips was picked from each replicate thrips cohort and tested by DAS-ELISA for the presence of TSWV N protein. The ELISA absorbance values for thrips fed on transgenic tissue were always lower than those of the corresponding non-transgenic tissue in each experiment. ELISA test of the leaf tissue on which the thrips fed conducted after the AAP showed that the different leaflets have similar relative virus titers suggesting that the differences in virus titer in the thrips are not due to differences in the amount of virus in the tissue (Fig. 3.13).

Lower TSWV titers detected in thrips after feeding on transgenic TSWV plants suggest that virus infection is also occurring in these groups of thrips but that the degree of infection is lower in comparison to thrips fed on non-transgenic, TSWV-infected plants. A total of 12 replicates (independent acquisition events, AAP) were done per treatment (3 per experiment, 4 independent experiments) and in four out of the 12 replicates for transgenic plant, the thrips sample was determined as positive for TSWV in comparison with 12 replicates for non-transgenic plant that were positive. The remaining samples for transgenic plants were not determined as positive by the ELISA criterion but higher absorbance values were observed than in the buffer and non-exposed thrips controls. These results suggested that the thrips feed on transgenic plant tissue acquired TSWV although at lower levels. The lower titer observed for a sample consisting of 15 pooled thrips may indicate (i) a lower percentage of thrips infected with the virus in the cohort, (ii) a lower level of infection in the individual infected thrips or (iii) a

combination of these two variables. Independently of the factors contributing to the lower overall virus titer observed, the results suggest that the transgenic plants are interfering with the acquisition of TSWV by *F. occidentalis*.

Normalized abundance of TSWV-N RNA in thrips fed on TSWV-infected transgenic tissue is significantly lower than in thrips fed on non-transgenic plants 24h after AAP

In order to confirm the results obtained by ELISA for virus titer in groups of thrips (n = 15) real-time quantitative reverse transcriptase-PCR (qRT-PCR) was used to analyze four individual thrips randomly selected (out of 10 sampled 24h after AAP) per repetition for a total of 24 individuals per experiment. Thrips were analyzed this way for three out of the four experiments described herein. The results supported that TSWV titer in thrips exposed to TSWV-infected transgenic plants is significantly lower ($P \leq 0.0002$) than in thrips exposed to non-transgenic plants (Fig. 3.14); and therefore, that the transgenic plant interfered with the infection of thrips by TSWV. However, looking into our goal, to decrease virus transmission, we need to test if the lower virus titers in thrips fed on transgenic plants correspond to lower percentage of TSWV transmission. Therefore, transmission assays were set using thrips from the three experiments analyzed by qRT-PCR.

F. occidentalis cohorts show reduced transmission of TSWV when acquired from transgenic G_N-S::GFP tomato plants

A significant lower number of adult *F. occidentalis* individuals transmitted TSWV to leaf discs after an IAP of 48h when they had fed for virus acquisition on TSWV-infected transgenic tomato tissue in comparison to thrips that acquired the virus from non-transgenic plants (Table 3.9 and Fig. 3.15). The difference in transmission were observed in all replicates (total 24, 12 for transgenic and 12 for non-transgenic) from three independent assays. Overall, transmission rates higher than 60% were recorded for thrips fed on non-transgenic plants; meanwhile, transmission ranged from 0 to 50% when thrips fed on transgenic tissue. These results show that the lower virus titers detected 24h after acquisition in thrips feed on TSWV-infected plants correspond to lower number of individuals capable of transmitting the virus as adults.

Discussion

Tomato transgenic plants expressing TSWV G_N glycoprotein or a soluble form (G_N-S) were generated. TSWV G_N glycoprotein localizes to the Golgi, the site of TSWV particle budding (Kikkert et al., 1999; Kikkert et al., 2001; Ribeiro et al., 2008). In accordance, G_N::GFP protein in plants had a punctate localization pattern suggestive of Golgi localization. G_N-S::GFP plants showed a fluorescent signal different from the G_N::GFP plants. G_N-S::GFP displayed a reticulate-like pattern indicative of ER localization. Additionally, a defined ring of fluorescence was observed in many cells, and it apparently corresponds to the lumen of the nuclear envelop that is continues with the ER lumen. G_N glycoprotein during initial stages of its expression localized at the ER in plant protoplasts (Ribeiro et al., 2008), suggesting that without the transmembrane domain and cytoplasmic tail, it is retained at the ER.

ELISA, western blot and quantification data showed that varying amounts of recombinant protein are produced among different transgenic lines. Amounts of G_N-S::GFP protein ranged from 0.47% of the total soluble protein in the plant to less than 0.001% in leaf tissue samples. As a reference, the expression of Dengue virus E glycoprotein domain III in tobacco plants rendered amounts between 0.13 and 0.25% of total soluble protein in the transgenic leaf tissue (Kim et al., 2009). The results on T0 and T1 generations for G_N::GFP and T0 to T3 generations for G_N-S::GFP suggested that by repeated cycles of selecting high expressing plants and obtaining their progeny, plants with high levels of recombinant protein can be obtained. In these research the T3 generation of G_N-S::GFP plants displayed a significant increase in the amount of protein detected in the leaf tissue.

Contrary to what may be expected; challenging the plants with TSWV apparently did not trigger a transgene silencing phenotype nor, as a consequence, resistance to the virus. In most of the plants inoculated with TSWV, both the virus and the recombinant protein were detected 15 days after mechanical inoculation. The plants show varying severity of symptoms including stunting, leaf deformation, yellowing patterns and necrotic lesions, similar to the ones observed in the non-transgenic plants. In reference to a control strategy dependent on the presence of the recombinant protein in the plant, the stability of the protein expression is a positive characteristic. Also, no apparent change in the subcellular localization of the recombinant protein

was observed in presence of the virus. Overall, it appears that TSWV infection on the transgenic plants did not affect the expression nor the behavior of G_N-S::GFP protein.

Thrips feed on TSWV-infected G_N-S::GFP transgenic plants showed lower virus titer 24h after the acquisition access period (as determined by ELISA and confirmed by qRT-PCR of individual thrips) in comparison with thrips exposed to non-transgenic plants, and as a consequence a reduction in TSWV transmission by adults. The results show a similar trend but a higher impact on transmission than the ones observed for the rice brown planthopper (*Nilaparvata lugens*) and *Rice ragged stunt oryzavirus* (Reoviridae), when the vector was fed prior to virus acquisition in transgenic or non-transgenic rice plants expressing spike protein (S9) of the virus (Shao et al., 2003). The level of blockage in TSWV transmission reached per repetition within an experiment ranged between 37.5% and 100% (zero transmission) reduction in the number of thrips transmitting the virus to leaf discs in a 48h IAP. These results are very promising and suggest that G_N-S::GFP transgenic plants may have an impact in TSWV spread in a crop.

The results on TSWV acquisition and subsequent transmission by *F. occidentalis* suggest a dose-dependent relationship in the virus-vector interaction as was previously proposed by Rotenberg *et al*. (2009). Albeit few reports study the quantitative aspects of plant virus acquisition and transmission, the data supports a quantitative parameter involved in the phenomenon for circulative plant viruses (Vandenheuvel et al., 1991; Ng et al., 2004). In our system, it appears that the number of virus particles that start the infection makes a difference in terms of later virus transmission by the individual thrips. We hypothesize that the initial infection of the midgut requires reaching certain titer threshold in order to spread and potentially reach the salivary glands during a specific time/development window. The virus-vector interaction at the dose level and the host cellular response to virus replication in this system have just started to be characterized (Rotenberg et al., 2009; Rotenberg and Whitfield, 2010). Further research is required in order to understand the interplay between TSWV and thrips host cell responses to it, and how these interactions will define vector competence of thrips as has been suggested for mosquito vectors of animal-infecting viruses (Keene et al., 2004; Sanders et al., 2005; Sanchez-Vargas et al., 2009; Khoo et al., 2010). A balance may be reached between the virus replication cycle and thrips defense pathways which may vary depending on the level of initial infection.

The results herein are the concept proof that G_N glycoprotein of the virus can be exploited to interfere with virus acquisition and transmission of TSWV by *F. occidentalis*. Besides, these results further pinpoint G_N as an important determinant of the virus-vector interaction (Whitfield et al., 2004; Sin et al., 2005). The transgenic plants or modified versions of them without the fusion to GFP or with a tissue specific promoter to drive expression of the transgene may be planted as borders or interspaced in fields to interfere with the virus transmission cycle. It is important to emphasize that G_N-S::GFP transgenic plants are not a unique solution to control TSWV infection in fields and greenhouses but rather a new and promising option to include in integrated management schemes to render a sustainable and long term control of TSWV epidemics. Future research resulting from our findings includes the need to study the effect of the transgenic plants in the transmission of other tospoviruses in tomatoes and/or transmission of TSWV by other thrips species. Moreover, any other crop species or ornamental plants may also be transformed following this approach.

We showed that transgenic tomato plants expressing a recombinant form of the ectodomain of TSWV glycoprotein, G_N-S::GFP, are interfering with TSWV acquisition and transmission by western flower trips. The results contribute to the hypothesis that G_N is the attachment protein of the virus (Whitfield et al., 2004). Additionally, these transgenic plants are tools for further studying the virus-vector interaction and transmission specificity between virus and vector species. Overall the results herein exemplify how the understanding of the molecular aspects of plant virus-vector interactions allow to exploit the elements of the system to develop novel and ecological sound approaches to control the spread of plant viruses. Moreover, this understanding and application can be broadened and adjusted for the control of other plant viruses and contribute to understanding and control of animal and human infecting counterparts: other arthropod-vectored bunyaviruses.

Materials and Methods

Construction of expression vectors

Two expression vectors were constructed for the expression of two forms of TSWV glycoprotein G_N. One corresponds to the complete predicted ORF (Whitfield *et al*. 2004) of G_N

(wild type form); and another, G_N soluble (G_N-S), includes only the predicted ectodomain of the glycoprotein, excluding the transmembrane and cytoplasmic domains. In both constructs, a fusion to green fluorescent protein (GFP) was done. The sequence corresponding to TSWV glycoprotein G_N was amplified from plasmid pGF7 (Adkins *et al*. 1996). The sequence fragments for both forms of the glycoprotein were amplify using the primer pairs: forward primer G_N General Wt/S nt1-31 F (5'-CACCATGAGAATTCTAAAACTACTAGAACTAGTCG-3') and reverse primer G_N-Wt (-A) fusion nt 1356-1386 R (5'-CATAGACATGGGCATTTGAGACAAAATGATC-3') for G_N; and forward primer G_N General Wt/S nt1-31 F and reverse primer G_N-S fusion nt895-930 R (5'-AATGCTTTTTGAATATTTGATTATGCAATCTCTAAC-3') for G_N-S.

The expression clones were constructed using the Gateway® cloning technology (Invitrogen). Entry clones were generated by cloning gel purified PCR amplicons of the sequences of interest into pENTR/D-TOPO vector. The entry clones were recombined with the expression vector pSITE-2NB (Chakrabarty *et al*. 2007) to generate plant expression vectors for G_N and G_N-S with C-terminal fusions to EGFP (enhanced GFP): G_N::GFP and G_N-S::GFP.

Tomato transformation

Tomato (*Solanum lycopersicum*) transgenic plants were generated by the laboratory of Dr. Sunghun Park, Horticulture, Forestry and Recreation Resources Department, Kansas State University following standard protocols (Park et al., 2003). The genetic background for the transgenic plants was tomato var. Moneymaker, and the plant tissue was transformed using lines of *Agrobacterium tumefaciens* (strain LBA4404) carrying the expression clones described previously. Tomato plantlets obtained after transformation and *in vitro* culture were kept in a greenhouse, temperature 25°C day and 23°C, light cycle 16 hours light and 8 hours dark. Tomato fruits were periodically harvested from the plants and store at 4°C until processing for seed extraction. To confirm the transgenic nature of G_N::GFP plantlets, genomic DNA was extracted (DNeasy Plant Mini Kit, Qiagen, Valencia, CA, USA) and PCR reactions were set using the specific primer pairs G_N Front F (5'-GATAATTCGTGGAGACCA-3') and G_N Front R (5'-CAAGCAGTTGTTAGGGAG-3'); and NPT F (5'-GAGGCTATTCGGCTATGACTG-3') and NPT R (5'-ATCGGGAGCGGCGATACCGTA-3') to detect G_N::GFP and NPTII nucleotide

sequences, respectively. PCR reactions (GoTaq Flexi DNA Polymerase kit, Promega, Madison, WI, USA) were carried out in a final volume of 50 µl (1x reaction buffer, 1.25 units of GoTaq polymerase, 2.5 mM $MgCl_2$, 200 µM dNTPs mix, and 600 nM each primer) with 3 µl of template DNA. The thermocycler conditions were for G_N::GFP detection: 1x 95 °C for 2 min; 30 x (95 °C for 30 sec; 50 °C for 40 sec, and 72 °C for 30 sec); 1x 72 °C for 5 min; and for NPTII detection: 1x 95 °C for 2 min; 30 x (95 °C for 30 sec; 55 °C for 40 sec, and 72 °C for 1 min); 1x 72 °C for 5 min.

ELISA screening of transgenic plants

Enzyme linked immunosorbent assay (ELISA) was used to test transgenic plants for the presence of G_N::GFP and neomycin phosphotransferase II enzyme (NPTII). Presence of NPTII was assayed by a double antibody sandwich (DAS)-ELISA, using a commercial detection kit (Agdia Inc., Elkhart, IN, USA) following the manufacturer recommendations.

The presence of G_N protein fusions to GFP (wild type or soluble form) was tested by triple antibody sandwich (TAS)-ELISAs using either; (i) goat and rabbit peptide polyclonal antibodies generated against the ectodomain of G_N protein (GeneScript USA Inc., Piscataway, NJ, USA) or (ii) goat peptide polyclonal antibodies against G_N in combination with a rabbit polyclonal antibody against GFP (Invitrogen, Carlsbad, CA, USA). The peptide polyclonal antibodies recognize both, G_N and G_N-S forms of the glycoprotein. Details for each TAS-ELISA are given below under the corresponding subtitles.

Samples were prepared similarly for the different ELISAs being performed. A leaf disc (diameter ca. 13 mm) was cut off from the apical leaflet of the youngest completely developed leaf (leaf node number three) of each tomato plant (three weeks old) to be tested. The leaf disc was ground in 1 ml of the appropriate sample buffer. Samples for anti-G_N or anti-G_N/GFP ELISAs were extracted in general extraction buffer (GEB consisting of PBST [0.137 M NaCl, 10 mM Na_2HPO_4, 1.8 mM KH_2PO_4, 2.7 mM KCl, and 0.05% Tween-20, pH 7.4] supplemented with 10mM Na_2SO_3, 2% PVP [MW 40000], 0.2% powdered egg albumin [grade II], and 2% Tween-20, pH 7.4). Samples for NPTII ELISA were ground in the extraction buffer provided by the manufacturer (Agdia Inc.). All buffers, if not supplied by the company, were prepared

following Agdia Inc. standard protocols. A working volume of 100 µl per well was used for the different steps and ELISA tests.

In the case of NPTII ELISA, the cut off value to declare a sample positive corresponds to two times the mean of negative controls. For the ELISA tests to detect G_N fusions, either G_N or G_N/GFP mixture of antibodies, I used a cut off value corresponding to the mean of negative controls plus three times the standard deviation of the negative samples (Sutula et al., 1986).

Anti-G_N TAS-ELISA

Overnight coating of microtiter wells was done with 0.4 µg/ml of peptide polyclonal rabbit anti-G_N antibody diluted in carbonate coating buffer (15mM Na_2CO_3, 35mM $NaHCO_3$, pH 9.6). The next day, the ELISA plate was washed four times with PBST and samples were loaded. The ELISA plate was incubated overnight at 4 °C covered with plastic wrap. The following day, the ELISA plate was washed four times with PBST. Secondary antibody, peptide polyclonal goat anti-G_N antibodies #163 and #164, each one at 0.2 µg/ml in ECI buffer (PBST supplemented with 0.2% BSA and 2% PVP (MW 40000), pH 7.4), was incubated for two hours at room temperature and light agitation. The ELISA plate was washed four times with PBST and a rabbit anti-goat antibody conjugated to alkaline phosphatase (Bio-Rad) diluted 1:2000 in ECI buffer was added. The conjugated antibody was incubated at room temperature for one hour and light agitation. The ELISA plate was washed four times with PBST. Enzyme substrate, p-nitrophenyl phosphate dissolved to 1mg/ml in PNP buffer (0.5 mM $MgCl_2$ and 1 M diethanolamine, pH 9.8) was added and incubated for one hour at room temperature protected from light. ELISA plate was read at a wavelength of 405 nm after one hour of reaction.

Anti-G_N/GFP TAS-ELISA

Overnight coating was done with peptide polyclonal goat anti-G_N antibodies, #163 and #164, diluted to 0.4 µg/ml each, in buffer carbonates. The ELISA plate was washed four times with PBST the next day and samples were loaded. Samples were incubated overnight at 4°C wrapped with saran. The following day, the ELISA plate was washed four times with PBST. Secondary antibody was incubated for two hours at room temperature and light agitation. The secondary antibody was polyclonal rabbit anti-GFP (Invitrogen) diluted to 0.8 µg/ml in ECI buffer. The ELISA plate was washed four times with PBST and conjugated antibody added; goat anti-rabbit conjugated to alkaline phosphatase (Invitrogen) diluted 1:2000 in ECI buffer. The

conjugated antibody was incubated at room temperature for two hours and light agitation. The ELISA plate was washed four times with PBST. Enzyme substrate, p-nitrophenyl phosphate dissolved to 1mg/ml in PNP buffer was added and incubated for one hour at room temperature protected from light. ELISA plate was read at a wavelength of 405nm after one hour.

Quantification of recombinant protein in transgenic plants

The amount of recombinant protein (G_N-S::GFP or G_N-Wt::GFP) in selected transgenic plants was estimated using a quantitative GFP ELISA (MaxDiscovery Green Fluorescent Protein ELISA Kit, Bioo Scientific, Austin, TX, USA). Per every molecule of recombinant fusion protein there is one molecule of GFP; therefore, the amount of GFP in the plant tissue is an indirect measurement of the amount of the recombinant protein. Five hundred grams of transgenic leaf tissue was sampled per plant and grinded in 0.5 ml of protein extraction buffer included in the kit. The samples were treated and the ELISA conducted as indicated in the manufacturer protocol. Samples were standardized to 3 mg/ml of total soluble protein.

Control tomato plant was included in every ELISA. The ELISA absorbance value of the control sample was used as a plant background value to subtract from each sample's ELISA absorbance value before estimating the amount of GFP in the sample. Samples (3 mg/ml of total soluble protein) were diluted in the dilution buffer included in the ELISA to different ratios until reaching dilutions that gave absorbance values within the value range of a GFP standard curve included in each ELISA plate. Recombinant protein quantity was estimated using the linear equation of the best fit line to the standard curve.

Total protein in each sample was quantified using Pierce BCA Protein Assay Kit (Thermo Scientific). Samples were diluted 1:25 (10 µl in 240 µl of distilled water) and 70 µl of the diluted sample was combined with 1400 µl of BCA working solution (Solution A and B mixed 50:1 ratio) in 15 ml culture tubes. The reactions were incubated at 37°C with agitation for 30 min and immediately quantify by spectrophotometry at 560nm. A standard curve of bovine serum albumin (BSA) 2, 1, 0.5, 0.25, 0.125, 0.0625 and 0.01 mg/ml was included in each case. The standard curve was prepared from a concentrated 2 mg/ml stock solution and dissolved in 0.9% NaCl. For the standard curve the reference was set using BCA working solution with 70 µl of 0.9% NaCl and for the samples the reference was set using protein extraction buffer diluted

1:25. Protein concentrations were calculated using the linear equation of the best fit line to the standard curve.

The amount of recombinant protein in each sample was calculated using the estimate of GFP protein determined for each plant. The following formulas were used: *grams of G_N::GFP = Grams GFP *81265.07/23283* and *grams of G_N-S::GFP= Grams GFP *63416/23283*. To compare the relative amount of recombinant protein among plants, the amount (in nanograms) of G_N-S::GFP or G_N::GFP were expressed per milligram of total soluble protein in the sample or as a percentage of the total soluble protein.

SDS-Page and western blot

Protein expression was confirmed by separation of total protein extracts by sodium dodecyl sulfate-polyacrylamide gel electrophoresis (SDS-PAGE) and specific detection of the recombinant proteins by antibodies (Western blot). Equal amounts of protein were loaded into 10%-resolving - 5%-stacking polyacrylamide gels and run for 2:15 min at 100V in SDS-PAGE running buffer (25 mM Tris-Base, 250 mM glycine and 0.5% SDS). The identity of the protein bands was assayed by Western blot probing with G_N, N or GFP-specific antibodies. Gels were electrophoretically transfer to nitrocellulose membrane (Hybond-C Extra, Amersham) in transfer buffer (48 mM Tris-Base, 39 mM glycine, 0.0037% SDS, 20% methanol) at 30 mA and 4 °C, overnight (ca. 15 h). Membranes were blocked with phosphate-buffered saline (PBS) supplemented with 0.05% Tween (PBST) and 5% nonfat dry milk (NFDM) for 1 h and then incubated with primary antibodies for 2h. Primary antibodies were polyclonal peptide rabbit anti-G_N, and polyclonal rabbit anti-GFP (Invitrogen), diluted in PBS-NFDM at 1:2000, and 1:2500 respectively. The polyclonal peptide rabbit anti-G_N was costumed made during this work (GenScript) against a 14 amino acid peptide (SQTPGTRQIREEES) from the N-terminus region of G_N, starting at residue 78 from the start methionine of the polyprotein which corresponds to position 42 after the signal peptide sequence is removed. Secondary horseradish peroxidase-conjugated antibodies (Bio-Rad) were diluted 1:5000 and incubated for 1h. Three rinses, each 100µl PBST-5% NFDM for 5min, were done between incubations. Western blots were visualized with ECL Plus Western Blotting Detection System (GE Healthcare, Little Chalfont, BKM, UK) using 2 ml of reagent mix (A and B) per membrane.

Screening transgenic plants for the presence of green fluorescence by fluorescent microscopy

The presence of the GFP fused recombinant proteins in the transgenic leaf tissue (abaxial surface) was evaluated by fluorescence microscopy of leaf sections (0.5 x 0.5 cm) mounted in distilled water. The plant leaf tissue was observed by epifluorescence microscopy (Zeiss Axioplan 2 IE Mot microscope) or by confocal microscopy (Zeiss Axiovert 200M microscope equipped with a Zeiss LSM 510 META system or a LSM 700 Confocal Laser Scanning microscope with Zen Efficient Navigation software).

Seed extraction and decontamination

Tomato fruits coming from the same plant were smashed in a sealed plastic bag by hand pressure until most of the pulp was broken down. The bag was filled with one volume of tap water (a ratio of water to broken tomato 1:1) and was left overnight in the greenhouse for the tomato mixture to ferment. The next morning (ca. 15h fermentation), the plastic bag was opened and the contents were carefully mixed by pressing the bag to allow some oxygen to get into the tomato mixture. The bag was sealed again and periodically checked throughout the day until a large number of seeds had settled at the bottom of the bag. Once this occurred, the contents of the bag were poured into a 2 L beaker and stirred. Seeds were allowed to settle at the bottom for 2 min; afterwards, half of the volume of liquid was decanted slowly and discarded without disturbing the seeds at the bottom. The beaker containing the seeds was filled with tap water and the procedure was repeated until the solution is clear and most of the tomato pulp and debris was clean out without losing the seeds. The beaker with the tomato seeds was filled once more with tap water and the complete volume of liquid was decanted through a sieve to separate the seeds from the rest of the tomato mixture. The seeds were collected from the sieve into a paper towel and left to dry overnight. Dry seeds were stored in paper envelopes with a desiccant pouch (silica gel) at 10°C.

Challenge of G_N-S::GFP transgenic plants with TSWV

Three week old transgenic G_N-S::GFP tomato plants that had tested positive for the presence of the recombinant protein were inoculated with TSWV in order to evaluate the response of the plants to TSWV infection and to evaluate if G_N-S::GFP is detectable in plant tissue after virus infection. Eighteen T1 and 57 T2 plants were mechanically inoculated in two independent experiments. In each experiment, 20 non-transgenic tomato plants were inoculated as controls. Leaf tissue from symptomatic, ELISA-positive tomato plants three weeks after inoculation, was used as virus source. Tomato plants were evaluated for virus presence 15 days after inoculation, apparent negative plants were re-inoculated immediately and re-tested 15 days after the second inoculation.

As a way to indirectly test for a possible recovery or resistance phenotype to virus infection, leaf tissue samples (1.3cm-diameter disc) were collected from inoculated leaf tissue (old leaf) and from new systemic tissue (new leaf) for each plant. The terminal leaflet of the second true leaf (from bottom to top) was used to collect the mechanical inoculated leaf sample or local infection sample; and the terminal leaflet of the second younger leaf (from top to bottom) was collected as the systemic infection sample. Each leaf disc was homogenized in general extraction buffer and aliquots were tested separately for G_N-S::GFP and TSWV N presence by TAS-ELISA (described previously) and by DAS-ELISA (anti-TSWV reagent set, Agdia) protocols respectively. In the case of anti-TSWV DAS-ELISA, samples were considered positive when the absorbance value was higher to three times the mean absorbance value of the negative controls (non-inoculated, healthy tomato plants of the same age as the inoculated ones).

TSWV acquisition test on transgenic tissue

In order to determine the effect of transgenic tomato plants on TSWV acquisition by thrips, four independent experiments were conducted. For each experiment, leaflets (leaf node six from the top of the plant) from TSWV-infected transgenic and non-transgenic plants were placed in 15% agar plates. Three replicates (plates) were done per treatment (transgenic or non-transgenic) per experiment. Plants G_N-S::GFP#9.302 and non-transgenic#113 were used in experiment one, and plants G_N-S::GFP#9.517 and non-transgenic-C were used for the other three experiments. Plants G_N-S::GFP#9.302 and non-transgenic#113 were mechanically inoculated

and plants G_N-S::GFP#9.517 and non-transgenic-C were thrips-inoculated with TSWV and confirmed by ELISA to be positive for TSWV and G_N-S::GFP presence 15 days after inoculation as described previously. First instar larval thrips (L1s) 0-18 hours old were placed into 15% agar plates with the appropriate plant tissue and sealed with parafilm. The plates were kept at an incubator (25°C with a photoperiod of 12h light and 12h dark) for a 24h acquisition access period (AAP). The larval thrips were moved to plastic cups with green beans for another 24h period to allow virus replication inside the thrips and clearing of TSWV-infected plant tissue from the gut lumen. From each cup (replicate), 15 thrips were collected into a 1.5ml microcentrifuge tube and homogenized with a micro pestle (Kontes) in 150 µl of ice-cold GEB. Samples were vigorously vortexed (30sec) and incubated on ice 30min. Control thrips non-exposed to TSWV-infected tissue were also sampled. Thrips cups were placed back into the incubator and fresh green beans add until adult eclosion.

Determination of TSWV acquisition by qRT-PCR

To determine the normalized abundance of TSWV in thrips after an AAP on transgenic and non-transgenic TSWV-infected tissues, four thrips (L1s 42-50h old) were collected per replication 24h after the AAP into individual RNase free 1.7ml microcentrifuge tubes, flash frozen in liquid nitrogen and stored at -80°C. RNA was extracted from individual thrips, real time quantitative reverse transcriptase-PCR was done and TSWV N normalized abundance was calculated as described previously (Rotenberg et al., 2009).

Inoculation access period (IAP)

Adult thrips (24h after eclosion) from each thrips cohorts (experiments 2, 3 and 4) exposed to transgenic and non-transgenic TSWV-infected tissue were individually placed into 15 ml microcentrifuge tubes with a leaf disc (1.5 cm in diameter) of *Datura stramonium* third leaf (top to bottom) from four weeks old plants. Thrips were left for a 48h IAP in an incubator (25°C with a photoperiod of 12h light and 12h dark). Afterwards, leaf discs were floated in water for four additional days to allow virus replication in the leaf tissue. Leaf discs were triturated in 1 ml of GEB and tested for the presence of TSWV by DAS-ELISA with antibodies specific against TSWV (Agdia).

Statistical analyses

Data sets from the different objectives were tested for normality and when found to be not normal distributed comparisons and analyses were done using non-parametric tests with a combination of statistical programs (Graphpad Prism v.5; Minitab v.14; and SAS). Comparisons of two treatments were done by Mann-Whitney test and comparisons of three or more data sets were done with Kruskal-Wallis test followed by Dunn's multiple comparison for pairwise comparisons of means. Contingency tables were analyzed by Fisher's exact test.

Tables and Figures

Table 3.1. Percentage of germination and percentage of T1 G_N::GFP plants with detectable amounts of recombinant protein by ELISA (anti-G_N/GFP).

	Percentage (number of germinated or positive / total)	
Transgenic line[1]	**Germination[2]**	**G_N::GFP**
T1 G_N::GFP#1.xx	46.0% (23/50)	91.3% (21/23)
T1 G_N::GFP#2.xx	58.0% (29/50)	72.4% (21/29)
T1 G_N::GFP#6.xx	80.0% (40/50)	0 (0/34)

[1] The transgenic plant identification number consists of a series of numbers separated by dots. Each number corresponds to the plant number assigned at each transgenic generation starting with T0 from which the line was derived and ending with the most recent generation. The "xx" represents all the plants of a specific line of that generation and will vary from one to the total number of seedlings, i.e. 1 to 23 in the case of G_N::GFP#1.xx because there were a total of 23 plants for that T1 line.

[2] Germination of non-transgenic tomato seeds sown simultaneously and obtained from tomato plants that grew and were processed simultaneously than the T0 G_N::GFP parental plants was 82% (41/50).

Table 3.2. Percentage of germination and percentage of transgenic tomato T1 plants positive for the presence of recombinant G_N-S::GFP protein and the selection marker NPTII.

T1 G_N-S::GFP Lines[1]	Percentage (number of germinated or positive plants / total)		
	Germination[2]	G_N-S::GFP[3]	NPTII[4]
G_N-S::GFP#3.xx	84% (42/50)	12.1% (4/33)	93.9% (31/33)
G_N-S::GFP#6.xx	6.7% (8/120)	62.5% (5/8)	71.4% (5/7)
G_N-S::GFP#7.xx	7.1% (5/70)	75% (3/4)	75% (3/4)
G_N-S::GFP#9.xx	26% (13/50)	85.4% (88/103)	79.6% (82/103)
G_N-S::GFP#11.xx	56% (28/50)	55.6% (15/27)	88.9% (24/27)

[1] The transgenic plant identification number consists of a series of numbers separated by dots. Each number corresponds to the plant number assigned at each transgenic generation starting with T0 from which the line was derived and ending with the most recent generation. The "xx" represents all the plants of a specific line of that generation and will vary from one to the total number of seedlings, i.e. 1 to 42 in the case of G_N-S::GFP#3.xx because there were a total of 42 plants for that T1 line.

[2] Germination of non-transgenic tomato seeds sown simultaneously and obtained from tomato plants that grew and were processed simultaneously than the T0 G_N-S::GFP parental plants was 74% (37/50).

[3] Detected by ELISA using specific antibodies against G_N or a combination of antibodies against G_N (capture antibody) and GFP (secondary antibody).

[4] *Neomycin phosphotransferase II* gene product that confers resistance to kanamycin. Detected by a commercial DAS-ELISA kit (Agdia Inc).

Table 3.3. Percentage of germination and of transgenic tomato T2 plants positive for the presence of recombinant G_N-S::GFP protein and the selection marker NPTII.

T2 G_N-S::GFP Lines[1]	Percentage (number of germinated or positive plants / total)		
	Germination[2]	G_N-S::GFP[3]	NPTII[4]
G_N-S::GFP#9.10.xx	14.2% (17/120)	100% (17/17)	100% (17/17)
G_N-S::GFP#9.27.xx	42% (42/100)	100% (42/42)	100% (42/42)

G_N-S::GFP#9.207.xx	20% (8/40)	100% (8/8)	100% (8/8)

[1] The transgenic plant identification number consists of a series of numbers separated by dots. Each number corresponds to the plant number assigned at each transgenic generation starting with T0 from which the line was derived and ending with the most recent generation. The "xx" represents all the plants of a specific line for that generation and will vary from one to the total number of seedlings, i.e. 1 to 17 in the case of G_N-S::GFP#9.10.xx because there were a total of 17 plants for that T2 line.

[2] Germination of non-transgenic tomato seeds sown simultaneously and obtained from tomato plants that grew and were processed simultaneously than the T1 G_N-S::GFP parental plants was 80% (56/70).

[3] Detected by ELISA using specific antibodies against G_N or a combination of antibodies against G_N (capture antibody) and GFP (secondary antibody).

[4] *Neomycin phosphotransferase II* gene product that confers resistance to kanamycin. Detected by a commercial DAS-ELISA kit (Agdia Inc.).

Table 3.4. Percentage of germination and of transgenic tomato T3 G_N-S::GFP plants with detectable amounts of recombinant protein.

T3 G_N-S::GFP Lines[1]	**Percentage (number of germinated or positive plants / total)**	
	Germination[2]	**G_N-S::GFP[3]**
G_N-S::GFP#9.10.7.xx	54% (27/50)	100% (27/27)
G_N-S::GFP#9.10.11.xx	32% (16/50)	100% (16/16)
G_N-S::GFP#9.27.5.xx	12% (6/50)	100% (6/6)
G_N-S::GFP#9.27.27.xx	10% (5/50)	100% (5/5)
G_N-S::GFP#9.207.2.xx	12% (6/50)	100% (6/6)
G_N-S::GFP#9.207.3.xx	24% (12/50)	100% (12/12)

[1] The transgenic plant identification number consists of a series of numbers separated by dots. Each number corresponds to the plant number assigned at each transgenic generation starting with T0 from which the line was derived and ending with the most recent generation. The "xx"

represents all the plants for the specific line of that generation and will vary from one to the total number of seedlings, i.e. 1 to 27 in the case of G_N-S::GFP#9.10.7.xx because there were a total of 27 plants for that T3 line.

[2] Germination of non-transgenic tomato seeds sown simultaneously and obtained from tomato plants that grew and were processed simultaneously than the T2 G_N-S::GFP parental plants was 86% (43/50).

[3] G_N-S::GFP detected ELISA using a combination of antibodies against G_N (capture antibody) and GFP (secondary antibody).

Table 3.5. Contingency table for the detection of *Tomato spotted wilt virus* (TSWV) and G_N-S::GFP by ELISA in inoculated leaf tissue (old leaf tissue). The second true leaf after the cotyledons of transgenic tomato plants expressing G_N-S::GFP was mechanically inoculated with TSWV and was sampled 15 days after virus inoculation. Samples were simultaneously tested for the presence of virus and recombinant protein. The number of plants positive for both (virus and recombinant protein) for either one or for any are summarized.

	Detection of G_N-S::GFP[2]		
Detection of TSWV[1]	Positive (+)	Negative (-)	**Totals**
Positive (+)	42	12	54
Negative (-)	19	2	21
Totals	61	14	75

[1] Detected by a DAS-ELISA commercial kit (Agdia).

[2] Detected by ELISA using specific antibodies against G_N or a combination of antibodies against G_N (capture antibody) and GFP (secondary antibody).

Table 3.6. Contingency table for the detection of *Tomato spotted wilt virus* (TSWV) and G_N-S::GFP by ELISA in systemic leaf tissue (new leaf tissue). The second leaf from top to bottom from transgenic tomato plants expressing G_N-S::GFP and that were previously mechanically inoculated with TSWV at a different leaf was sampled 15 days after virus inoculation. Samples were simultaneously tested for the presence of virus and recombinant

protein. The number of plants positive for both (virus and recombinant protein) for either one or for any are summarized.

	Detection of G_N-S::GFP		
Detection of TSWV	Positive (+)	Negative (-)	**Totals**
Positive (+)	45	23	68
Negative (-)	5	2	7
Total	50	25	75

Table 3.7. Contingency table for the comparison of TSWV detection[1] pattern in local (old) and systemic (new) leaves between transgenic and non-transgenic inoculated plants.

	Pattern of TSWV detection: old/new leaf[2]				
Plant	**+/+**	**+/-**	**-/+**	**-/-**	**Total**
Non-transgenic	26 (65.0%)	2 (5.0%)	11 (27.5%)	1 (2.5%)	40 (100%)
Transgenic	49 (65.3%)	5 (6.7%)	19 (25.3%)	2 (2.7%)	75 (100%)
Total	75	7	30	3	115

[1] TSWV was detected by DAS-ELISA (Agdia Inc., Elkhart, IN, USA) 15 days after virus mechanical inoculation.

[2] Percentages per row (plant type) are given in parenthesis.

Table 3.8. Contingency table for the comparison of G_N-S::GFP detection[1] pattern in local (old) and systemic (new) leaves between transgenic plants non-inoculated or inoculated with TSWV.

	Pattern of G_N-S::GFP detection: old/new leaf				
Plant	**+/+**	**+/-**	**-/+**	**-/-**	**Total**
Non-inoculated	12 (63.2%)	2 (10.5%)	1 (5.3%)	4 (21.0%)	19 (100%)
TSWV-inoculated	50 (66.7%)	11 (14.7%)	0 (0%)	14 (18.7%)	75 (100%)
Total	62	13	1	18	94

[1] TSWV was detected by DAS-ELISA (Agdia Inc., Elkhart, IN, USA) 15 days after virus mechanical inoculation.

[2] Percentages per row (plant type) are given in parenthesis.

Table 3.9. Contingency table for the total number of adult thrips (from three independent experiments) that transmitted or not TSWV to leaf discs during an 48h IAP after feeding as larvae on transgenic or non-transgenic TSWV-infected tissue for a 24h AAP.

Tomato plant on which thrips fed:	**Number of thrips**		
	Transmission positive (+)	Transmission negative (-)	Total
Transgenic	12	78	90
Non-transgenic	67	23	90
Total	79	101	180

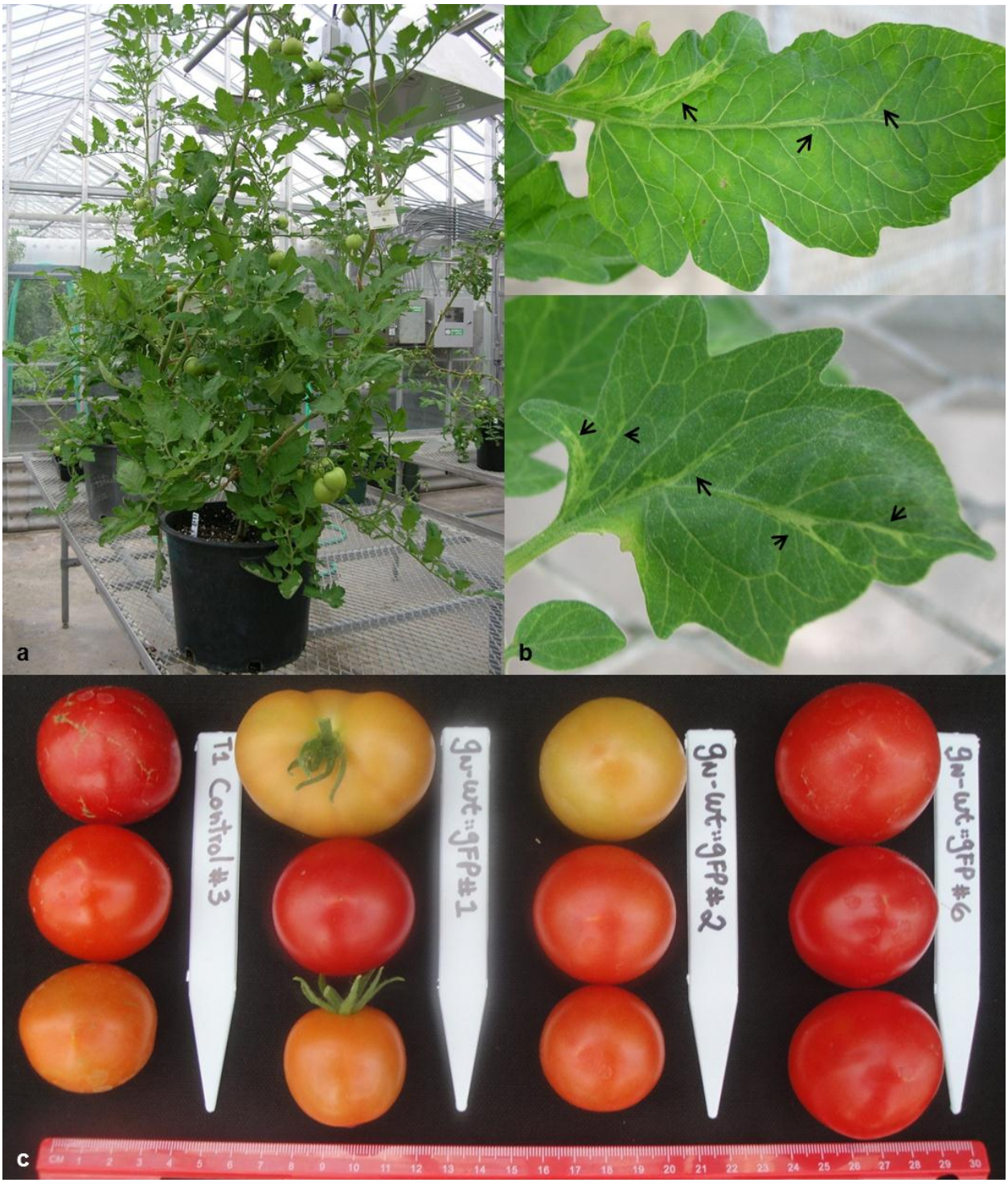

Figure 3.1. General appearance of T0 G_N::GFP transgenic tomato plants.

T0 G_N::GFP transgenic tomato plants in the greenhouse (a) and enation-like morphology (black arrows) of few veins per leaflet in plant T0 G_N::GFP#2 (b). Sample of three tomato fruits for the three T0 plants obtained for G_N::GFP and for a non-transgenic plant that was

growing simultaneously in the greenhouse. Plant T0 G_N::GFP#2 tested highest by ELISA for presence of G_N::GFP recombinant protein followed by plant #1; the recombinant protein was not detected by ELISA or confocal microscopy for plant #6.

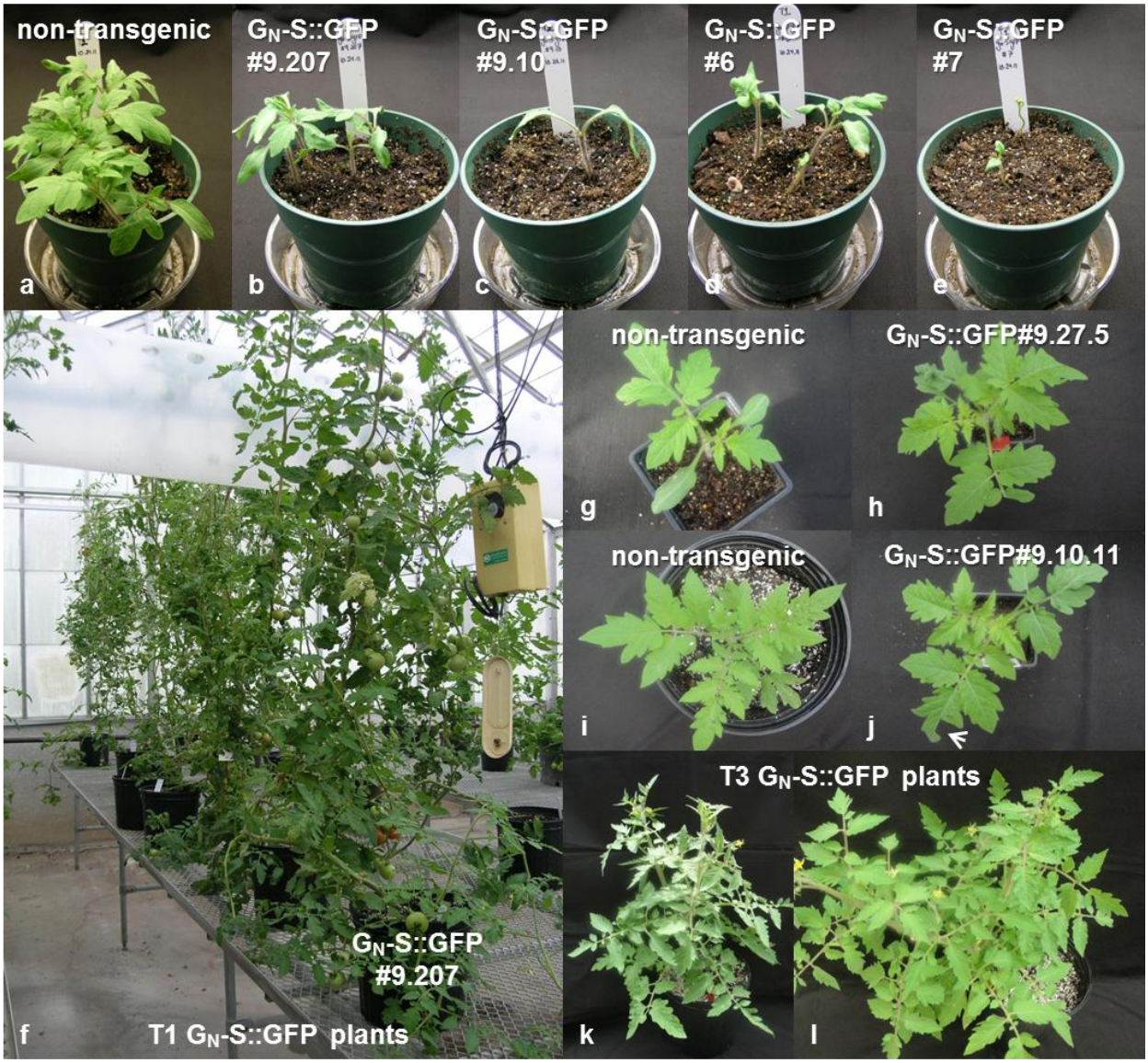

Figure 3.2. General appearance of G_N-S::GFP transgenic tomato plants.
Seed pots showing germination for seeds from a non-transgenic tomato plant (a), and transgenic plants G_N-S::GFP#9.207 (b), #9.10 (c), #6 (d) and #7 (e). T1 transgenic plants in the greenhouse, first plant in the row is plant G_N-S::GFP#9.207 (f). Transplanted seedlings after germination in seed pots for individual screening to detect the presence of the

recombinant protein; non-transgenic control plants (g and i) and T2 transgenic plants G_N-S::GFP#9.27.5 (h) and #9.10.11 (j). Notice the terminal leaflet of plant #9.10.11 missing a section of leaf blade (white arrow) which corresponds where the sample for ELISA was taken during screening of the plants. T3 plants selected for harvesting tomatoes due to high expression of the recombinant protein, G_N-S:GFP#9.27.27.2 (k) and #9.207.2.1 (l).

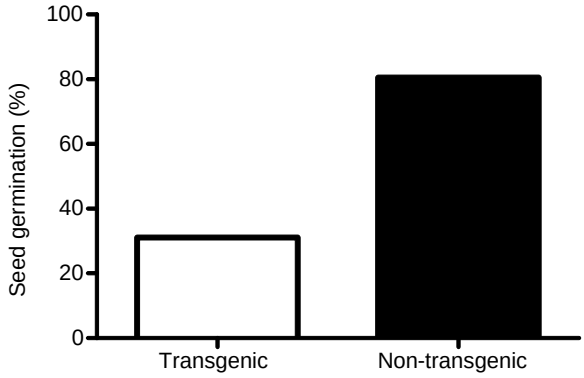

Figure 3.3. Percentage of seed germination in transgenic and non-transgenic plants. Comparison of all transgenic seed (G_N::GFP and G_N-S::GFP plants, all generations tested) vs. all non-transgenic seeds tested. Germination is significantly different ($P < 0.0001$) as determined by Fisher exact test of the corresponding 2x2 contingency table.

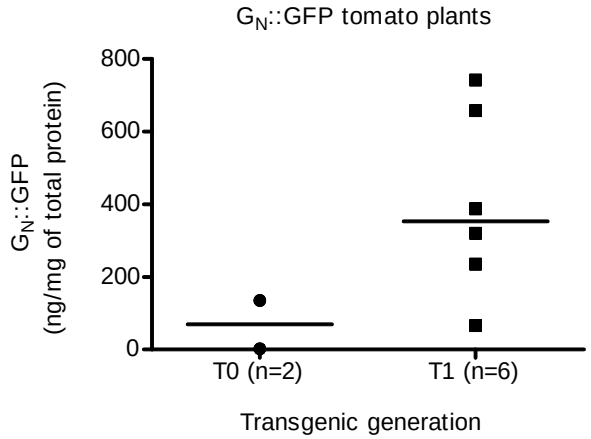

Figure 3.4. Amount of recombinant protein estimated in a subsample of G_N::GFP tomato transgenic plants, T0 and T1 generations.

The horizontal line (—) represents the median. No statistical comparison was made because T0 only has two data points which is less than what is required for the Mann Whitney test.

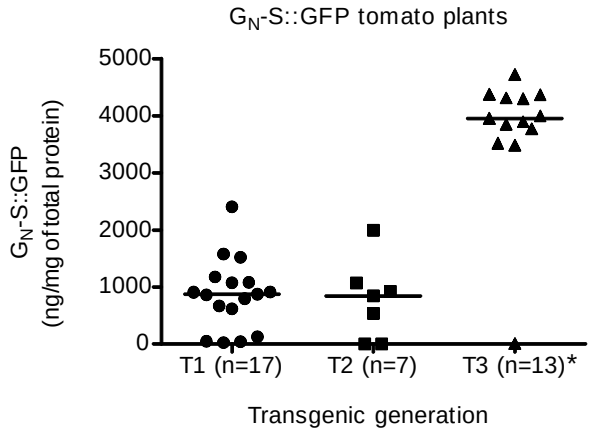

Figure 3.5. Amount of recombinant protein estimated in a subsample of G_N-S::GFP tomato transgenic plants, T1, T2 and T3 generations.

The horizontal line (—) represents the median and the asterisk (*) indicates significant difference of the transgenic generation in comparison with the other generations ($P < 0.05$, determined by Dunn's multiple comparison test).

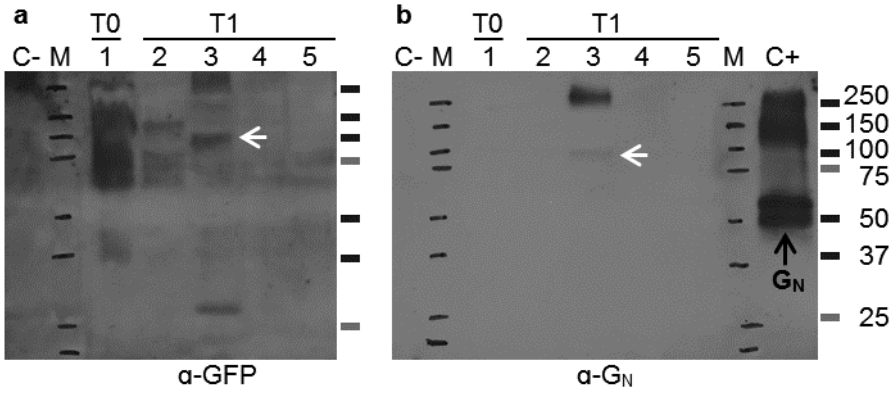

Figure 3.6. Western blots for G_N::GFP transgenic plants tested with specific antibodies against GFP (a) or G_N (b).

The white arrows signal a band between of the expected size, approximately 84 kDa, detected with anti-GFP and anti-G_N antibodies in one T1 sample, lane 3. A band or signal was also detected around the molecular size for two other plants, lanes 1 and 2, with anti-GFP antibody. Samples are T0 plant G_N::GFP#2 (1), T1 #1.10 (2), #1.13 (3), #2.1 (4) and #2.3 (5); and control non-transgenic tomato (C-) and TSWV-infected *Datura stramonium* (C+). TSWV G_N is approximately 55 kDa and GFP is approximately 29 kDa.

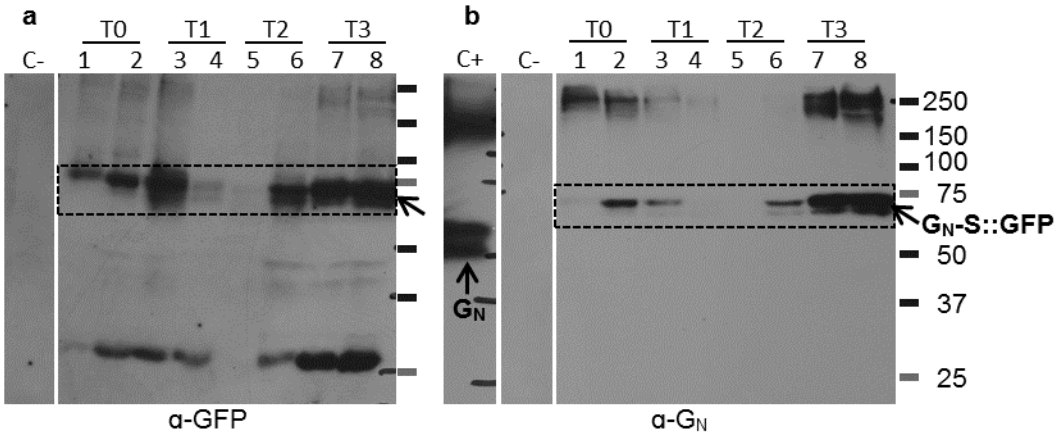

Figure 3.7. Western blots for G_N-S::GFP transgenic plants tested with specific antibodies against GFP (a) or G_N (b).

G_N-S::GFP bands are highlighted by a dashed rectangle. Samples are T0 plants G_N-S::GFP#7 (1), and #9 (2); T1 #7.4 (3) and #9.514 (4), T2 #9.10.11 (5) and #9.207.7 (6) and T3 #9.10.11.11 (7) and #9.207.3.10 (8); and control non-transgenic tomato (C-) and TSWV-infected *Datura stramonium* (C+). The predicted size of G_N-S::GFP protein is approximately 63 kDa; TSWV G_N is approximately 55 kDa and GFP is approximately 29 kDa.

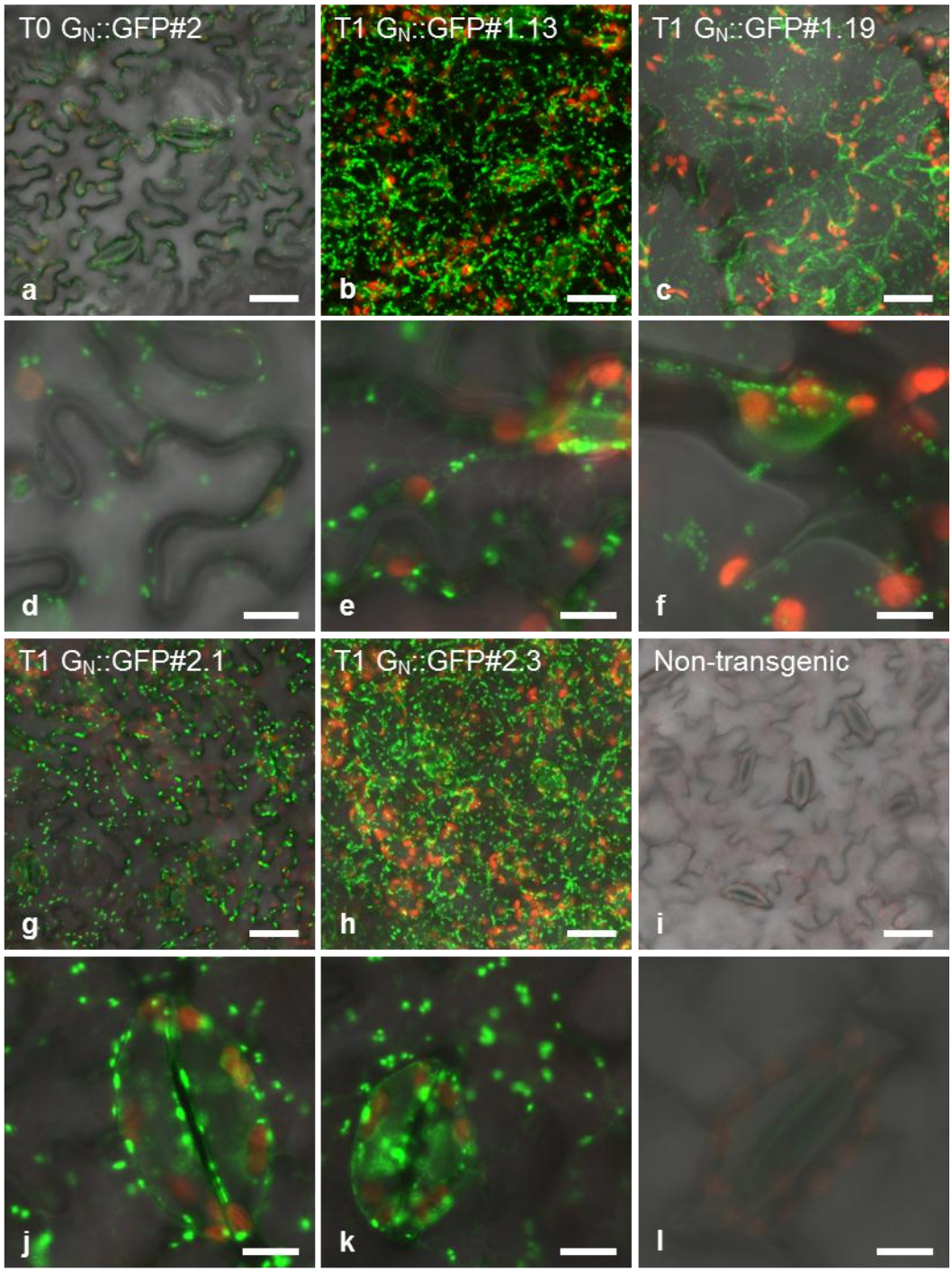

Figure 3.8. Confocal microscope images of G_N::GFP transgenic plants.

Notice the punctate pattern of G_N::GFP (green) and also a faint reticulate pattern (panel e). Images are merge of channels for bright field (DIC), green (G_N::GFP fluorescence) and red. Panels a and d are optical sections; all other panels are projections. Panels d – f and l –

k are details at 1600x of panels a – c and g – i (400x) , respectively. Scale bars represent 50 µm in panels a – c and g – i (280x); and 10 µm in panels d – f and j – l.

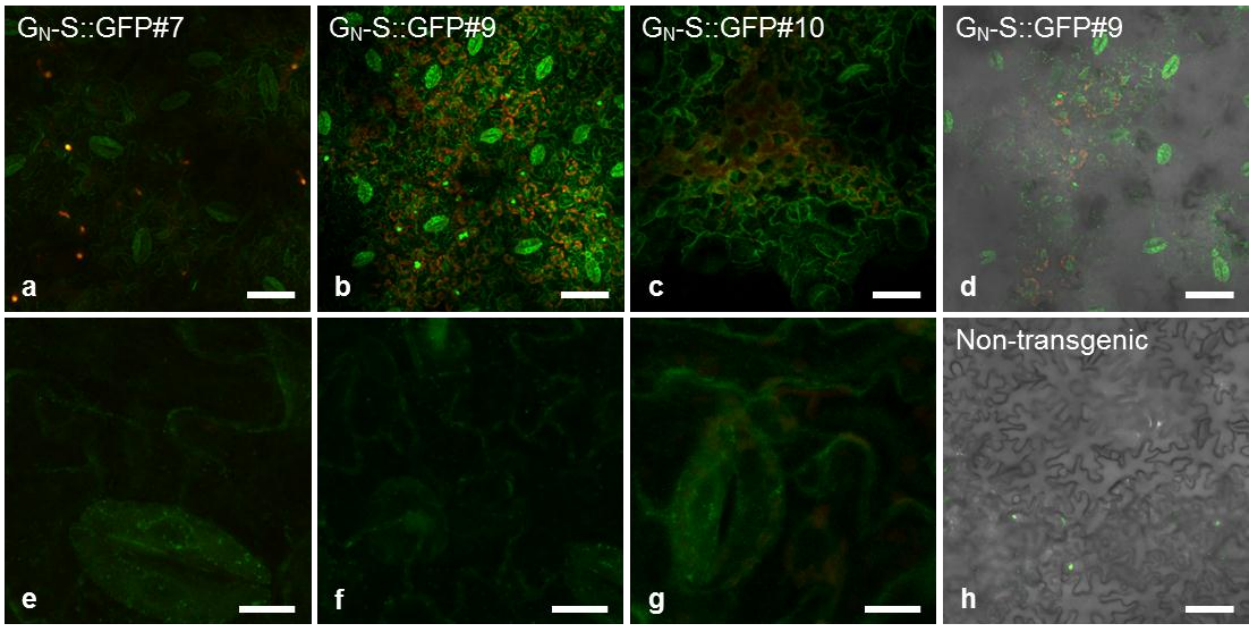

Figure 3.9. Confocal fluorescence images for T0 G_N-S::GFP transgenic tomato plants. Projections at 280x of lines #7 (panel a) , #9 (panel b) and #10 (panel c) and details at 1600x of these lines, panels e, f and g respectively. Each image is a merge of channels for green: G_N-S::GFP fluorescence, and red for chloroplasts (chlorophyll auto-fluorescence). Optical section of T0 G_N-S::GFP#9 (panel d) and a control non-transgenic tomato plant (panel h). Optical section images are a merge of bright field (DIC), green and red channels. Scale bars represent 50 µm (panels a – d and h) and 10 µm (panels e – g).

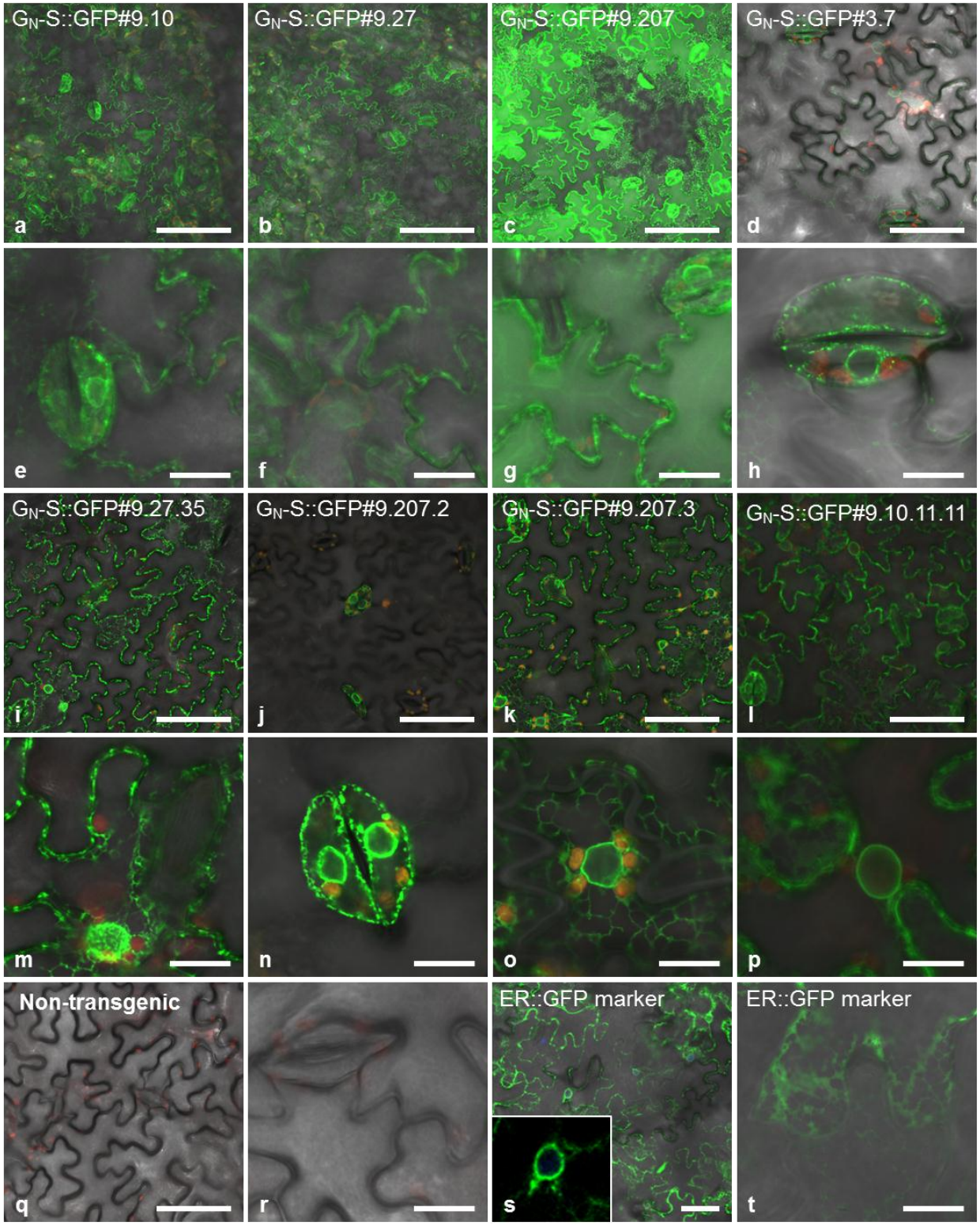

Figure 3.10. Confocal fluorescence images for T1, T2 and T3 G_N-S::GFP transgenic tomato plants.

Note the reticulate-like pattern (m, o and p), fluorescent ring-like structures (e, h, I, j, k, l, n, o, and p) and strong or restricted fluorescence in stomas (a, d, h, j and n). Optical sections at 400x of different transgenic lines or non-transgenic control plant, panels a – d, i – l and q. Details at 1600x for the same transgenic lines or non-transgenic control plant, panels e – h, m – p and r. Endoplasmic reticulum marker fused to green fluorescent protein (ER::GFP) transiently expressed in *Nicotiana benthamiana* is showed in panels s and t. Inset in s: detail of the nuclear envelop highlighted by fluorescent signal. Detail of reticulate pattern (panel t). Each image (panels a – r) is a merge of channels for green: G_N-S::GFP fluorescence, red: chloroplasts (chlorophyll fluorescence) and bright field (DIC). Panels s and t are a merge of channels for green: ER::GFP, blue: nuclear marker (DAPI) and bright field (DIC). Scale bars represent 50 µm (panels a – d, i – l, q and s) and 10 µm (panels e – h, m – p, r and t).

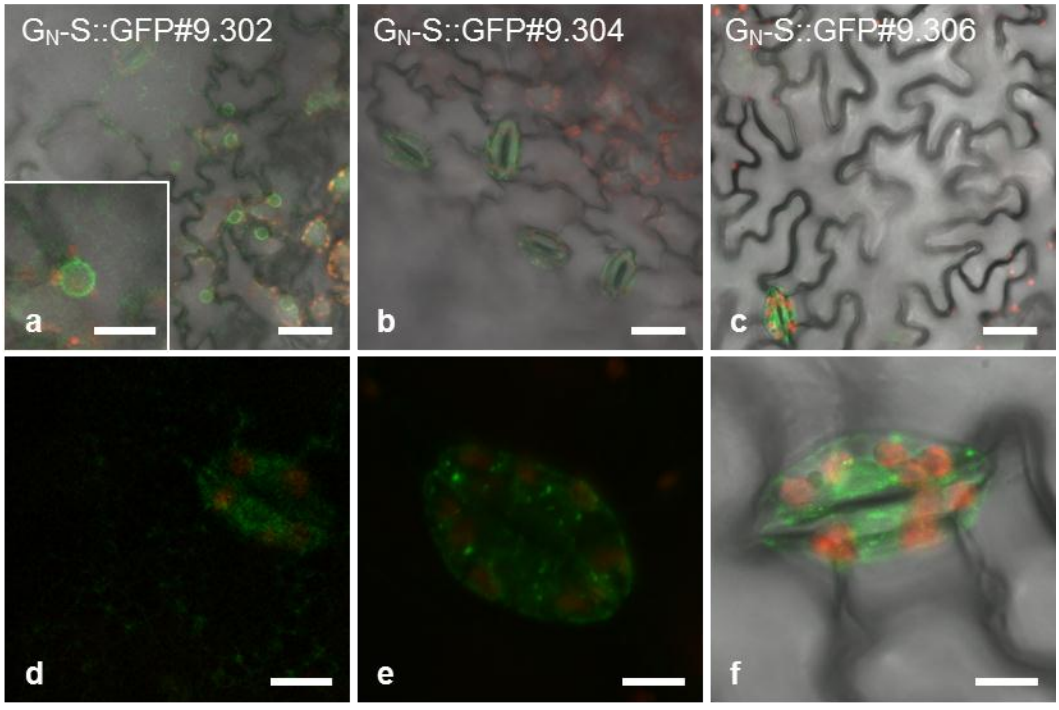

Figure 3.11. Images of G_N-S::GFP fluorescence in TSWV-infected tomato transgenic plants.

Fluorescent "rings" (nuclear envelop, panel a and inset) and reticulate pattern (panel d) suggesting ER localization. Stronger fluorescent signal or the only fluorescent signals were

observed at guard cells of stomata in some plants (panels b-c, e-f). Optical sections (a, d) and projections (b, c, e, f) of merged images for bright field (DIC), green channel (G_N-S::GFP) and red channel (chloroplasts), except for d and e which are only green and red channels. Scale bars in a – c represent 50 µm and in a-inset and d – f are 10 µm.

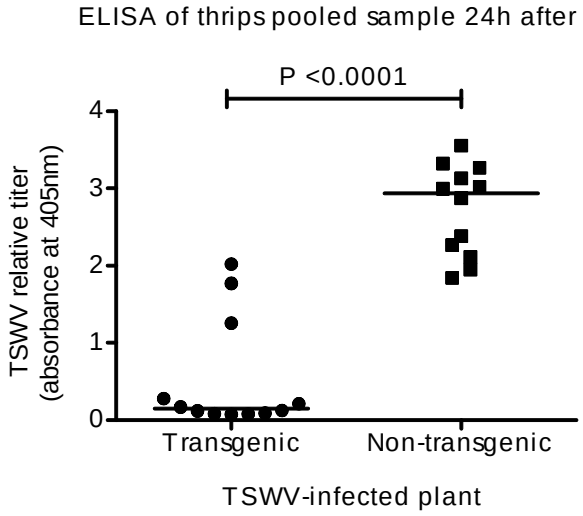

Figure 3.12. Detection of TSWV nucleocapsid protein (N) in thrips cohorts given a 24h acquisition access period (AAP) on TSWV-infected, G_N-S::GFP transgenic or non-transgenic tomato leaf tissue.

TSWV was detected by DAS-ELISA in samples of pooled thrips (n = 15). The graph depicts twelve data points (replicates) per treatment out of four independent experiments. The horizontal line (—) indicates the median of the data points. Medians were determined as significant different ($P < 0.0001$) between the two treatments (transgenic or non-transgenic) by the Mann Whitney test.

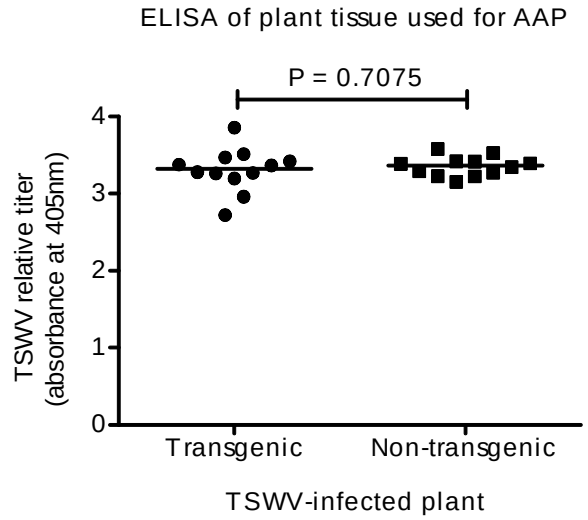

Figure 3.13. Detection of TSWV nucleocapsid protein (N) by DAS-ELISA in tissue used for thrips AAP.

The graph depicts twelve data points (replicates) per treatment out of four independent experiments. The horizontal line (—) indicates the median of the data points. Medians between the two treatments (transgenic or non-transgenic) were compared by the Mann Whitney test.

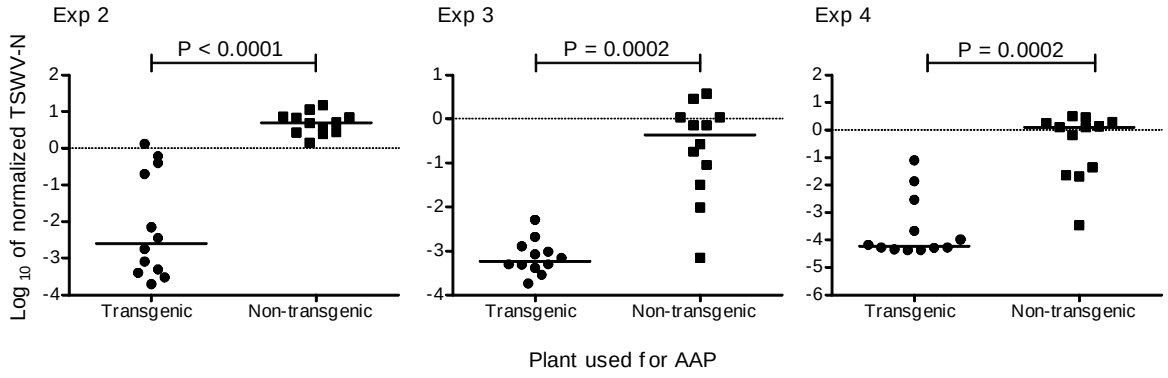

Figure 3.14. Normalized abundance (Log_{10} transformed) of *Tomato spotted wilt virus* (TSWV) N RNAs in thrips fed in transgenic and non-transgenic TSWV-infected plants. Larval thrips (0-18h old) were exposed to a G_N-S::GFP transgenic plant or to a non-transgenic plant, both TSWV-infected, and allowed to feed for a 24h AAP. A second 24h feeding period was done on green beans and sampled. Twelve thrips per treatment and

three independent experiments are shown. Virus abundance in thrips fed on the transgenic plant was significantly different from thrips fed on non-transgenic plant as determined by the Mann Whitney test.

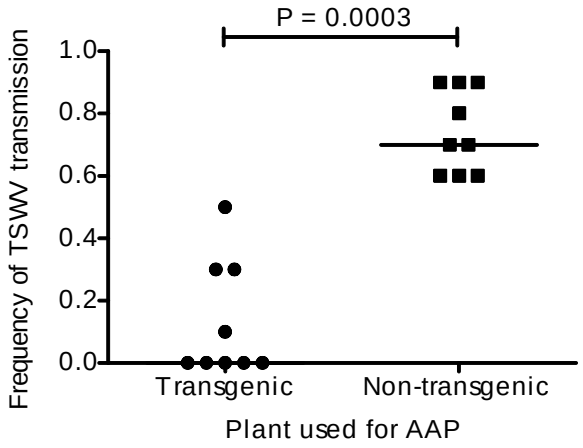

Figure 3.15. Frequency of transmission of TSWV by adult *Frankliniella occidentalis* individuals fed as larvae on transgenic and non-transgenic TSWV-infected plant tissue. Each data point represents the frequency out of ten thrips tested individually for TSWV transmission by a 48h IAP in leaf discs of *Datura stramonium*. The treatments are significantly different as determined by the Mann Whitney test.

Chapter 4 - *Dynamics of TSWV infection and spread in its insect vector Frankliniella occidentalis with an emphasis on the principal salivary glands.*

Abstract

Tomato spotted wilt virus (TSWV), an economically important plant virus belonging to the genus *Tospovirus*, is transmitted by thrips in a circulative-propagative manner. The virus-vector interaction is very complex and aspects of it are poorly understood, including the route of virus dissemination in the vector and infection of principal salivary glands (PSGs). The PSG is an important organ in the virus transmission cycle, because the virus needs to infect it for transmission to occur. The goal of this work was to study the morphology, infection and route of TSWV into the PSGs of the thrips vector *Frankliniella occidentalis*. Information on morphology and general organization of the salivary glands was obtained by confocal fluorescence microscopy. PSGs have three distinct regions, the central and main one composed of large bi-nucleated cells, and a complex branched lumen that discharges into an efferent duct (ED). Tubular salivary glands (TSGs) appear to be also composed by bi-nucleated cells defining a central lumen. TSGs have an enlarged clavate section (CS) and fine terminal thin apical section (TAS). A ligament-like filament connects each TSG to the corresponding PSG; the ligament runs superficially on the PSGs and is attached to the anterior region of MG1. TSWV infection was tracked by immunolabeling the virus glycoprotein, G_N, at four key points throughout the life cycle of *F. occidentalis*. The virus established a strong and conspicuous infection of midgut region 1 (MG1) in contrast to low frequency, very limited and apparently low titer infections in the foregut (FG) and midgut sections 2 and 3 (MG2 and MG3). Moreover, the infection of MG1 appeared less frequent in adults in comparison to larval thrips, 52% vs. 88% respectively. In general, infection of TSGs was detected prior to PSG infection and we hypothesize that the TSGs and associated EDs and ligaments are a putative route for PSG infection by TSWV. PSGs showed uneven infection between one pair of glands and within each gland. Virus infection was observed in cells in the three regions of PSGs and strong signal could be detected in bi-nucleated cells and their lumen. Virus infection was also tracked by ELISA against the nucleocapsid (N)

protein in two independent experiments at several time points throughout the life cycle of *F. occidentalis*. Congruencies between the immunolabeling experiments and ELISA curves were recognized; all the infection patterns showed a steep increase the first hours after acquisition access period (AAP) reaching a peak at late L1 or at L2 stage followed by a decrease of TSWV signal or titer. Additionally, ELISA results showed that the virus reached a low point between prepupae and adults 24h after eclosion; and finally tended to increase again during adulthood. TSWV transmission rate by adults 24h after eclosion was over 83% for the four time-course experiments. No differences were observed for transmission or for the infection of PSGs between genders. Overall, new information on PSG morphology was generated and the TSG is proposed as route for TSWV infection of the PSGs in *F. occidentalis*.

Introduction

Tomato spotted wilt virus (TSWV) is an economically important plant virus transmitted to plants by several species of insects in the order Thysanoptera (thrips). TSWV is the type member of the genus *Tospovirus*, the only plant infecting genus within the *Bunyaviridae*; and it has been catalogued as one of the top ten most important plant viruses due to the economic losses associated to it and its biological properties. Moreover, the diseases caused by tospoviruses, as for many animal infecting bunyaviruses, are emerging and increasingly gaining in importance due to detection of new virus species, expansion of geographical and host ranges and the spread of thrips vectors to new areas, among other factors (Goldbach and Peters, 1994; Whitfield et al., 2005b; Pappu et al., 2009; Scholthof et al., 2011; Walter and Barr, 2011; Mandal et al., 2012).

Like the mammal-infecting bunyaviruses, tospoviruses replicate in their insect vectors (circulative-propagative interaction).Virus-vector interactions are complex and for other plant virus systems, where circulation but no viral replication occurs in the vector, several barriers including different tissue-specific receptors, other molecules and genetic inherited traits have been proposed as variables regulating the interaction (Gray and Banerjee, 1999; Burrows et al., 2006; Cilia et al., 2011a; Cilia et al., 2011b). In the case of thrips-tospovirus interactions, it is established that larvae, predominantly L1s, need to acquire the virus in order for adults to

transmit it (van de Wetering et al., 1996). Additionally, another requisite for an adult to transmit TSWV is infection of the principal salivary glands (Kritzman et al., 2002).

Thrips gender and their specific behavior is another factor determining the rate of virus transmission. Male thrips have been reported to have higher transmission efficiency than females from the same cohort. This difference is explained by distinct feeding behaviors between genders; females feed more vigorously and localized creating large areas of dead cells. These cells will not be conducive for initiating a viral infection. Conversely, male thrips show more probing behavior during which small amounts of cell contents are ingested, thus producing a significantly less scarring. It is hypothesized that the probed cells are capable of supporting viral infection since they are not irreversibly damaged (van de Wetering et al., 1998; van de Wetering et al., 1999; Stafford et al., 2011). On the other hand, female thrips were shown to contain an absolute higher number of virus RNA but males contain a higher proportion of viral RNA in relation to the total RNA content. A higher virus abundance (TSWV normalized N-RNA) was positively correlated with frequency of TSWV transmission by female and male individual thrips (Rotenberg et al., 2009).

Although the principal salivary gland is a very important organ in terms of virus transmission by thrips, there is a lack of information regarding its morphology and virus infection of this tissue. It is not known if there are morphological differences nor if there are differences in salivary gland infection between genders (i.e. a gender specific infection barrier). Moreover, it is not clear the route through which TSWV reaches the principal salivary glands. There are two hypotheses: (i) a stage-developmental theory in which virus will move from the midgut to the salivary gland by direct contact between the tissues (Moritz et al., 2004) or (ii) that the virus will move through the ligament-like structures that connect each principal salivary gland to the anterior region of MG1 (Nagata et al., 1999; de Assis Filho et al., 2002). A clear understanding of the factors determining virus infection and transmission by individual thrips is necessary in order to design new strategies to block the virus-vector interaction; and therefore, abolish the crop infection and its economic consequences. Additionally, such information will be valuable as well for a better understanding of the virus-vector interactions for bunyaviruses and identification of conserved features of vector-virus interactions for this important virus family.

The objectives of this work were first to describe the morphology and organization of *F. occidentalis* salivary glands by fluorescent confocal microscopy in combination with actin and

nuclear markers. A second objective was to track, at specific time points, TSWV infection in the gut and salivary tissues of *Frankliniella occidentalis* individuals, in order to localize TSWV infection in these tissues. As a third objective, we aimed to compare the morphology and infection status of salivary glands from adult male and female thrips. Here we present new information on the possible route by which TSWV reaches the principal salivary glands and on the morphology of these tissues.

Results

Morphology of the principal and tubular salivary glands of Frankliniella occidentalis

Principal salivary glands (PSGs)

The principal salivary glands (PSGs) of *Frankliniella occidentalis* are a pair of ovoid structures with three distinct regions (Fig. 4.1). Each gland appears to have a rounder side, the base, and an opposite more angular side, the apex. The majority of each gland, in the central region (CR), consists on relatively large sized, loose-packed bi-nucleated cells (BiN). Among these cells there is a branched lumen (L) highlighted by acting labeling and which seems to be generated by the interconnecting lumen of each BiN cell (Fig. 4.1b to e). In average 11.3±3.3 (median = 12, n = 65) big nuclei were counted in each central region of each principal salivary gland; which implies there are approximately six BiN cells per gland. At opposite sides of the CR, at the base and apex, there are two regions of smaller single-nucleated cells, an apical (AR) and basal region (BR). The pair of glands is connected to each other at the base, through the connection of the basal single-nucleated cell regions of each gland (Fig. 4.1b). The region of single-nucleated cells at the apex appears as a triangular-like structure wrapping the angular end of the gland (Fig. 4.1b, c and d). The AR was also observed, in some samples, as a layer of cells in only one side of the gland's apical end (Fig. 4.1e). The main lumen of each PSG continues into an efferent duct (ED) that projects out of the gland at the apical side of it (Fig. 4.1c to d). Observed under the bright field (DIC), the PSGs are translucent structures where the three regions described herein and the ED can be distinguished (Fig. 4.1f).

No difference in the organization of the tissues and cells was observed between female and male adult thrips; however female PSGs were larger than male ones (Table 4.1). Several size

parameters: short and long axis, perimeter and area of each principal salivary gland, were measured for adult female and male thrips. Only intact PSGs were included in the size comparison because some glands from the total observed appeared to be damaged during the dissection and immunolabeling steps. All measurements of PSG size revealed a significant difference between female and male PSGs (all $P < 0.001$). PSGs from females or males were analyzed based on sex regardless of virus infection status because no statistical difference was found by a two-way ANOVA analyses between the size parameters measured and the virus status of the tissue: (i) non-exposed, (ii) exposed and negative, and (iii) exposed and positive. However, a tendency to an increase in the mean value of each parameter was observed in that same order (i to iii) indistinctly of thrips gender (Fig. 4.2). This observation suggested the possibility that TSWV infection in PSGs is triggering swelling or an inflammation-associated response.

Ligament-like connecting structure (Lig) and efferent duct (ED)

A filament-like structure, referred as a ligament (Lig), rich in actin (strong phalloidin-conjugate labeling) appears to be attached superficially to each PSG, and to run from base to apex (Fig. 4.1a to e). The ligament projects into opposite directions of the principal salivary glands (Fig. 4.1b). The side projecting from the base of each gland seems to correspond to the ligament-like structure previously reported to connect each gland with the anterior region of MG1 (Ullman et al., 1989). The opposite side, projecting from the apex of the PSG, appears to connect to the tubular salivary gland (TSG). We hypothesize that the ligament-like structure serves structural purpose maintaining the position of the PSGs by anchoring them to the midgut and TSGs. The ligament seems to be very elastic and resistant because during dissection it was stretched to more than double of its length without tearing off and as the tension ceases it retracted to its original length.

The efferent duct from each PSG also appears to be connected to the tubular salivary gland, thus two connections exist between each PSG and its corresponding TSG (Fig. 4.3e). In several samples a very small dot or ovoid spot of DAPI signal was observed in the center of the free structure connecting the principal and corresponding TSG. Therefore, we hypothesize that the ED is a cell based structure and apparently the connection between tubular and principal salivary glands is a single elongated cell (Fig. 4.1c and 4.3c and e). The Lig and ED are very

important structures for transmission of virus to a new host plant or dissemination in the vector; they represent a cellular route connecting the midgut with the principal and the tubular salivary glands.

Tubular salivary glands (TSGs)

The tubular salivary glands (TSGs) are a pair of tubule-like structures with polarity. At the basal end, the one in contact with the muscle cells wrapping the midgut, each TSG is a blunt tubule of uniform width; meanwhile, at the apical end, the one attached with the PSGs, there is a clavate section (CS) followed by a thin-apical section (TAS) (Fig. 4.3a). A longitudinal lumen is highlighted by actin staining along all the structure. The CS is the site where the ligament and ED from the PSGs seem to attach to the TSG. The whole tubule-like structure seems to consist of single cells slightly overlapping one next to other. DAPI and actin staining suggested that the cells along the TSGs are also bi-nucleated (Fig. 4.3b-d). The TSGs are relatively long and during the dissection they can be stretched out to approximately half the length of the body of the thrips without tearing off. This observation suggests that the tubular glands are elastic and simultaneously very strong structures, contrary to the PSGs that are easily torn off during dissection.

Initial TSWV infection of Frankliniella occidentalis

In order to observe the initial infection of thrips by TSWV and to test the immunolabeling protocol, larval thrips were dissected and processed after three hours clearing in 7% sucrose following a 18h AAP on *Emilia sonchifolia* or *Datura stramonium* TSWV-infected or healthy tissue. Strong signal, after probing against G_N, was observed localized to a specific area of the anterior midgut region 1 (MG1) near the cardiac valve (CV) (Fig. 4.4a and b) confirming previous observations on the site of initial infection (Nagata et al., 1999; Kritzman et al., 2002). Additionally, in some guts multiple foci of TSWV signal were observed throughout the midgut (Fig. 4.4c and d). In other guts, the virus was distributed in an even pattern along the MG1 in what apparently are the muscle cells (Fig. 4e and f).

TSWV infection of gut and salivary tissues of F. occidentalis

TSWV was detected by immunolabeling with an antibody against G_N in the foregut, midgut and salivary tissues of *F. occidentalis*. The frequency (Tables 4.2 and 4.3), apparent intensity and distribution (Figs. 4.5 and 4.6) of TSWV signal through the individual tissues were variable. Virus signal appeared as foci of variable size with irregular boundaries and random shape (Fig. 4.5i and j, and 4.6). In contrast, in some TSWV non-exposed control thrips a variable degree of background signal was noticed, but it was generally faint and the pattern of the signal was different from the one observed for TSWV. Background signal appeared as few fine green dots randomly distributed through the tissue (Figs. 4.5a to h, and 4.8d).

TSWV signal in MG1 was variable but overall more frequent and stronger than the signal observed in the other sections of the digestive track (Tables 4.2 and 4.3; Figs. 4.6 and 4.7). Signal in MG2 and MG3 was observed at lower frequency and intensity than in MG1, in total 23% (42/180) of the observed MG2 and MG3 had signal vs. 65% (112/172) of MG1s. Likewise, the FG seldom had signal, only 19% (31/166), and when present it was relatively faint and of limited distribution through the structure (Fig.4.6l and o). The cardiac valve appeared as a barrier to virus spread because TSWV signal was seen in MG1 but not in the corresponding FG in 71% (76/107) of the samples (Fig. 4.6d); and in 100% of the individuals where signal was detected in the FG the corresponding MG1 was also positive. The tissue tropism of TSWV suggested differences in the susceptibility/permissibility of cells in MG1 region of the digestive track and therefore it suggested that there is differential cell specialization at the continuous sections of the MG and at the FG.

In the salivary tissues, TSWV signal was moderate in the TSG but it could be very strong in the PSGs (Figs. 4.8 and 4.9). In TSGs virus signal followed the dense actin strands that are apparent along the tubule-like structure (white arrows in Fig. 4.8b, c and e). Despite the presence of background fluorescence in the TSG of a TSWV non-exposed thrips (white arrows in Fig. 4.8d), the dense actin strands did not show labeling with TSWV signal. In some images, virus signal seemed to fill the whole volume of the TSGs cells suggesting that a high virus load in this tissue is also a possibility (Fig. 4.8a and b).

TSWV infection of the PSG was variable in intensity (Fig. 4.9c to h, and Fig.4.10), distribution (Fig. 4.11) and partial infections of one or both PSGs are common (Fig. 4.12). All the regions of the PSG were susceptible to infection (Fig. 4.9a and c). In the central region, one

or few single bi-nucleated giant cells displayed TSWV signal rather than a uniformly distributed infection throughout the CR (Fig. 4.8e to h). In some samples, the only visible signal was found at the central portion of the branched lumen (what seems to be the common area of the lumen discharging into the ED) (Fig. 4.8d). Meanwhile, in other samples the signal was found in one or various individual lumens throughout one PSG (Fig. 4.8e-h).

The connecting structures: (i) the ligament connecting the PSG to the corresponding MG1 and TSG and (ii) the ED from the PSG that seems to be in contact with the CS of the TSG are possible bridges for the passing of virus from one structure to another. This possibility is supported by the observations reported herein (morphology section of results) suggesting that these structures are specialized cells rather than an extracellular matrix connection. TSWV signal was observed in 29% (8/28) and 21% (13/63) from the total observed number of MG1 to TSG ligaments and TSG to PSG ligaments/EDs, respectively. The signal appears, as with the TSG, as small foci along the structures (Fig. 4.9a and b).

TSWV infection at four time points of Frankliniella occidentalis life cycle

Four time points, L1, L2, A24 and A96, in the life cycle of *F. occidentalis* were selected for immunolabeling to track TSWV infection and spread through the thrips body (Tables 4.2 and 4.3). The time points are thought to represent critical points in TSWV infection and/or thrips life cycle. The first larval instar (L1) is known to be the best stage for acquisition and subsequent transmission of TSWV in later development stages; it will represent a relatively early stage in the infection. We selected a late L1 (24h after a 24h AAP) because the initial infection seems to be limited to the anterior region of MG1 and will not be as informative for examination for possible routes of escape from the midgut. The late second larval instar is a point in which the insect is preparing to enter into the pupal stages when physiological and anatomical changes occur. Moreover, there is clearing of epithelium tissue during the pupal stage making it important to know virus location prior to the pupal stages. Sampling adults 24h after eclosion allowed visualizing the virus infection state shortly after the changes occurred during the pupal stages. Additionally, early adult thrips are more likely to transmit TSWV, and the frequency in transmission of individual thrips decreases with age (van de Wetering et al., 1999; Rotenberg et al., 2009). The 24h-old adult stage was used to test TSWV transmission during a 48h inoculation

access period (IAP). The last time point analyzed, adults 96h after eclosion (4 days old), showed the status of TSWV inside its vector as it ages and corresponded to a point in which the frequency of TSWV transmission by individual thrips is starting to decrease (van de Wetering et al., 1999).

Analyzing the frequency of infection in individual tissues by immunolabeling at each time point in combination to the observed intensity of infection allowed indirect speculation on virus route and infection through the insect life cycle (Tables 4.2 and 4.3; Fig. 4.7 to 4.9). We focus on MG1 as the site for virus entry and main site for replication; and for the interest of this work on salivary gland tissues. Overall, (i) it was observed that TSG infection occurs prior to detection of virus signal in the PSGs. TSWV signal in general was detected in the TSGs since the first time point, 21% in late L1; at the same time point any signal was detected in the PSGs (Fig. 4.7). TSWV was observed in the PSGs at or after L2-72h stage (Fig. 4.7). Additionally, a contingency table for the presence or absence of TSWV in TSGs and corresponding PSGs (n = 53 paired samples) revealed that there is a significant association (co-occurrence, $P = 0.0052$) in the presence or absence of TSWV in TSGs and corresponding PSGs of each individual thrips. This result supports the hypothesis that the TSGs are a route for TSWV spread into the PSGs.

Second (ii), the percentage of infection of MG1 had a significant tendency ($P < 0.0001$) to decrease through the thrips life cycle suggesting that the load of virus decreased from larval to adult stages; at least in terms of G_N detection. Additionally, the apparent intensity and spread of the signal is much lower (Fig. 4.6m and 4.9a). TSWV infection on MG1 apparently behaves inversely to PSG infection because the frequency of TSWV-positive PSGs increases at the adult stages (Fig. 4.7) and the signal intensity is higher in PSGs than in the corresponding MG1s (Fig. 4.6m and 4.9a). Together, these observations suggest that MG1 is the main site of TSWV infection in larval thrips; and conversely, the PSGs are a main site of virus replication in adult thrips. The results and suggestion also support the idea that development has an impact on virus infection because the susceptibility of different organs or virus tropism apparently changes from larval to adult thrips (Ullman et al., 1992).

For experiment one of immunolabeling, MG1 at late L1 stage had the highest percentage of infection (94%) and after this time point, the percentages decreased (Table 4.2) which indirectly may be interpreted as clearing of the virus in certain percentage of the thrips or as areas with less concentration of the virus below the detection limit of the immunolabeling

technique. Infection of PSG was detected for adult thrips but no at larval stages in this experiment and percentage of transmission by adults 24h after eclosion was 86.7% and 93.3% for males and females, respectively. In contrast, PSG frequency of infection for individuals from the same cohort was 100% and 66.7% for females and male, respectively. In the case of the second immunolabeling experiment, a minimal increase in TSWV signal was noticed between L1 and L2 stages (from 91% to 93%) and infection of the PSG was observed at late L2 stage (Table 4.3). Transmission for this cohort of thrips was 80% and 100% for females and males respectively but again the percentage of infection detected by immunolabeling for 24h-old thrips PSGs was lower, with 0 and 50% for females and males, respectively. The results support the idea that certain percentage of TSWV infection is not detected by the immunolabeling technique suggesting that viral infection, or G_N, in some tissues or samples was present at a concentration below the detection level of the technique.

Tracking TSWV through F. occidentalis life cycle by ELISA

To further understand the immunolabeling observations of TSWV in the thrips guts and have additional information on virus titer through development for this strain of virus and isolate of thrips, we tracked TSWV at different time points during *F. occidentalis* life cycle by ELISA using antibodies against the nucleocapsid protein (N). The ELISA results (Fig. 4.13) revealed a general tendency for TSWV to reach a high titer level between late L1 and L2 instars; a noticeable decrease in viral titer during the pupal stages. The virus titer tends to increase again as the adult thrips ages from one to four days after eclosion. By using this approach, TSWV is being tracked at the protein level (as with the immunolabeling approach) but testing against N protein that is a component of the viral ribonucleoprotein and has important functions in virus transcription and replication. In plants, TSWV can exist and move through the plants as RNPs without the need of the viral glycoproteins (Nagata et al., 2000; Sin et al., 2005). Therefore, low levels of G_N may be independent of actual titer of RNP units in thrips cells. Moreover, the ELISA technique is dependent on an enzymatic reaction and spectrophotometry, a more sensitive assay than the immunolabeling technique. In addition to the four time points sampled for immunolabeling, the initial stage of infection (3h after AAP) and the pupal stages: prepupae (P1)

and pupa (P2), were also sampled in two individual acquisition and transmission time-course experiments.

The two ELISA time course experiments (Fig. 4.13) suggested that the virus has a phase of high replication at the initial stages of infection after a 24h AAP. This behavior was suggested by a relatively steep curve in TSWV titer from the initial sampling point, 3h after AAP, to 24h or 48h after AAP. The results were in accordance with the immunolabeling data that suggest that at 3h after AAP there is just a limited infection in the anterior MG1 area just after the CV (Fig. 4.4). Observations at late L1 (Fig. 4.6a to e) tend to show increased distribution and intensity of TSWV signal within MG1; coinciding with the increase of virus titer detected by ELISA (Fig. 4.13). The ELISA experiments agreed with the immunolabeling observations that at late L2 stage the virus signal (Fig. 4.6f to h) or ELISA titer (Fig. 4.13) started to decrease and showed a down peak between the pupal stages and adults 24h after eclosion. After eclosion adult thrips seem to have a low titer of virus and the curves showed a tendency to increase as the adult ages (Fig. 4.13).

The virus titer determined by ELISA and the curve behavior seem to have biological significance since there is accordance between ELISA values and transmission. Experiment B showed relative higher ELISA values throughout the time points and 100% transmission by 24h-old adults. Experiment A had a much lower TSWV titer at 3h after AAP and a relatively lower absorbance value throughout the curve; but a similar general curve pattern than experiment B. In accordance, transmission rate for experiment A was relatively lower in comparison to B (almost significantly different, $P = 0.052$) but still considered a high rate of transmission, 83.3%. Overall, the results lead us to suggest that the initial infection up to the middle of L2 where there is active and high virus replication may be a crucial step for virus-vector interaction and determination of the transmitting status of the resulting adult individuals.

Comparison of adult female and male infection of the salivary glands and its relation to TSWV transmission

The immunolabeling results indicate that there is no difference in the frequency, extent or intensity of infection between female and male PSGs. These findings suggest that there are no differential barriers or factors determining differential TSWV infection of PSG between genders.

Differences that have been noticed for TSWV transmission between female and male adult thrips may be solely due, as hypothesized previously, to different feeding behaviors, with males more prone to transmit TSWV because their feeding behaviors result in a greater number of probes that induce less cell death (van de Wetering et al., 1998; van de Wetering et al., 1999; Stafford et al., 2011). Alternatively, it is possible that barriers exist but under the conditions of the experiments reported herein were not manifested since there were no differences in transmission rate between genders for these experiments (*P*s > 0.05; Table 4.4). Also the sensitivity of immunolabeling is a limitation.

Different comparisons of PSG infection frequencies by TSWV between genders indicate that there are not significant differences between female and male PSGs infection. The general frequency of infection of single PSGs for adult thrips (24 and 96h after eclosion) is similar for females and males, 50% and 54.8% respectively (contingency table, $P = 0.7998$). Whole pairs of PSGs were observed for a total of 27 individuals. These PSGs were separated in three categories: (i) both PSGs on one pair were non-infected; (ii) both PSGs on one pair were infected or (iii) one PSG out of one pair was infected and the second one was non-infected. There is no difference in the frequency of PSGs within these categories between female and male thrips ($P = 1.0$, Fisher exact test; Fig.4.12). Males have a higher percentage (72.5%) of pairs of PSGs infected (one or two lobules) in comparison to female thrips (66.6%); but the percentage of PSGs with both lobules infected out of the total number of infected pairs is higher for females (50%) than males (38.5%). In general a tendency (not statistically significant) for a higher frequency of infection of salivary glands was observed for males.

In agreement with the data on frequency of TSWV infection of PSGs, analysis of the amount and extent of infection also showed no significant differences between female and male thrips. The amount of infection was measured indirectly by the intensity of the fluorescent signal in the PSGs, and a wide range of fluorescence intensity values were recorded for male and female PSGs with no significant difference between genders (Fig.4.10). The extent of infection was measured as the percentage of each PSG area that has fluorescent signal. Likewise, both adult male and female PSGs displayed varying percentages of their area with signal without a significant difference between genders (Fig.4.11).

Discussion

Confocal imaging complemented with cellular stains (for actin and nuclei) enabled a detailed description of *Frankliniella occidentalis*' PSG and TSG morphology. Both types of salivary glands are apparently composed mainly of bi-nucleated cells and have differentiated areas based on different cell morphology and organization. PSGs have three regions, a central (CR) one composed of large bi-nucleated cells that define a branched lumen (L) and two smaller regions at opposite sides of the CR, the basal (BR) and apical (AR) regions composed of small single-nucleated cells. The TSGs have a tubular longitudinal lumen (L) defined by single cells and have a differentiated apical terminus with a clavate section (CS) and a thin apical section (TAS). Both salivary glands seem to be connected by pairs of efferent ducts and by ligament-like filaments that anchor each PSG to the anterior part of MG1, run superficially along each PSG and then extends to apparently attach to the CS of each TSG.

The localization of TSWV within *F. occidentalis* midgut and salivary tissues was determined by immunolabeling of dissected thrips tissues using antibodies against TSWV G_N and conjugates with Alexa Fluor 488 (green signal). TSWV signal was observed at the FG and MG in the digestive system and at the PSG, TSG, ligament-like filament and ED of the salivary tissues. MG1 appeared as a crucial tissue for virus infection of thrips. Initial infection localized and was limited to the anterior part of MG1 (Fig. 4.4) and the whole MG1 seemed to support a higher viral load than the adjacent FG, MG2 and MG3 sections (Fig. 4.7). Also, from this tissue the virus may spread to the PSGs for transmission to occur; thus, MG1 is the initial site of entry into *F. occidentalis* cells, a site of virus replication and a prerequisite for PSG infection.

The route TSWV follows to infect the PSGs is not well clarified. The virus needs to infect, replicate and spread in MG1 and escape to the surrounding muscular cells wrapping the gut epithelium. After this point several possibilities have been proposed and all seem plausible based on our observations. (i) The virus may move by direct contact between the muscular cells of MG1 and the PSGs at larval stages before eclosion of adults in a developmental-dependent process (Moritz et al., 2004). In this work dissection of thrips distorted the actual position of the PSGs, but PSGs appeared to be in contact with the anterior region of MG1 in several samples (Fig. 4.6c) and an apparent different intensity of signal was observed before and after pupation supporting the idea that development has an important impact on virus infection in the thrips tissues. (ii) TSWV may spread to the PSGs by the ligament-like filament anchoring the PSGs to

MG1 (Nagata et al., 1999; de Assis Filho et al., 2002). In accordance with this hypothesis virus signal was observed on 29% of the ligaments. (iii) Based on the results reported in this work, we hypothesize that the TSG and associated ligament and ED are a possible route for the infection of thrips PSGs by TSWV, and by extension of any *Tospovirus*. TSWV signal was observed in TSGs before or simultaneously with its detection in 52% of the corresponding PSGs (Tables 4.2 and 4.3 and Fig. 4.7). The co-occurrence of TSWV signal in TSGs and corresponding PSGs was significant ($P = 0.0052$); and TSWV was also observed in 21% of the ligament and/or ED connections between the two types of salivary glands. The proposed routes are not mutually exclusive and indeed, the three of them may occur. In any case, virions will need to cross non-cellular, extracellular matrix layers which constitute a significant obstacle; however, mechanisms by which virus cross this type of barriers in insects have begun to be elucidated (Means and Passarelli, 2010; Passarelli, 2011). Further research in the route of TSWV into the PSGs, the mechanism it utilizes to cross non-cellular barriers, and the extent of organs infected is required in order to fully understand this aspect of the virus-vector interaction and recognize potential molecules or processes to target in order to block the interaction and control virus transmission.

Observations of TSWV signal pattern and localization in the salivary tissues suggested that TSWV may be exploiting the vesicle trafficking mechanisms of thrips cells (Wijkamp et al., 1993; Ullman et al., 1995; Ohnishi et al., 2001; Walter and Barr, 2011). TSWV signal was observed in TSGs mainly followed the dense actin strands that are apparent along the tubule-like structure (white arrows in Fig. 4.8b, c and e). This pattern suggested that the virus signal localized to the lumen wall or at the union site of a self-folding cell or between adjacent cells. The virus signal was observed as continuous traces of foci at these strands along the TSG suggesting that possibly these foci represent vesicles containing virus particles or vesicles decorated with G_N spanning through their membranes. It also may suggest how the virus is moving from one cell to another by budding out from one cell membrane and getting in by endocytosis in the adjacent membrane. Likewise, TSWV signal was strong at the actin reach lumen of PSGs. As a hypothesis, the signal in the lumen may represent masses of virus particles in the saliva held there by the fixation and size constraints of the ED may prevent washing from the lumen during dissection. Alternatively, the signal that appears to be in the lumen may localize to the wall and cells surrounding the lumen, inside exocytosis vesicles going to discharge their contents into the lumen (Wijkamp et al., 1993).

No differences between thrips gender were found in our trials for PSGs frequency, extent or level of infection, suggesting that there are no differential barriers or susceptibility to TSWV between female and male PSGs. In the two immunolabeling experiments 86.7 and 80% of females transmitted TSWV; meanwhile 93.3 and 100% of males transmitted the virus. Both experiments showed a slightly higher percentage of male transmitters during a 48h IAP; however the differences are not significant. The lack of difference in the frequency, extent and intensity of PSG infection by TSWV in our experiments may be because for the particular AAP events analyzed no gender differences in transmission were observed. The results indicate that the final degree of salivary gland infection was similar for these AAP events. Moreover, the transmission results for the experiments to detect TSWV titer by ELISA in several thrips stages showed similar behavior with no significant differences between genders. Previous results on TSWV transmission experiments previously conducted in our laboratory (Rotenberg et al., 2009) also showed no significant differences in transmission between genders. The strain of the virus, the specific genotype of the thrips colony and other factors during acquisition and development may be not conducive for gender differences in TSWV transmission in our conditions.

Finally, high frequency of TSWV infection in MG1 and high intensity and distribution of virus signal within *F. occidentalis* tissues was observed. It is interesting to question what the effect is of this high virus load on thrips cellular functioning and overall physiology. Several anecdotal observations during this research lead to speculation that TSWV may be pathogenic to thrips in accordance with the idea that tospoviruses evolved from thrips infecting viruses. (i) The results suggested possible virus effects on thrips PSGs size. (ii) In two out of the four total time-course experiments reported herein, a delay in the development of the TSWV-exposed thrips cohort was observed in comparison to TSWV-non-exposed controls. (iii) Clearance by host autophagy mechanism of *Sin Nombre hantavirus* G_N glycoprotein was shown recently (Spiropoulou et al., 2003; Hussein et al., 2012); and autophagy was previously reported for TSWV proteins in *F. occidentalis* cells based on observations by electron microscopy (Ullman et al., 1995). During this work a decrease in the detection of TSWV G_N was observed for MG1. In general G_N signal intensity seemed to decrease even when the frequency of TSWV-positive tissues increased. A possible explanation for this observation may be an autophagy mechanism triggered by G_N (Spiropoulou et al., 2003; Hussein et al., 2012). Understanding the effect (pathological?) of virus replication in insect vectors and the host cellular responses is of

increasing interest for human virus-vector systems (Keene et al., 2004; Girard et al., 2005; Sanders et al., 2005; Girard et al., 2007; Sanchez-Vargas et al., 2009; Bartholomay et al., 2010; Girard et al., 2010; Khoo et al., 2010; Lopez-Montero and Risco, 2011; Sim et al., 2012) and the first steps to study it in the *Tospovirus*-thrips system have been made (Rotenberg and Whitfield, 2010; Badillo-Vargas et al., 2012). Future research toward this question would help to identify host components mediating virus replication and distribution within vectors and would allow recognizing novel targets for control of animal- and plant-infecting viruses.

Materials and Methods

Plant materials and TSWV inoculum

Emilia sonchifolia and *Datura stramonium* plants were kept in a growth chamber set at 24°C and a photoperiod of 14h light/10h dark. TSWV (isolate TSWV-MT2) infected plant tissue for AAP was obtained by mechanical inoculation of two-week old *E. sonchifolia* plants or three-week old *Datura stramonium*. Mechanical inoculation was done using *E. sonchifolia* TSWV-symptomatic tissue from thrips-inoculated plants kept in the greenhouse and no older than two months after exposure to thrips. Infected tissue was ground with -20°C cold mortar and pestle in 10ml of ice-cold 100mM Na_2SO_3 buffer. Plants to be inoculated were dusted with carborundum and gently rubbed with a cotton swab wet with inoculum. Twelve days after mechanical inoculation, symptomatic leaves were harvested and assembled into bouquets and placed into plastic deli cups used for AAP. Similar harvesting of leaf tissue was done for non-inoculated plants of the same age used as control. *D. stramonium* leaf discs were used to test virus transmission from thrips. The third youngest leaf from the apex of four-week old plants was used to obtain 1.5-cm-diameter discs for the inoculation access period (IAP) in transmission assays.

Thrips rearing and acquisition access periods (AAP)

A western flower thrips (*Frankliniella occidentalis*) colony was maintained on green pods (*Phaseolus vulgaris*) as previously described (Ullman et al., 1992). First instar larval thrips (L1s) 0 to 8 hours old were collected from green beans obtained from the colony; where previously adult thrips have fed and laid eggs. The beans were brushed to clean from any thrips

and placed on plastic cups and incubated for 8h to allow eggs to hatch. Collected L1s were allowed to feed on TSWV-infected and healthy *E. sonchifolia* leaf tissue on independent plastic cups for an acquisition access period (AAP) of 18h in an incubator at 25°C with a photoperiod of 12h light and 12h dark. After the AAP, thrips were transferred to cups with green beans and kept in the incubator. Every three days, new green beans were added and the old ones looking dry or getting spoiled were removed.

Sampling points for thrips immunolabeling time course experiment

Thrips were sampled after the AAP at four time points throughout their life cycle at two independent experiments in order to collect individual thrips for dissecting and immunolabeling. The sampling points were first instar larval thrips 24h after AAP, second instar larval thrips 72h after AAP, adult thrips 24h and 96h after adult eclosion. Approximately 40 individuals were picked per time point and treatment (TSWV-exposed and non-exposed) with a fine paint brush under a dissecting stereoscope and placed into a plastic cup cover with a double layer of parafilm for three hours. One hundred microliters of 7% sucrose solution are loaded in between the parafilm layers for thrips to feed on it and clear their guts from any plant material to avoid interference or background fluorescent signals due to presence of antigen in the gut lumen. The time points to sample were selected in accordance with the following criteria: (i) to observe virus infection of the larval thrips at a relatively early point (L1 24h, that is a 45-53h old thrips [0-8h hatching + 18h AAP + 24h after AAP + 3h clearing]) and at the end of the larval life stage before going into prepupa stage (L2 72h, that is 93-101h old thrips). Then, the interest was to sample adult thrips relatively young, 24 h after eclosion that we used in the laboratory consistently for inoculation access periods (IAP) in transmission experiments. Last, a relatively older adult, 96 h (four days) after eclosion, was sampled in order to evaluate the viral infection in the tissues as adult thrips age.

Dissecting and Immunolabeling of thrips guts and salivary glands

Thrips were dissected by head decapitation method to obtain the gut and salivary glands and these tissues were fixed and immunolabeled (Bressan and Watanabe, 2011)(Whitfield et al., 2004). Individual thrips were placed on a glass slide with ice-cold phosphate buffer-saline (PBS) and the head was decapitated using Teflon coated razor blades under a dissecting stereoscope.

The abdomen was gently pressed to help the gut and attached salivary glands to come out of the body cavity. The thrips was moved to a Tissue tack slide (Polysciences Inc., Warrington, PA, USA) and placed on a drop of ice-cold PBS surrounded by an incubation chamber (Electron Microscopy Sciences, Hatfield, PA, USA). The gut was cut off the body by aiming to cut at the foregut but it also happened at MG3 or MG2 depending on how much of the gut was exposed outside the body cavity. After processing all the guts intended for the slide, the whole incubation chamber area was covered with PBS and the slide was left to sit on an ice-cold surface inside a humid box for several minutes. PBS was removed and the slide was left to sit for some minutes until it is almost air dried. The incubation chamber was filled with 4% paraformaldehyde in 50 mM sodium phosphate (pH 7.0) and incubated for 1 hour at room temperature in a humid box. The slide was rinsed once with PBS and left overnight at 4°C with PBS-1% Triton X-100. Next day all incubations were done at room temperature in a rocker with slight movement inside a humid box. The slide were washed three times with PBS and incubated in blocking buffer (PBS, 0.1% Triton X-100 and 10% normal goat serum (NGS)) for 30min. After blocking, the guts and salivary glands were incubated with peptide rabbit antibody against TSWV glycoprotein G_N at a concentration of 50 µg/ml in PBS supplemented with 0.1% Triton X-100 and 1% NGS for 2.5h. The following remaining incubations were done in a humid box wrapped in aluminum foil to protect the slides from the light. The slides were washed three times with PBS and incubated with chicken anti-rabbit antibody conjugated with Alexa Fluor 488 (Invitrogen, Carlsbad, CA, USA) at 10 µg/ml in PBS supplemented with 0.1% Triton X-100 and 1% NGS for 2.5h. The slides were washed three times with PBS and incubated for 2 hours with phalloidin conjugated to Alexa Fluor 594 and with DAPI (4',6-diamidino-2-phenylindole, dihydrochloride) at 4 units/ml and 125 µg/ml respectively (Invitrogen). The slides were washed three times with PBS and then rinsed three times with distilled water. The incubation chamber was removed and the slides air dried. Thirty-five microliters of PBS-50% glycerol were added on the area were the guts were placed, covered with a cover slip and sealed with nail polish. Slides were kept at 4°C and protected from light. The procedure for infection of thrips and immunolabeling were optimized during two independent preliminary experiments. Initial infection of *F. occidentalis* by TSWV, 3h after AAP, was evaluated during these two preliminary experiments without the use of actin marker (phalloidin Alexa Fluor conjugate 495).

Confocal fluorescent microscopy

The slides for the preliminary tests on initial TSWV infection of thrips midgut were observed by confocal fluorescence microscopy with a Zeiss LSM 700 Confocal Laser Scanning microscope with Zen Efficient Navigation software and 40X oil- immersion objective with variable scan zooms using channels for bright field, blue signal (405nm, laser at 2%) and green signal (488nm, laser at 2%) and a short pass filter, SP490. Gains and pinholes were adjusted for bright field and blue signal at each image; meanwhile, green channel gain (550) and pinhole (119µm) was kept constant.

The slides of thrips guts and salivary tissues from the time course experiments were observed by confocal fluorescence microscopy with a Zeiss Axiovert 200M confocal microscope eq(Sutula et al., 1986)uipped with a Zeiss Laser Scanning System LSM 510 META for image acquisition. Images were observed and handled with Zeiss LSM Image Browser Version 4.2.0.121. The confocal microscope settings were: a 405 nm laser diode at 5% transmission for detecting DAPI fluorescence with a bandpass (BP) filter 420-480 nm and pinhole aperture of 56 µm; a 488 nm Argon laser at 5% transmission for detecting Alexa Fluor 488 with a BP filter 505-530 nm and pinhole aperture of 64 µm; and a 543nm HeNe laser at 80% transmission for exciting Alexa Fluor 594 with a BP filter 585-615nm and pinhole aperture of 76 µm. Gain was fixed at 500 for the green channel in order to be able to compare the intensity of TSWV signal among images. Gain settings for the other channels were adjusted as necessary in order to obtain the best detail of nuclei and actin in each image as well as the bright field background. To study the tissue and acquire images a 40X oil- immersion objective was used with variable scan zoom. Differential interference contrast (DIC, also known as Nomarski Interference Contrast, NCI) method was used to visualize the bright field. Z-stacks were taken at the four channels with an automatic calculated optimum of 0.37µm per slide and projections were generated selecting the option for maximum transparency.

Time course experiments tracking TSWV by ELISA in F. occidentalis

To gain more information on TSWV infection of *F. occidentalis*, TSWV titer was determined at different time points in the life cycle of *F. occidentalis* by DAS-ELISA (Agdia Inc., Elkhart, IN, USA) with antibodies against TSWV nucleocapsid (N) protein in two

independent acquisition and transmission cohorts of thrips (experiments) following AAP, IAP and conditions as described herein in the other sections. The time point samples included the four time points from the immunolabeling experiments and in addition, L1 thrips 3h after AAP, L2 thrips 120h after AAP for experiment A; prepupae (P1) and pupae (P2) stages. Six samples consisting of 15 thrips pooled together were tested by ELISA per time point and absorbance average value was used as an estimate of the relative virus titer at the corresponding time point.

Transmission Assay

A transmission assay utilizing individual thrips and *Datura stramonium* leaf discs was used to determine the transmission rate of each cohort (experiment) of thrips. Fifteen female and fifteen male adults, 24h after eclosion, were randomly picked from the TSWV-exposed cohort of thrips. Each thrips was placed in a 15 ml centrifuge tube with a 1.5 cm *D. stramonium* leaf disc for an Inoculation Access Period (IAP) of 48h. A piece (ca. 2x2cm) of Kimwipe tissue was placed at the bottom of the tube to absorb excess of humidity. The tubes were kept in an incubator at 25°C with a photoperiod of 12h light and 12h dark. After the IAP, the leaf discs were floated on tap water (24-well plates) for four days to allow virus replication in the plant tissue. The number of leaf discs infected with virus was determined by DAS-ELISA using commercial antibodies against TSWV (Agdia Inc.). Leaf discs were ground in 4°C-cold general extraction buffer (GEB) and the ELISA proceeded as indicated by the manufacturer's protocol. Absorbance of plates was read after one hour at 405nm, and samples with absorbance values higher than 3 times the mean absorbance values of controls (virus-free leaf discs) were considered positive (Sutula et al., 1986).

Quantitative analysis of PSGs images: fluorescence signal and size parameters

In order to relatively compare TSWV infection in the individual PSGs between female and male adult thrips, ImageJ software was used to analyze TSWV fluorescence signal. Each image was opened in ImageJ software, and the color channels were split into individual images. All individual images were closed except for the image for the green channel that was converted to an 8-bit gray image and the automatic scale removed to obtain pixels as the units of the measurements thus that images at different magnifications are comparable because the properties

measured are all in pixels. The exact area of MG1 was delimited with the freehand selection tool and several properties of the area of interest were measured using the 'Measure' option including: Area, Mean Intensity, Percentage of Area or Area Fraction ('%Area'), and Raw Integral Density ('RawIntDen').

TSWV relative level of infection was indirectly estimated from the fluorescence data by quantifying the mean intensity of the fluorescent signal for TSWV (green channel, Alexa Fluor 488) in PSGs. The mean intensity of the green fluorescent signal (MIS, arbitrary units) was calculated as the RawIntDen divided by the area with fluorescent signal (*MIS= RawIntDen/[(Area*%Area)/100]*). The degree of spread of TSWV infection within the tissue was indirectly estimated from the percentage of area with green fluorescent signal (%Area) from the total area of the PSG (Area). Additionally, the length of vertical and horizontal axis, the perimeter and the area of each PSG was measured using Zeiss LSM Image Browser v.4.2.0.121 capabilities.

Statistical Analyses

Data sets were tested for normality and the appropriate transformations and tests conducted (parametric or non-parametric) using commercial statistic software (Minitab v.14 and Graphpad Prism v.5). Size parameters were compared between genders by t-tests and by general linear models for a two-way analysis of variance (ANOVA) for the fixed factors gender and infection-status. Area of PSGs was transformed by root square to obtained a normalized distribution and included in ANOVA analyses; otherwise non-transformed area was compared between genders by the Mann-Whitney test. Analyzes of frequency of TSWV detection by immunolabeling were done by contingency tables and Fischer exact test. ELISA time-course data sets were tested by Kruskal-Wallis test followed by Dunn's multiple comparison test. Analysis of transmission frequency between genders and among experiments and different comparisons for the frequency of PSGs infection and between genders was analyzed by contingency tables and Fishers exact tests. Intensity and spread of TSWV signal in PSGs was compared between genders by the Mann-Whitney test.

Tables and Figures

Table 4.1. Size parameters[1] measured for the principal salivary glands of adult *Frankliniella occidentalis* individuals.

Gender	Long axis (µm)	Short axis (µm)	Perimeter (µm)	Area (µm^2)
Females	125.17 ± 5.09	57.91 ± 2.40	303.18 ± 11.83	5798.73 ± 385.97
(*n* = 34)	(59.82 – 180.49)	(27.30 – 85.34)	(157.90 – 461.49)	(1512.75 – 11142.68)
Males	97.90 ± 3.52	47.80 ± 1.78	244.80 ± 8.90	3842.92 ± 248.23
(*n* = 45)	(48.99 – 153.88)	(26.01 – 85.10)	(133.97 – 435.82)	(1653.72 – 7711.12)

[1] Averages are given with the standard error and in parenthesis the range of the measurements

Table 4.2. Percentage of tissues determined as positive for TSWV presence by immunolabeling with antibodies against G_N glycoprotein for immunolabeling experiment 1.

	Percentage of TSWV-positive thrips (total positive / total observed) by life stage[1] and gender							
			Adults, 24h			Adults, 96h		
Structure	L1, 24h	L2, 72h	Cohort	Females	Males	Cohort	Females	Males
Overall infection	93.8 (15/16)	60.9 (14/23)	72.2 (13/18)	57.1 (4/7)	81.8 (9/11)	56.8 (21/37)	52.4 (11/21)	62.5 (10/16)
Foregut (FG)	25.0 (4/16)	0 (0/23)	25.0 (3/12)	0 (0/3)	33.3 (3/9)	29.7 (11/36)	25.0 (5/20)	37.5 (6/16)
Midgut-1 (MG1)	93.8 (15/16)	60.9 (14/23)	66.7 (10/15)	50.0 (2/4)	72.7 (8/11)	48.6 (18/36)	40.0 (8/20)	62.5 (10/16)
Midgut-2 (MG2)	7.7 (1/13)	14.3 (3/21)	45.5 (5/11)	33.3 (2/6)	60.0 (3/5)	29.7 (11/28)	44.4 (8/18)	30.0 (3/10)
Midgut-3 (MG3)	0 (0/2)	0 (0/3)	25.0 (1/4)	0 (0/1)	33.3 (1/3)	8.1 (3/10)	25.0 (2/8)	50.0 (1/2)
Principal Salivary Glands (PSG)	0 (0/10)	0 (0/27)	80.0 (8/10)	100 (4/4)	66.7 (4/6)	29.7 (11/22)	58.3 (7/12)	40.0 (4/10)
Tubular Salivary Glands (TSG)	35.3 (6/17)	0 (0/39)	23.1 (3/13)	0 (0/6)	42.9 (3/7)	16.2 (6/34)	19.2 (5/26)	12.5 (1/8)
Ligament/ED PSG-TSG	66.7 (2/3)	0 (0/14)	75.0 (3/4)	50.0 (1/2)	100 (2/2)	0 (0/9)	0 (0/5)	0 (0/4)
Ligaments PSG-MG1	0 (0/2)	0 (0/7)	100 (3/3)	100 (1/1)	100 (2/2)	0 (0/1)	0 (0/1)	0 (0/0)

[1] Life stages are first instar (L1) and second instar (L2) larvae 24 and 72 hours after an 24 h acquisition access period (AAP) on TSWV-infected or non-infected *Emilia sonchiflora* tissue; and adult thrips 24 and 96 hours after eclosion.

Table 4.3. Percentage of tissues determined as positive for TSWV presence by immunolabeling with antibodies against G_N glycoprotein for immunolabeling experiment 2.

	Percentage of TSWV-positive thrips (total + / total observed) by life stage[1] and gender							
			Adults, 24h			Adults, 96h		
Structure	**L1, 24h**	**L2, 72h**	**Cohort**	**Females**	**Males**	**Cohort**	**Females**	**Males**
Overall infection	90.9 (20/22)	92.9 (13/14)	59.3 (16/27)	53.8 (7/13)	64.3 (9/14)	64.0 (16/25)	70.0 (7/10)	60.0 (9/15)
Foregut (FG)	4.5 (1/22)	28.6 (4/14)	13.0 (3/23)	23.1 (3/13)	0 (0/10)	25.0 (5/20)	40.0 (4/10)	10.0 (1/10)
Midgut-1 (MG1)	90.9 (20/22)	92.9 (13/14)	56.0 (14/25)	53.8 (7/13)	58.3 (7/12)	38.1 (8/21)	50.0 (5/10)	27.3 (3/11)
Midgut-2 (MG2)	10.5 (2/19)	60.0 (6/10)	22.2 (4/18)	22.2 (2/9)	22.2 (2/9)	18.8 (3/16)	37.5 (3/8)	0 (0/8)
Midgut-3 (MG3)	0 (0/12)	75.0 (3/4)	0 (0/6)	0 (0/3)	0 (0/3)	0 (0/3)	0 (0/3)	0 (0/0)
Principal Salivary Glands (PSG)	0 (0/8)	40.0 (2/5)	29.4 (5/17)	0 (0/7)	50.0 (5/10)	64.7 (11/17)	100.0 (1/1)	62.5 (10/16)
Tubular Salivary Glands (TSG)	9.5 (2/21)	56.3 (9/16)	7.1 (2/28)	0 (0/12)	12.5 (2/16)	25.0 (5/20)	30.8 (4/13)	14.3 (1/7)
Ligament/ED PSG-TSG	0 (0/5)	0 (0/0)	7.7 (1/13)	0 (0/5)	12.5 (1/8)	46.7 (7/15)	50.0 (1/2)	46.2 (6/13)
Ligaments PSG-MG1	0 (0/4)	0 (0/0)	25.0 (1/4)	0 (0/1)	33.3 (1/3)	25.0 (4/16)	0 (0/1)	26.7 (4/15)

[1] Life stages are first instar (L1) and second instar (L2) larvae 24 and 72 hours after an 24 h acquisition access period (AAP) on TSWV-infected or non-infected *Emilia sonchiflora* tissue; and adult thrips 24 and 96 hours after eclosion

Table 4.4. Transmission[1] of *Tomato spotted wilt virus* (TSWV) by individual *Frankliniella occidentalis* adults 24 hours after eclosion (n = 30) for five experimental cohorts.

	Percentage of TSWV transmission by individual thrips (number of TSWV transmitter thrips/total thrips tested)		
Experiment	**Females**	**Males**	**Cohort**
Immunolabeling-1[1]	86.7% (13/15)	93.3% (14/15)	90.0% (27/30)
Immunolabeling-2	80.0% (12/15)	100% (15/15)	90.0% (27/30)
ELISA curve-A	73.3% (11/15)	93.3% (14/15)	83.3% (25/30)
ELISA curve-B	100% (15/15)	100% (15/15)	100% (30/30)
Totals	**85.0% (51/60)**	**96.7% (58/60)**	**90.8% (109/120)**

[1] TSWV transmission was determined by ELISA with antibodies against TSWV nucleocapsid (N) protein done on leaf disc samples in which thrips were fed for a 48h inoculation access period. There were no significant differences between females and males at any experiment or in total (*P*s > 0.05, Fisher exact test).

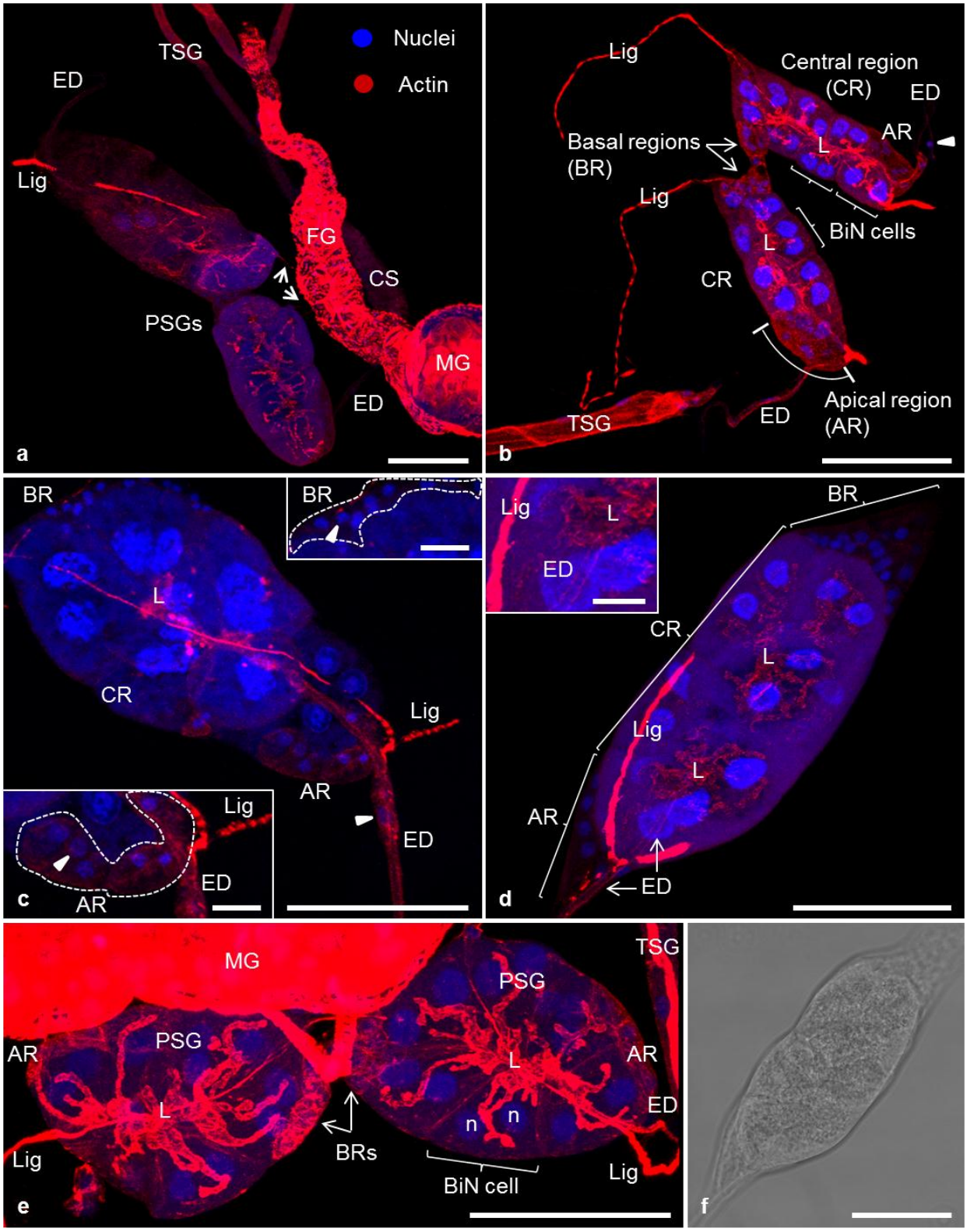

Figure 4.1. Morphology of principal salivary glands (PSGs) of *Frankliniella occidentalis*.

The morphology of *F. occidentalis* PSGs was observed by confocal fluorescent microscopy with actin (red color, phalloidin conjugated to Alexa Fluor 594) and nuclear (blue color, DAPI) markers. Pair of PSGs from a female thrips 24h after eclosion showing the general organization of PSGs and comparison to other associated tissues, foregut (FG), midgut (MG), tubular salivary gland (TSG) and its clavate section (CS). The efferent ducts (ED) from both PSGs are shown and the section of each ligament (Lig) connecting the PSGs to the MG is signaled by thick white arrows. Adult PSGs are elongated structures (a). Three regions are distinguished in the PSGs: a basal region (BR), central region (CR) and apical region (AR), and are highlighted for a male 24h (b), a male 96h (c), a female 96h (d) after eclosion and for late L1 thrips (e). The CR is composed of bi-nucleated cells (BiN) with large nuclei (n) (b, e) and the BR and AR are composed of smaller single-nucleated cells. Insets in panel c show magnifications of this regions and arrow heads signal to a single small nucleus. The ligaments run attached to the surface of each PSGs and project in opposite directions (b, c, e). A branched lumen (L) highlighted by actin staining is found in the CR of each PSG (b, c, d, e) and an ED drains out the contents of the lumen (c, d).Arrow head in panel b and c signal a nucleus in the ED. Inset in panel d shows the transition from the lumen to the ED still inside PSG. Larval PSGs have the similar organization as in adults; but are rounder in shape (e). Bright field image of the translucent PSG (same of panel d) is shown in f. Scale bars represent 50 µm in main panels and 10 µm in inset panels.

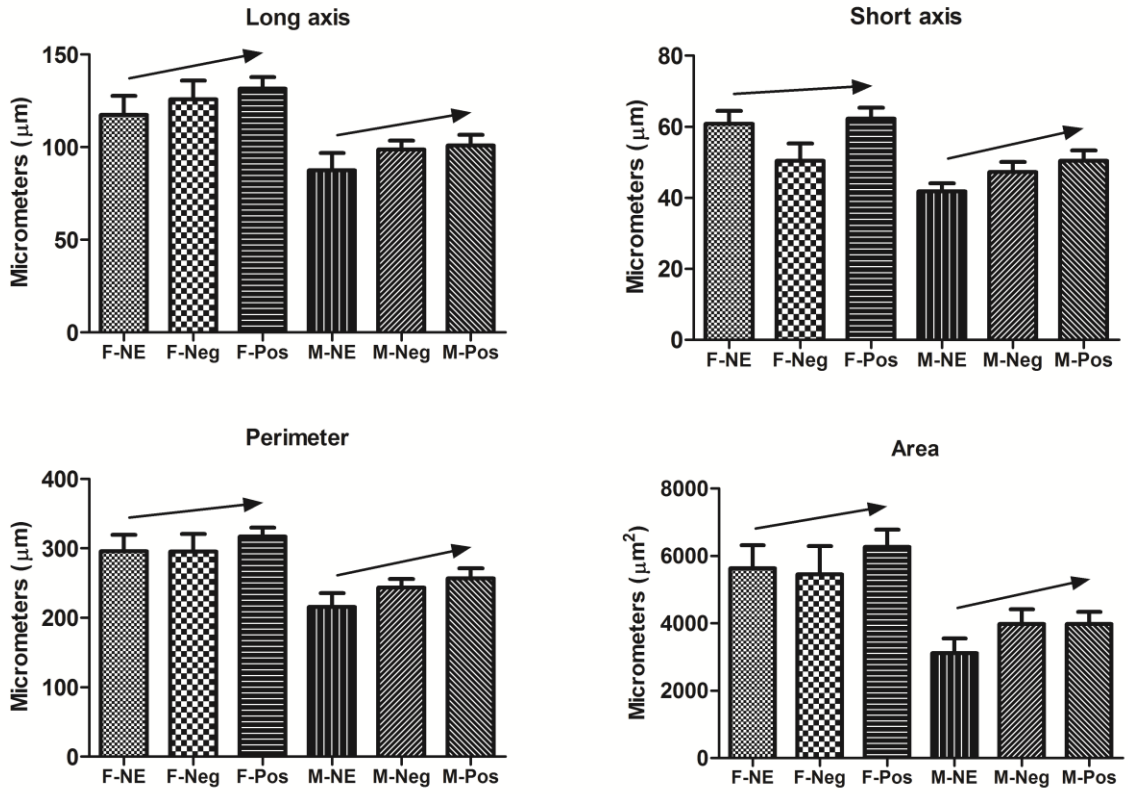

Figure 4.2. Size parameters measured for principal salivary glands (PSGs) of adult *Frankliniella occidentalis* individuals 24 and 96 hours after eclosion.

PSGs measures were separately analyzed by *Tomato spotted wilt virus* (TSWV) infection status: non-exposed (NE), exposed but determined virus negative (Neg) and exposed and determined virus positive (Pos); and by gender: females (F) or males (M). Arrows (line slope generated by connecting the average value of NE with the average value of Pos) show the tendency of size parameter to increase, for both genders, from non-exposed individuals to exposed and positive ones. The tendency observed in response to infection status and gender was not significant for the parameter infection status in a 2-way ANOVA, *P* = 0.235, 0.073, 0.272 and 0.363, for long axis, short axis, perimeter and area, respectively.

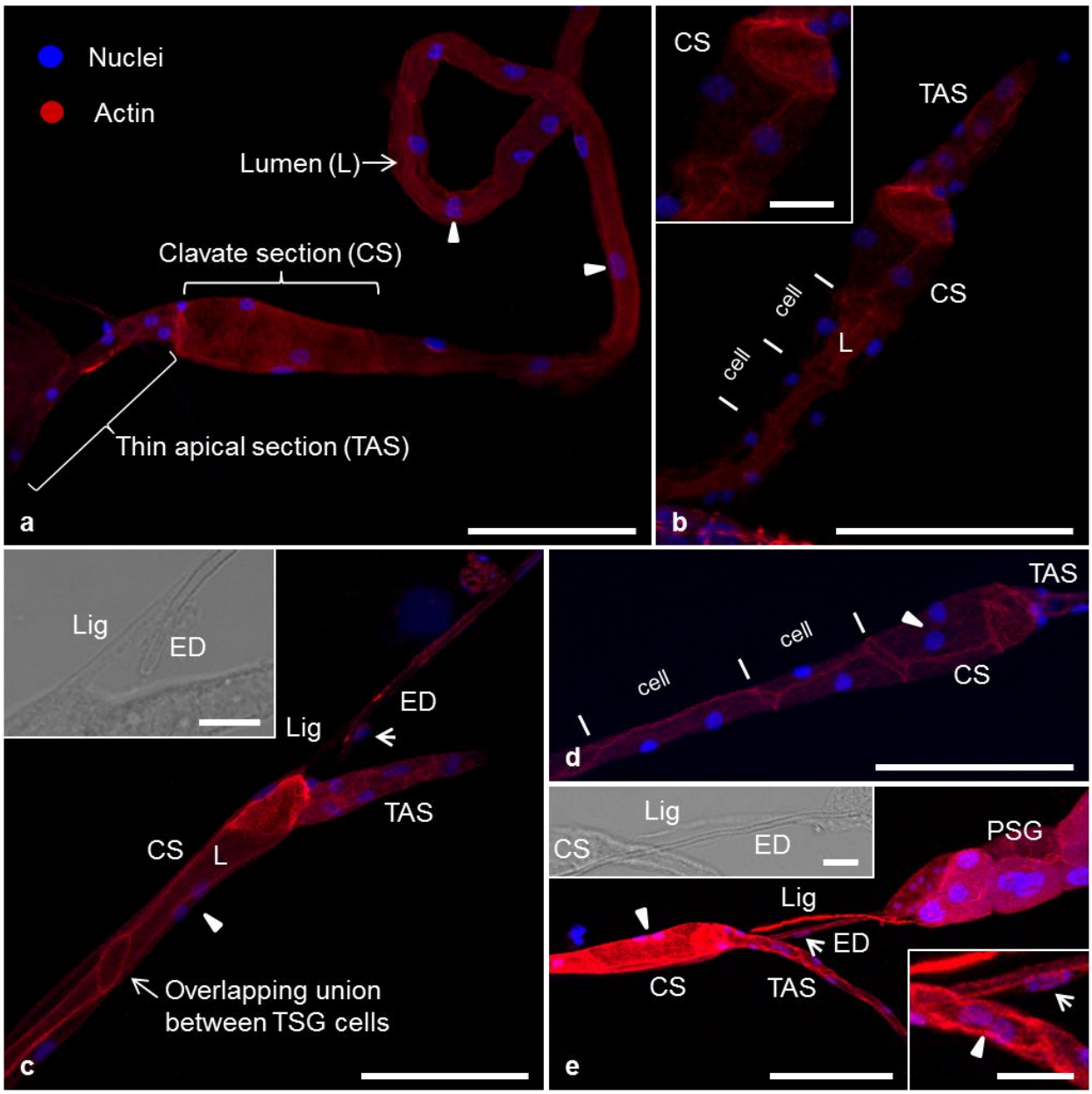

Figure 4.3. Morphology of the tubular salivary glands (TSGs) of *Frankliniella occidentalis*. TSGs were observed by confocal fluorescent microscopy with actin (red color, phalloidin conjugated to Alexa Fluor 594) and nuclear (blue color, DAPI) markers. TSG images are shown for female 96 h after eclosion (hae) (a, c), late L1 (b), male thrips 96 hae (d) and 24 hae (e). The TSGs are tubule-like structures with a lumen (L) cavity running along the structure. The apical section is differentiated with a clavate section (CS) and ending in a thin and blunt apical section (TAS). Cells in the TSG appear to be bi-nucleated as suggested by pairs of nuclei (arrow heads) (a). The clavate section has a differentiated

organization and the lumen seems to enlarge at this point (b and inset in b). The TSGs appear to be composed of cells attached one after another longitudinally by slanted, overlapping unions as the actin staining highlights (b, c, d). A ligament (Lig) and efferent duct (ED) connecting each TSG with a corresponding PSG are observed in association with the CS (c, e, and insets for bright field details). A single nucleus is marked by a thick white arrow in the ED (c, e). The TAS section is composed by few smaller cells that appear to have pairs of nuclei (arrow head in bottom-right inset in e). Scale bars represent 50 µm in main panels and 10 µm in inset panels.

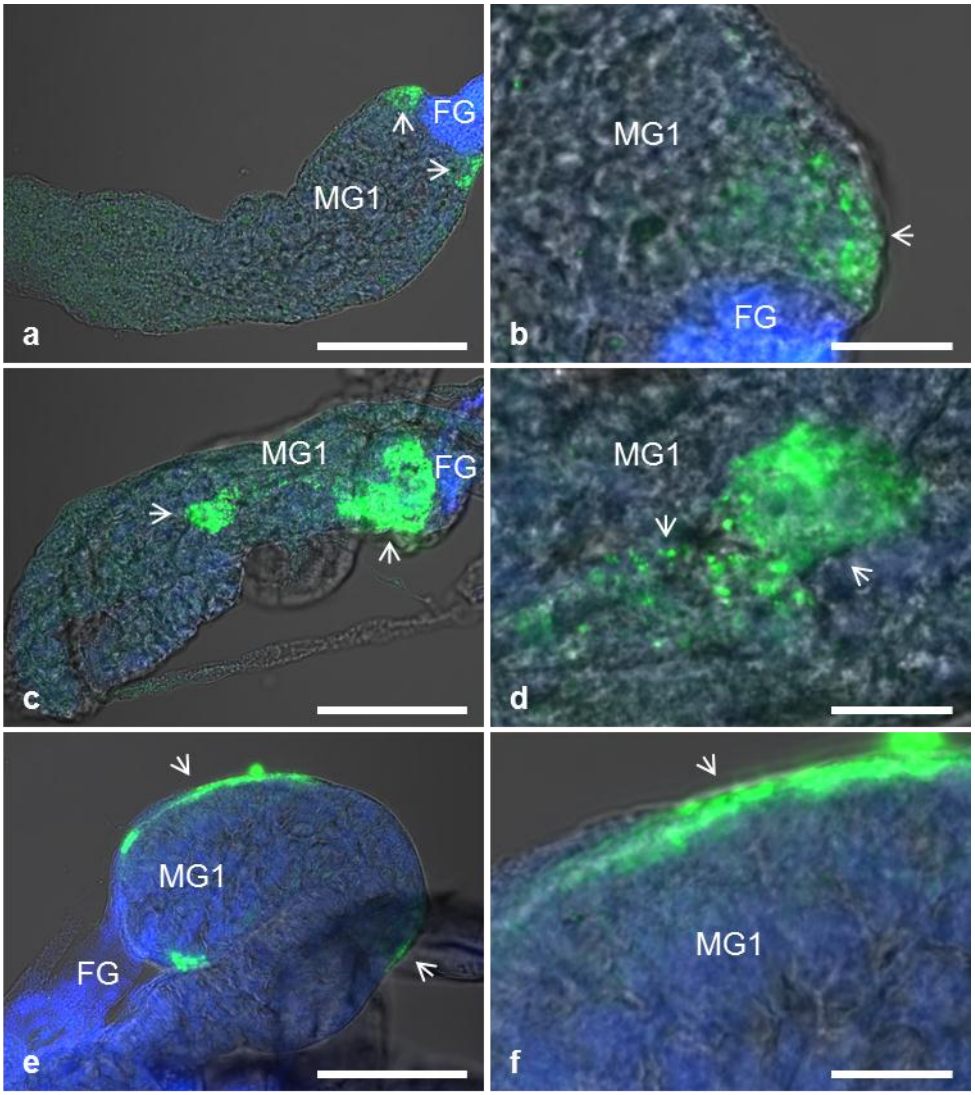

Figure 4.4. Initial infection of *Frankliniella occidentalis* by *Tomato spotted wilt virus* (white arrows) is detected as localized fluorescence in the anterior region of midgut 1 (MG1) just after the foregut (FG).

Initial infection was visualized in late first instar thrips three hours after a 24 hours acquisition access period on TSWV-infected plant tissue. TSWV infection started as discrete foci in MG1 next to the CV (a and b); the infection seemed to distribute through MG1 with the appearance of secondary foci of infection (c and d) or the virus apparently localized to the muscular cells surrounding the midgut epithelial cells (e and f). *F. occidentalis* digestive track was observed by confocal fluorescent microscopy using peptide polyclonal rabbit anti-G_N antibodies and a secondary Alexa Fluor 488 conjugated. Counterstaining was done with DAPI. Images are a merge of bright field (DIC), green and

blue channels. Panels b, d and f are magnifications of panels a, c and e, respectively. Scale bars represent 50 µm in a, c and e; and 10 µm in b, d and f.

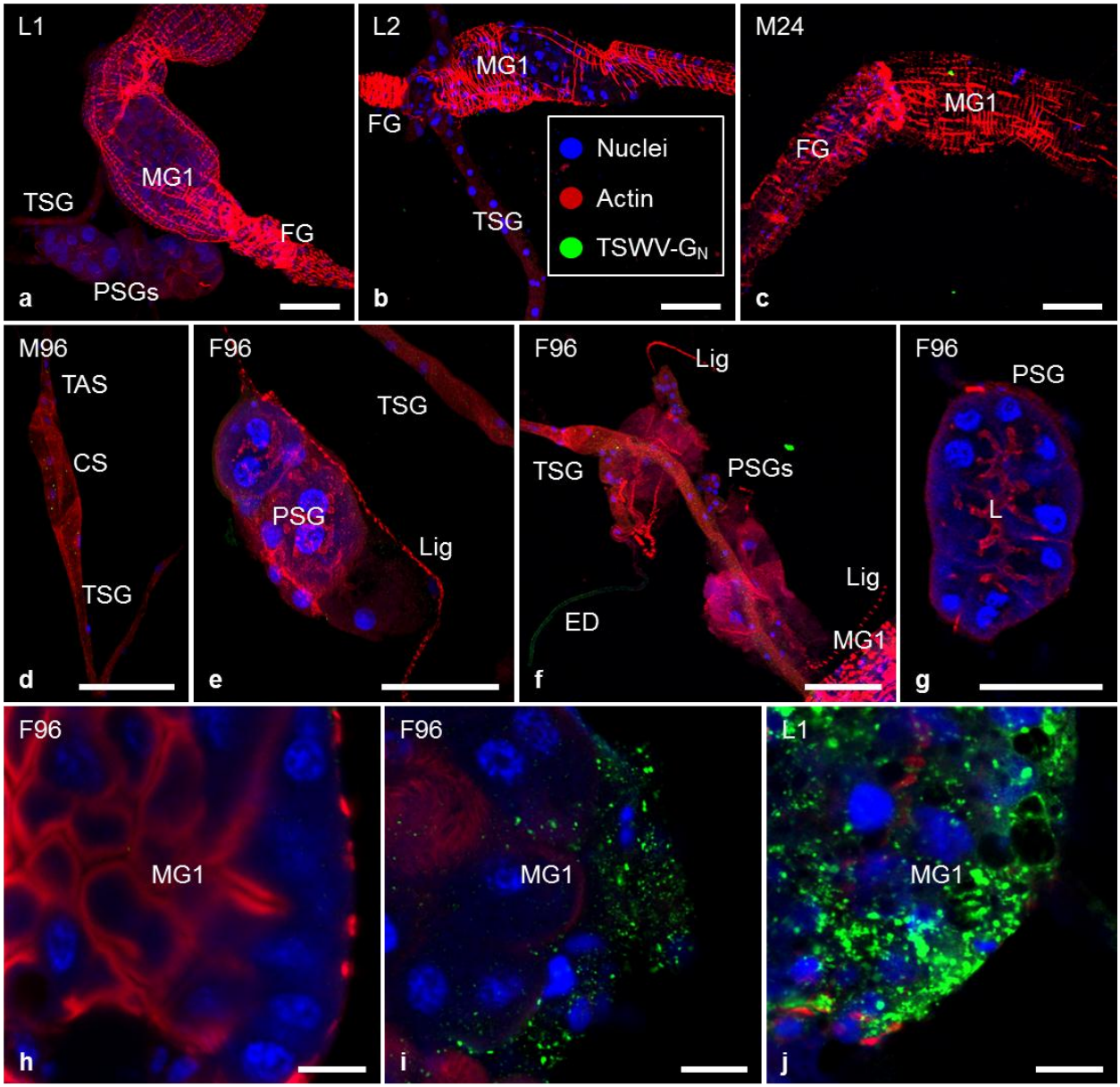

Figure 4.5. Background and TSWV-associated signals in *Frankliniella occidentalis* guts and salivary tissues after immunolabeling procedures.

Background signal observed in *Frankliniella occidentalis* guts and salivary tissues from *Tomato spotted wilt virus* (TSWV) non-exposed individuals after immunolabeling with antibodies against TSWV G_N glycoprotein and secondary Alexa Fluor 488 conjugated

antibody. Also, tissue was treated with cell marker stains for actin (phalloidin conjugated to Alexa Fluor 495) and nuclei (DAPI). Foregut (FG), midgut region 1 (MG1), principal salivary glands (PSGs), tubular salivary glands (TSGs) and associated structures, ligament-like filament (Lig) and efferent duct (ED) are shown. Background signal (random spots) is noticeable in c to f; and auto-fluorescence of the ED is observed in f. A detail of non-infected MG1 tissue is shown in h and TSWV-infected MG1 are shown in i and j for comparison. Scale bars represent 50 µm (a-g) and 10 µm (h-j). Images depict four time points sample during the research: late first (L1) and late second (L2) larval instars, and adult females (F) and males (M) 24 and 96 hours after a 24 hours acquisition access period.

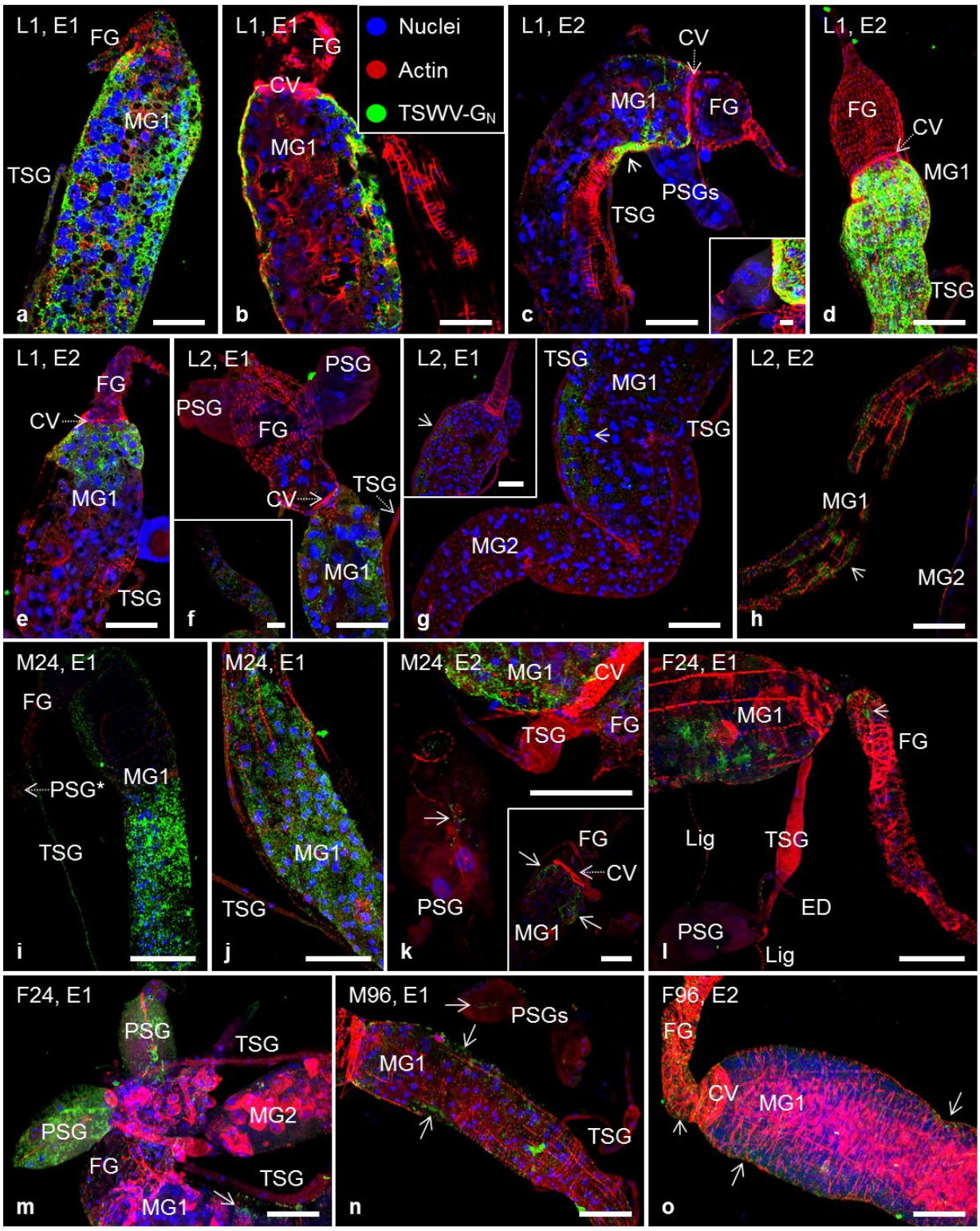

Figure 4.6. ***Tomato spotted wilt virus*** **(TSWV) infection of** ***Frankliniella occidentalis*** **midgut (MG) and associated tissues at four time points during the thrips life cycle.**

TSWV was detected by confocal fluorescent microscopy with an Alexa Fluor 488 conjugate to signal TSWV G_N presence, and marker for actin (red color, phalloidin conjugated to Alexa Fluor 594) and nucleus (blue color, DAPI). Time points were late first instar larvae (L1), late second instar (L2) thrips, adult thrips, females (F) or males (M) 24 or 96 hours after eclosion from two independent experiments (E1 and E2). TSWV infection was first observed in the first section of the midgut (MG1) of L1s as high signal throughout all the tissue in E1 and E2 (a, b, d) or as initial infection limited to the anterior region of MG1 in E2 (c, e). TSWV signal was less intense and with a reduced spread in second larval instar individuals (f-h). In adults, TSWV signal was mostly limited (white whole arrows) to small foci and with relative low intensity (i-o). Tubular salivary glands (TSGs) and principal salivary glands (PSGs) are observed with signal in some occasions. Signal in the foregut (FG) and second section of the midgut (MG2) was seem seldom, very localized and with low intensity. Dashed arrows signal specific structures when the tags are not directly on or next to the structure. White whole lines signal areas of TSWV signal and an asterisk (*) indicates a degraded tissue due to dissection. Scale bars represent 50 µm, except for inset in panel c that represents 10 µm. Insets depict details of the main panel or other tissues from the same individual from the main panel.

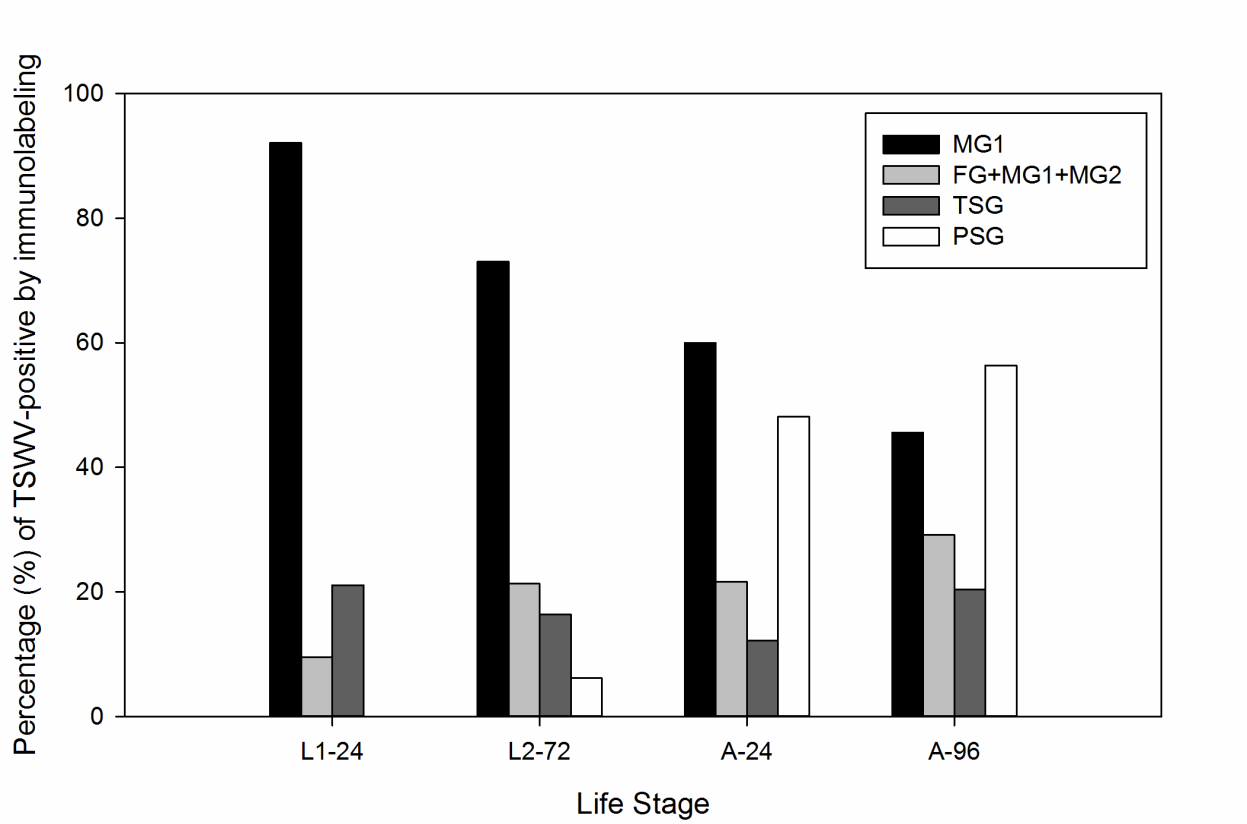

Figure 4.7. Percentages for the total number of *Tomato spotted wilt virus* (TSWV) positive tissues observed at four time points through *Frankliniella occidentalis* life cycle. Combined results from in two independent immunolabeling experiments. Tissues displayed in the graph are (i) midgut region 1 (MG1), (ii) combined data for foregut and midgut regions 2 and 3 (FG+MG2+MG3), (iii) tubular salivary glands (TSG) and (iii) principal salivary glands (PSG). TSWV was detected using antibodies against G_N protein and Alexa Fluor 488 secondary conjugates. Time points were late first instar larvae 24 hours after acquisition access period (haa, L1-24); second instar larvae 72 haa (L2-72), adult thrips 24 (A-24) and 96 (A-96) hours after eclosion (hae). Overall the change in the percentage of TSWV-positive tissues observed over time is significant for MG1 ($P < 0.0001$), FG+MG2+MG3 ($P = 0.0105$) and PSG ($P < 0.0001$) as determined by Fisher exact test.

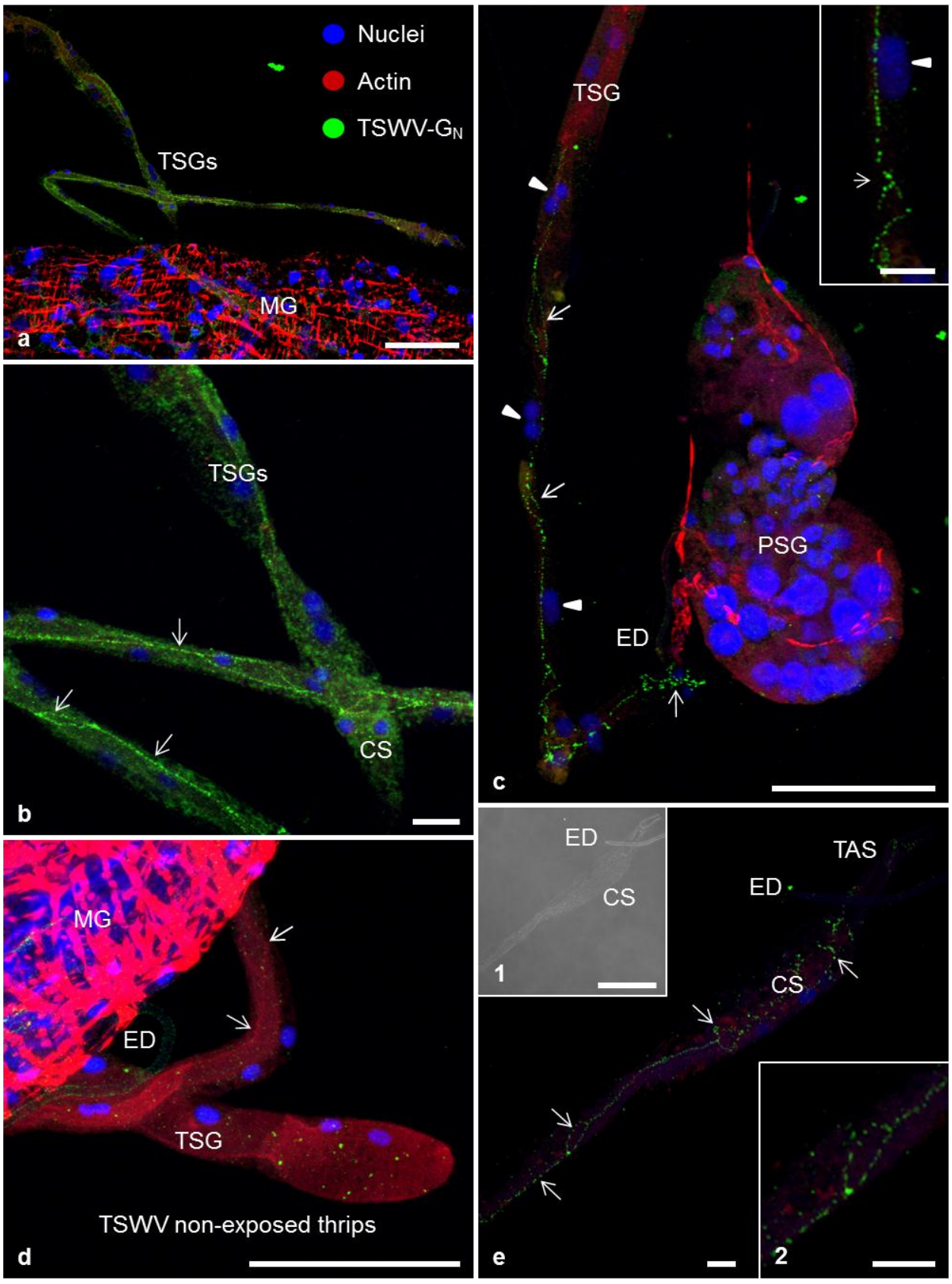
Nuclei
Actin
TSWV-G$_N$
TSGs
MG
a
TSGs
CS
b
TSG
PSG
ED
c
MG
ED
TSG
TSWV non-exposed thrips
d
ED
CS
1
TAS
ED
CS
e
2

Figure 4.8. *Tomato spotted wilt virus* infection of *Frankliniella occidentalis* tubular salivary glands (TSGs).

TSWV was detected by confocal fluorescent microscopy with an Alexa Fluor 488 conjugate to signal TSWV G_N presence, and marker for actin (red color, phalloidin conjugated to Alexa Fluor 594) and nucleus (blue color, DAPI). L1 TSGs (a-c) depicting TSWV signal generalized throughout all the TSGs (a, b) and with higher intensity (b) or only signal in larvae (c) and adults (e) localizing as small foci along high actin lines along the gland that appear to delimit the lumen and the union between cells (white arrows, b, c). Arrow head signal pairs of nuclei from a single bi-nucleated cell (c). TSWV non-exposed TSG from a female thrips (d) depicting the average background observed for TSGs and dull auto-fluorescence of the efferent duct (ED).

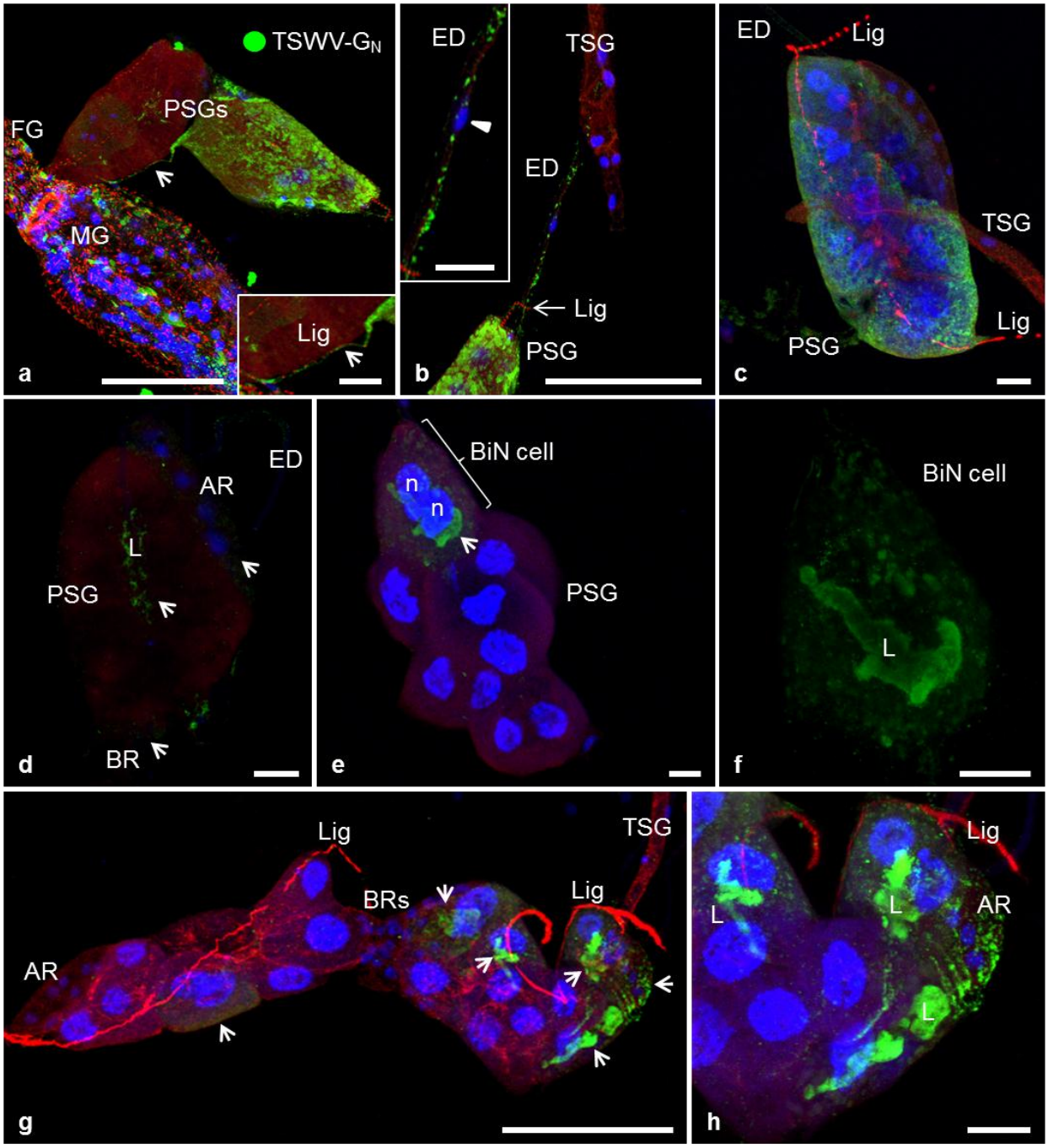

Figure 4.9. ***Tomato spotted wilt virus*** **(TSWV) infection of** ***Frankliniella occidentalis*** **principal salivary glands (PSGs).**

TSWV was detected by confocal fluorescent microscopy with an Alexa Fluor 488 conjugate to signal TSWV G_N presence, and marker for actin (red color, phalloidin conjugated to Alexa Fluor 594) and nucleus (blue color, DAPI). TSWV signal in PSGs was very variable and often different between the two glands from an individual thrips, where one PSG

showed strong and generalized signal for TSWV in contrast to the second PSG that has almost no signal. The corresponding midgut (MG) and foregut (FG) have limited and low intensity foci of TSWV signal. The ligament (Lig, signaled by a white arrow) shows strong TSWV signal (a). The efferent duct (ED) connecting a PSG (completely depicted in panel a) with the corresponding TSG showed foci of TSWV signal. Arrow head in the inset signals the single nucleus in the ED (b). PSG with TSWV signal localizing mainly in the periphery than toward the lumen (c). On the contrary, some PSGs showed limited and low intensity signal around the common lumen of the PSG and in some cases in the basal (BR) and apical regions (AR) (d). TSWV infection localized to one or few separated cells within the PSGs in female (e, f) and male (g, h) thrips. An single large bi-nucleated (n) cell showed signal and strong highlighting of the cells lumen (L) suggesting that TSWV accumulates in the lumen cavity or walls (e, f). At least five independent large bi-nucleated cells had TSWV signal in a pair of PSGs (white arrows, g). TSWV signal was also observed in the apical region (h).

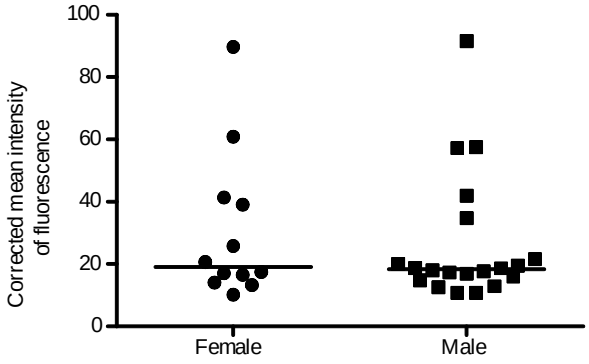

Figure 4.10. Mean intensity (arbitrary units) of TSWV signal in PSGs of female and male *Frankliniella occidentalis* adult thrips.

Fluorescent signal was determined by immunolabeling and confocal microscopy and quantified using ImageJ software. There was no significant difference between genders (*P* = 0.7703, Mann Whitney test).

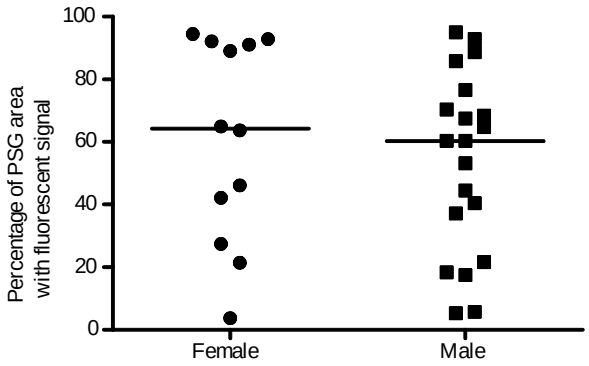

Figure 4.11. Percentage of area of principal salivary glands (PSGs) with TSWV signal. The area of PSGs with virus signal was determined by immunolabeling and confocal microscopy for adult *Frankliniella occidentalis* female and male thrips. The percentage of area was calculated using ImageJ. There was no difference for the percentage of area infected with TSWV between genders (*P* = 0.4958, Mann Whitney test).

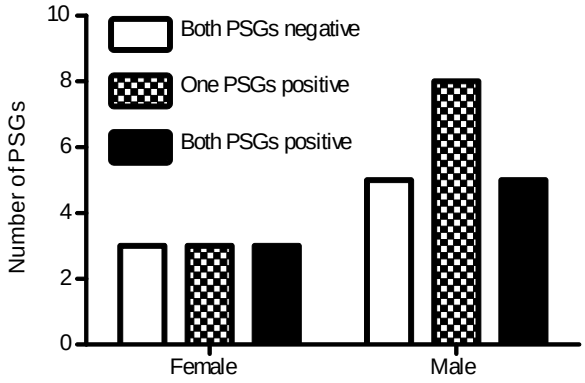

Figure 4.12. Comparison of infection status of the pair of principal salivary glands of adult *Frankliniella occidentalis* female and male thrips.
TSWV-infection categorized as both PSGs out of a pair without TSWV signal, one out of the pair with signal and both PSGs with TSWV signal. There is no statistical difference between genders as determined by Fisher exact test, P = 1.000).

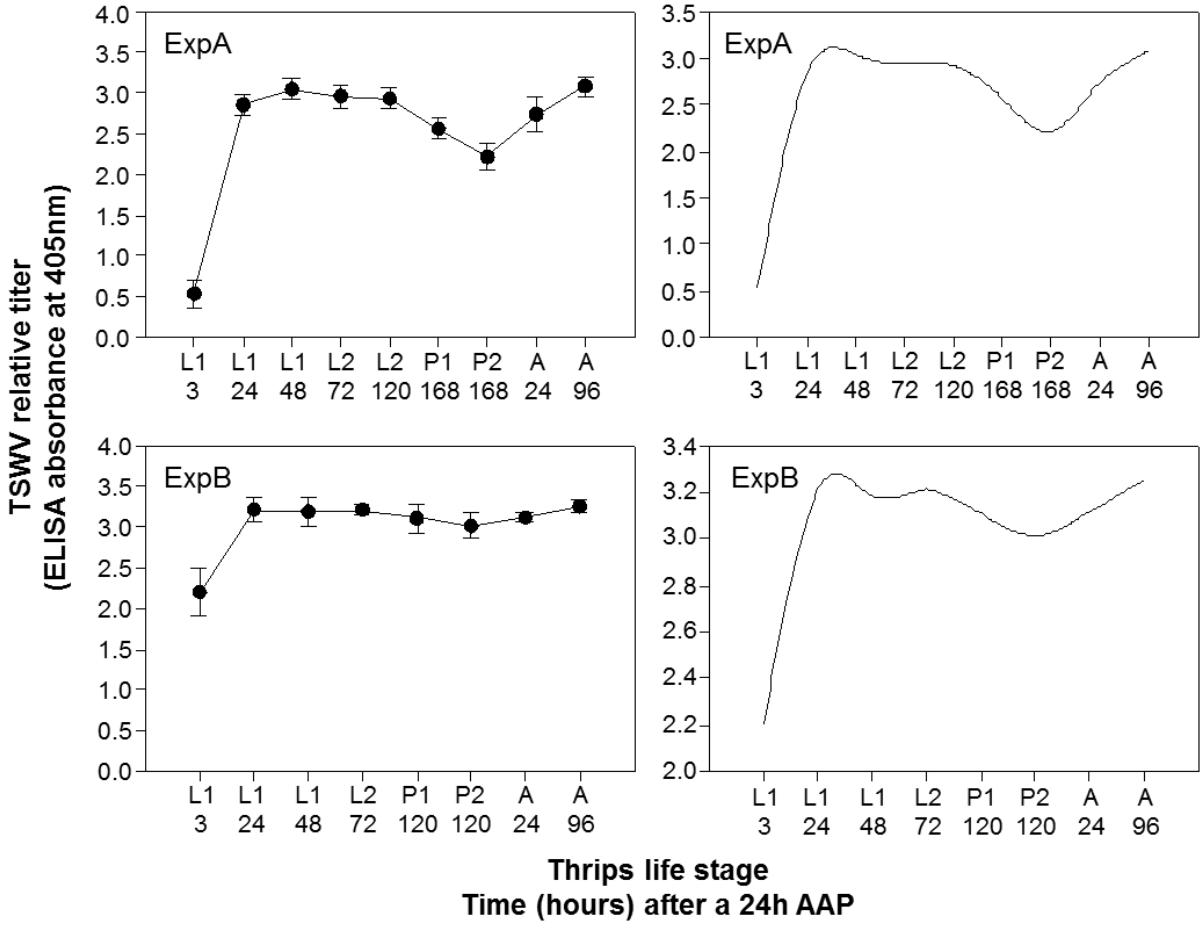

Figure 4.13. ***Tomato spotted wilt virus*** **(TSWV) relative titer at different time points during the life cycle of** ***Frankliniella occidentalis*****.**

Virus titer was determined by ELISA against TSWV-N protein. Life stages sampled were first instar larval thrips (L1) 3, 24 and 48 hours after a 24h AAP; second instar larval thrips (L2) 72 and in the case of experiment A, 120 hours after AAP; prepupae (P1), pupa (P2) and adults (A) 24 and 96 hours after eclosion. Each time point consists of six samples (15 thrips each) and in the case of adult thrips, half (3) the samples are females and half (3) are males. All samples were determined as positive for TSWV by the ELISA.

Chapter 5 - General discussion and future perspectives

Summary of results and products

Tomato spotted wilt virus (TSWV) is a plant-infecting virus in the family *Bunyaviridae*. Like other bunyaviruses, TSWV is transmitted in a circulative-propagative manner by the arthropod vector. Although a good deal of research has dissected aspects of the virus biology and interactions with the thrips vector, still many factors are unknown. The work in this dissertation aimed to develop novel control strategies against TSWV through a better understanding of the virus-vector interaction. The specific goals of my research were to track the route of TSWV in thrips using confocal microscopy and to further examine the utility of disrupting the virus-vector interaction for effective virus control. To achieve these goals, I examined the localization of glycoprotein G_N, the reported viral attachment protein, and expressed soluble and insoluble forms of the protein in plants transiently and transgenically. The findings of my experiments indicate that transgenic expression of G_N-S in tomato plants may have the potential to prevent secondary spread of virus. The route of TSWV in the thrips vector was described in detail using immunolabeling and cytoskeletal and organelle markers. I have described novel features of the primary salivary glands and documented that TSWV has the potential to use multiple dissemination pathways to move from the midgut region to the principal salivary glands. The transgenic plants and new knowledge generated of the virus-vector interaction are promising tools to improve the commercial management of TSWV and a model to approach the control of other virus-vector systems.

The work focused on G_N glycoprotein, a viral protein found on TSWV envelope and recognized as an important determinant of virus transmission by thrips. G_N previously was reported to be the viral attachment protein, the molecule mediating attachment of virus particles to the corresponding receptor in the epithelial cells of vector thrips (Whitfield et al., 2004). Moreover, a soluble form of this protein (G_N-S) was able to cause a decrease in virus transmission by *Frankliniella occidentalis* (the western flower thrips), a plant pest and important vector of TSWV (Whitfield et al., 2004; Whitfield et al., 2008). In those experiments, G_N-S was produced in cultured insect cells and was fed exogenously to thrips prior to or simultaneously

with purified TSWV virions. In this work, we further expanded on this phenomenon by expressing G_N-S protein *in planta* and testing its effect on TSWV acquisition and transmission by *F. occidentalis*. Moreover, TSWV infection of thrips was explored with special emphasis to understand principal salivary gland (PSG) morphology and infection.

The major contributions of this dissertation are summarized below per chapter:

Chapter 2. Transient expression and cellular localization of *Tomato spotted wilt virus* glycoprotein G_N, a soluble form (G_N-S), and nucleocapsid protein (N) in *Nicotiana benthamiana*.

TSWV G_N, G_N-S and N proteins were transiently expressed and their localization and behavior *in planta* were determined. As a first step to study the effect of G_N-S expressed *in planta* on TSWV acquisition and transmission by thrips, expression clones for C-terminus fusions of these three proteins to GFP and RFP were constructed and tested by agroinfiltration in *Nicotiana benthamiana* leafs. G_N-S localization was compared to G_N and N proteins by fluorescent microscopy. The major results of this chapter were:

- G_N localized by transient expression to the Golgi apparatus as determined by a punctate pattern within cells and co-localization with a Golgi marker. The result was in accordance with previous reports in cultured mammalian cells and plant protoplasts (Kikkert et al., 2001; Ribeiro et al., 2008) and it is the first report for G_N cellular localization in intact plant tissue.
- G_N-S displayed a different localization pattern by transient expression in comparison to G_N. The distinct G_N-S::GFP localization is in accordance to the deletion of the cytoplasmic domain (C-terminus) and transmembrane domain of G_N protein. G_N-S localized to the endoplasmic reticulum (ER) and to the cytoplasm of cells (soluble-like pattern).
- N::GFP protein showed in transient expression a complex localization pattern consisting of variable number and size of fluorescent spots (foci) that changed over time. N::GFP foci were found throughout the cytoplasm of the cell and in close proximity to cell membranes. The size and number of this fluorescent foci changed over time, from conspicuous and very small dots of fluorescence one to two days after agroinfiltration

(daa) to few (in many cases one) and relative large foci six to nine daa. In addition, approaches for quantitative analysis of localization patterns using ImageJ (Abramoff et al., 2004) capabilities were developed.

Chapter 3. Transgenic G_N-S::GFP tomato plants interfered with TSWV acquisition and transmission by *Frankliniella occidentalis*.

The potential of G_N-S::GFP to interfere with TSWV-*F. occidentalis* interaction was studied by transforming tomato plants and using those plants for acquisition and transmission experiments. Transgenic tomato plants expressing G_N-S:GFP and G_N::GFP were generated and characterized as potential tools to control TSWV. Several generations of the transgenic plants were grown in the greenhouse and the presence, the amount and localization of recombinant protein was determined for selected lines. I aimed to identify transgenic lines capable to disrupt virus-vector interaction and with the potential to be incorporated in management strategies for TSWV. The main results obtained for this chapter were:

- G_N-S::GFP transgenically expressed in tomato plants showed a reticulate pattern of localization within cells. Meanwhile, G_N::GFP displayed a punctate cellular localization pattern in accordance with transient expression results.
- T1 and T2 G_N-S::GFP transgenic tomato plants showed no resistance to TSWV infection 15 days after virus inoculation. The plants had symptoms similar to non-transgenic TSWV-infected plants. Moreover, the pattern (old mechanically-inoculated vs. young-systemic tissues) and frequency of TSWV and of G_N-S::GFP detection in those plants did not differ from non-transgenic TSWV-infected or transgenic non-infected plants, respectively.
- Transgenic G_N-S::GFP plants interfered with the acquisition and transmission of TSWV by *F. occidentalis*. Thrips cohorts were fed on TSWV-infected transgenic and non-transgenic tissue for a 24h acquisition access period (AAP) and then left to feed on green beans for a 24h clearing period. There was a significant lower acquisition of TSWV from transgenic tissue as suggested by low ELISA absorbance values and by real time quantitative reverse transcriptase-PCR (qRT-PCR). In contrast, ELISA values and normalized abundance of TSWV-N RNAs in thrips fed on non-transgenic TSWV-

infected tissue were significantly higher. Moreover, the percentage of TSWV transmission by samples (n = 10) of 24h-old-adult thrips originated from those acquisition events was significantly lower for thrips fed as larvae on transgenic TSWV-infected tissue than for thrips cohorts fed on non-transgenic TSWV-infected tissue.

Chapter 4. Dynamics of TSWV infection and spread in its insect vector, *Frankliniella occidentalis* with an emphasis on the principal salivary glands.

TSWV infection of thrips was explored with special emphasis to understand PSG morphology and infection. The route of TSWV on *F. occidentalis* was studied in order to understand how the virus reaches the tubular salivary glands (TSGs). Thrips were dissected and TSWV infection was visualized by confocal microcopy with immunolabeling and cellular and organelle markers at four time points through the vectors life cycle. To complement this visual evaluation of virus infection, virus titer through the vector life cycle was tracked by ELISA. Transmission rate and infection of PSGs was compared between thrips genders for each time course experiment. The main results or conclusions from these experiments were:

- A description of the anatomy of *F. occidentalis* PSGs and TSGs was obtained by confocal fluorescent microscopy complemented with markers for actin and nuclei. The observations made complemented previous descriptions and offered further detail on the morphology and types of cells and structures constituting the PSGs and TSGs.
- Infection of TSGs is reported for the first time and I hypothesized the TSGs as a possible route for TSWV to spread from MG1 into the PSGs. Infection of TSGs was observed at larval stages and before TSWV was detected on PSGs. Additionally, TSWV signal was observed in the efferent duct (ED) connecting the TSGs with PSGs.
- The pattern of TSWV infection over time was characterized from time course experiments by immunolabeling (against G_N) or by ELISA (against N) detection of the virus at different time points. In general terms, the results described a pattern in accordance with previous reports (Nagata et al., 1999; de Assis Filho et al., 2002; Kritzman et al., 2002). TSWV infection showed an increase on titer and spread during the larval stages after AAP and reaching a maximum at certain time point between late L1 and L2 stage. After this peak the amount of virus in the tissues apparently started to

decrease reaching a low point between prepuae and 24h old adult stages. The virus seemed to increase again in titer during the adult stage of thrips.

General discussion

TSWV glycoprotein G_N and a soluble form lacking the transmembrane and cytoplasmic domains (G_N-S) were fused to GFP and expressed transiently in *Nicotianan benthamiana* and transgenically in transgenic tomato plants. Subcellular localization of the corresponding GFP fluorescent signals was determined by confocal fluorescent microscopy. G_N::GFP recombinant protein localized, in both cases, to Golgi stacks throughout the cells as indicated by a punctate pattern or co-localization to a Golgi marker (Fig. 2.4 and 3.7 to 3.9) in accordance with previous reports (Kikkert et al., 2001; Ribeiro et al., 2008). Moreover, some observations suggested that G_N is expressed to lower level or it is less stable in the plant tissue than G_N-S. In transiently transformed *N. benthamiana* leaves, fewer cells showed expression of G_N in comparison to G_N-S, and the intensity of the fluorescent signal was in appearance lower. In agreement with this observations, G_N::GFP *in vitro* explants were very difficult to generate and the amount of recombinant protein produced in transgenic plants was relatively lower ($P = 0.0863$) than in G_N-S::GFP plants of the same generation (T1, Fig. 3.5 and 3.6).

The apparent lower accumulation of G_N::GFP in *N. benthamiana* and tomato plants (in comparison to G_N-S::GFP) observed in Chapters 2 and 3 may be linked to the putative role of *Bunyaviridae* G_N protein in cell autophagy as discussed for Chapter 4. *Sin Nombre hanatavirus* G_N is proposed as a pathogen associated molecular pattern (PAMP) (Hussein et al., 2012), pathogen derived molecules that are recognized by surveillance mechanisms in cells and trigger host cellular defense responses. Plant cells and their defense mechanisms are known to respond to PAMPs as animal cells do (Caplan et al., 2008; Caplan et al., 2008; Mazzotta and Kemmerling, 2011). Therefore, the apparent lower expression or stability of TSWV G_N::GFP observed in plant cells may be the result of defense mechanisms that G_N is triggering in host cells.

G_N-S::GFP cellular localization was not as consistent between method of expression and plant host as it was for G_N::GFP localization which localized to the Golgi. In transiently transformed *N. bentamiana* cells it was observed mainly as a soluble-like pattern similar to the

pattern observed for GFP molecule alone. However certain percentage of cells had a clear reticulate pattern solely or in addition to the soluble-like pattern. In transgenically transformed tomato cells, G_N-S::GFP displayed mainly a reticulate pattern and highlighting of the nuclear envelope lumen, indicative of ER localization. G_N has been observed at early stages of expression in *in vitro* systems to localize initially to the ER as part of the post-translational processing of the protein (Kikkert et al., 2001; Ribeiro et al., 2008). The soluble-like pattern observed can be due to an excess production in *N. benthamiana* cells and/or differences in the ER characteristics between plant species. Some of the recombinant protein may possible leak into the cytoplasm. Additionally, the apparent soluble-like pattern may be an artifact caused by the plant cell central vacuole pushing the ER to the cell periphery and packing it together so that a continuous of fluorescence signal is observed along the cell periphery. Lastly, different confocal microscopes were used to screen *N. benthamiana* tissue, Zeiss Axiovert 200M microscope equipped with Zeiss LSM510 Meta system; meanwhile, tomato transgenic tissue was mostly screened with a Zeiss LSM 700 Confocal Laser Scanning microscope. The level of resolution achieved by both microscopes at similar conditions (40x oil immersion objective and scam zoom of 0.7, 1 and 4x) may be different.

The results, in general, seem to support a dose-dependent relationship for the virus-vector interaction. Virus acquisition *per se* do not seems to depend on a certain virus dose, because the results from Chapter 3 suggest that initial infection of the midgut can occur even if a small number of virions are able to bind and enter the epithelial cells. Nonetheless, the initial amount of virus particles establishing the initial infection seems to make a difference on the development of the infection and final transmission by adult thrips. A positive (Pearson correlation = 0.829) and significant correlation ($P < 0.001$) was found between TSWV titer 24h after AAP for cohorts of thrips and the percentage of transmission by 24h-old adults for the corresponding cohorts (combined data from Chapters 3 and 4, Fig. 5.1). The previous arguments and results throughout this thesis support the hypothesis of a dose-dependent and developmental-dependent midgut escape barrier for thrips which has been suggested previously (Ullman et al., 1992; Nagata et al., 1997; Nagata et al., 1999; Ohnishi et al., 2001; de Assis et al., 2005).

TSWV transmission results obtained in Chapters 3 and 4 displayed similar transmission rates for female and male thrips in contrast to previous reports that male thrips are more likely to transmit the virus (van de Wetering et al., 1998; van de Wetering et al., 1999). Transmission

rates for females and males observed throughout this research (Fig. 5.2) were not significantly different (combined transmission results from Chapters 3 and 4, $P = 0.9429$). Differences in the virus isolate, the thrips colony genetic background and/or the conditions at which the experiments were run did not support the differences in transmission previously reported for *F. occidentalis* genders. These differences in transmission rates due to distinct genotype of vector-host combinations or due to environmental conditions highlight the complexity of the system.

The main contributions of this work support the concept that G_N can be exploited to develop novel strategies to control TSWV. Transgenic plants expressing a soluble form of G_N, G_N-S, interfered with TSWV acquisition and transmission by *F. occidentalis*. Larval thrips fed on virus infected transgenic plants had lower TSWV titers 24h after virus AAP (Fig. 3.11) and the resulting adults showed lower rates of virus transmission (Table 3.9 and Fig. 3.13), in contrast to significantly higher TSWV titers and transmission rates displayed by thrips fed on non-transgenic TSWV-infected plants . These plants are promising tools for the management of TSWV in greenhouses and fields; as well as tools for future research on virus-vectors interactions. Second, immunolabeling results suggested that the TSGs are a possible route for TSWV spread into the PSGs of *F. occidentalis*. And lastly, TSWV infection of the PSGs was characterized; the virus may spread throughout the tissue or localize to single cells. The lumen of individual cells appears as a site of virus accumulation. Additionally, there are no apparent differences in TSWV infection of PSGs between genders.

Future research and perspectives

There is still a considerable lack of understanding on the factors and processes determining *Tospovirus*-thrips interactions. The results obtained throughout this work support the need to continue the study of G_N as a target for virus control and signal toward other interesting aspects of the virus-vector biology that need to be studied. Possible research lines that are noteworthy to follow up based on the results showed herein are listed below.

- Test if TSWV G_N-S would interfere with virus acquisition by other thrips species known to vector TSWV or with the acquisition and transmission of other *Tospovirus* species. In order to test this possibility, acquisition and transmission test as described herein

(Chapter 3) should be done with other thrips species, i.e *Thrips tabaci*. Also, transgenic plants should be inoculated with different tospoviruses and acquisition and transmission experiments conducted to test if TSWV G_N-S protein will interfere, as well, with other tospoviruses acquisition and consequent transmission. These investigations will determine a putative broader applicability of the transgenic plants to control the spread of other tospoviruses. They will also contribute to the understanding of virus-vector specificity among these viruses and thrips. Of high interest is that analysis of such results may contribute to unlock if different thrips share a common receptor for the viruses.

- Dose-dependent transmission of TSWV is suggested by this work and has previously been proposed (Nagata et al., 2000; Rotenberg et al., 2009), and determining its occurrence contributes to a better understanding of the interaction. A dose-dependent interaction has interesting implications for virus transmission; i.e. it suggests that higher concentration of recombinant G_N-S in plants may cause a complete blocking of TSWV acquisition and transmission. Moreover, it suggests that other strategies oriented to achieve a low virus titer in plants may also block the transmission cycle of the virus. To further study this phenomena, a possible approach will be to purify TSWV from plants and serial dilutions of the purified virions feed to larval thrips. Acquisition and transmission should be determined following the methodologies standardized during this work.
- Agronomic performance of the transgenic plants and long-term reaction toward TSWV infection is an important characterization for actual deploy of the plants in commercial settings. Yield of transgenic and non-transgenic, healthy or virus infected plants should be determined and compared. The reaction of the transgenic plants to TSWV infection and its effect on G_N-S::GFP expression was determined 15 days after inoculation for this thesis. Studies looking at longer periods of time after infection will determine if the desired effect of the plants is available through the whole production cycle that extends beyond 15 days in commercial settings, especially with indeterminate tomato varieties in greenhouses.
- To determine if TSWV N protein localizes to plasmodesmata and is involved with TSWV movement within and between cells. N protein seems to have a biological significant change of localization through time in *N. benthamiana* cells. A change in

localization pattern of N was also noted for *in vitro* mammalian cells transfected for the expression of N fused to yellow fluorescent protein (Snippe et al., 2005). Moreover, localization of fluorescent N::GFP foci at the boundaries between cells suggests that N protein may be involved with cell-to-cell movement of TSWV RNPs. TSWV N was shown to assist with long distance movement in the TMV system (Zhang et al., 2012). Initially co-localization or BiFC experiments using N and a plasmodesmata resident protein will indicate an association of TSWV N and the plasmodesmata. Simultaneously, the effect of inhibitors of actin and microtubule polymerization in the localization pattern of N::GFP will unlock possible participation of N protein in TSWV movement mechanisms (Harries et al., 2009; Simon et al., 2009a).

The specific research objectives listed before are just a sample from a long list of questions and hypothesis that need to be resolved for *Tospovirus*-vector interactions. Recent technological developments and new approaches to study virus-vector interactions are starting to reveal a new understanding of the complexity of tospoviruses and their interaction with thrips (Rotenberg et al., 2009; Rotenberg and Whitfield, 2010; Stafford et al., 2011; Badillo-Vargas et al., 2012). Simultaneously, ongoing research is unlocking the hidden biology of other arbovirus-vector systems. Based on these new developments and recent research results, it is expected that the coming years will bring an overwhelming and eye-opening series of discoveries contributing to the understanding of virus-vector interactions.

Tables and Figures

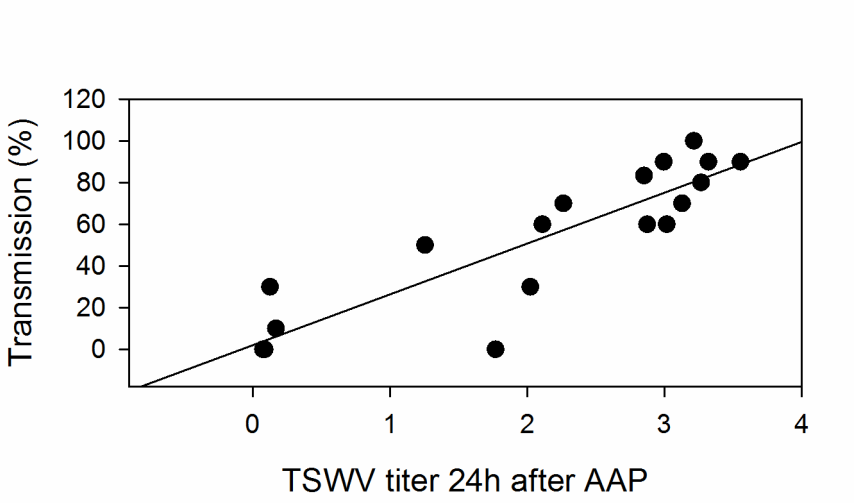

Figure 5.1. Correlation between *Tomato spotted wilt virus* (TSWV) titer and the corresponding percentage of transmission for cohorts of *Frankliniella occidentalis* thrips. TSWV was detected by ELISA 24h after AAP from experiments in chapter #3 and #4. Virus titer was determined from one or six (average) pooled samples of 15 thrips each. Transmission was calculated out of ten or 30 thrips tested. For statistical analysis purposes, ELISA absorbance values and transmission frequencies were transformed by calculating Log10[absorbance] or Arcsine[square root(frequency)], respectively. Transformed data was analyzed for correlation, Pearson correlation was 0.829 and *P* < 0.001).

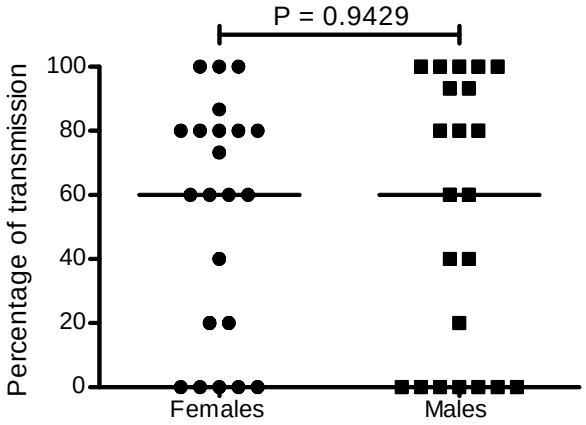

Figure 5.2. Comparison of the percentage of *Tomato spotted wilt virus* transmission for female and male *Frankliniella occidentalis* adults 24h after eclosion.

Transmission was calculated out of five or 15 thrips for cohorts of thrips. The horizontal line (___) represents the median. There is no difference between genders as determined by the Mann Whitney test.

References

Abramoff M.D., Magalhaes P.J., and Ram S.J. (2004). Image processing with ImageJ. **11,** 36-42.

Accotto G.P., Nervo G., Acciarri N., Tavella L., Vecchiati M., Schiavi M., Mason G., and Vaira A.M. (2005). Field evaluation of tomato hybrids engineered with *Tomato spotted wilt virus* sequences for virus resistance, agronomic performance, and pollen-mediated transgene flow. Phytopathology **95,** 800-807.

Adkins S., Choi T., Israel B.A., and Bandla M.D. (1996). Baculovirus expression and processing of *Tomato spotted wilt topsovirus* glycoproteins. Phytopathology **86,** 849-855.

Andersson A.M. and Pettersson R.F. (1998). Targeting of a short peptide derived from the cytoplasmic tail of the G1 membrane glycoprotein of Uukuniemi virus (Bunyaviridae) to the Golgi complex. J. Virol. **72,** 9585-9596.

Badillo-Vargas I.E., Rotenberg D., Schneweis D.J., Hiromasa Y., Tomich J.M., and Whitfield A.E. (2012). Proteomic analysis of *Frankliniella occidentalis* and differentially-expressed proteins in response to *Tomato spotted wilt virus infection*. J. Virol. **86, *in press***.

Bandla M.D., Campbell L.R., Ullman D.E., and Sherwood J.L. (1998). Interaction of *Tomato spotted wilt tospovirus* (TSWV) glycoproteins with a thrips midgut protein, a potential cellular receptor for TSWV. Phytopathology **88,** 98-104.

Bartholomay L.C., Waterhouse R.M., Mayhew G.F., Campbell C.L., Michel K., Zou Z., Ramirez J.L., Das S., Alvarez K., Arensburger P., Bryant B., Chapman S.B., Dong Y., Erickson S.M., Karunaratne S.H.P.P., Kokoza V., Kodira C.D., Pignatelli P., Shin S.W., Vanlandingham D.L., Atkinson P.W., Birren B., Christophides G.K., Clem R.J., Hemingway J., Higgs S., Megy K., Ranson H., Zdobnov E.M., Raikhel A.S., Christensen B.M., Dimopoulos G., and Muskavitch M.A.T. (2010). Pathogenomics of *Culex quinquefasciatus* and meta-analysis of infection responses to diverse pathogens. Science **330,** 88-90.

Bergeron E., Vincent M.J., and Nichol S.T. (2007). Crimean-Congo hemorrhagic fever virus glycoprotein processing by the endoprotease SKI-1/S1P is critical for virus infectivity. J. Virol. **81,** 13271-13276.

Bertolotti-Ciarlet A., Smith J., Strecker K., Paragas J., Altamura L.A., McFalls J.M., Frias-Staheli N., Garcia-Sastre A., Schmaljohn C.S., and Doms R.W. (2005). Cellular localization and antigenic characterization of Crimean-Congo hemorrhagic fever virus glycoproteins. J. Virol. **79,** 6152-6161.

Bertran A.G.M., Oliveira A.S., Nagata T., and Resende R.O. (2011). Molecular characterization of the RNA-dependent RNA polymerase from *Groundnut ringspot virus* (genus *Tospovirus*, family *Bunyaviridae*). Arch. Virol. **156,** 1425-1429.

Bressan A. and Watanabe S. (2011). Immunofluorescence localization of *Banana bunchy top virus* (family *Nanoviridae*) within the aphid vector, *Pentalonia nigronervosa*, suggests a virus tropism distinct from aphid-transmitted luteoviruses. Virus Res. **155,** 520-525.

Brittlebank C.C. (1919). Tomato diseases. J. Agric. Victoria **17,** 231-235.

Bucher E., Sijen T., de Haan P., Goldbach R., and Prins M. (2003). Negative-strand Tospoviruses and Tenuiviruses carry a gene for a suppressor of gene silencing at analogous genomic positions. J. Virol. **77,** 1329-1336.

Burrows M.E., Caillaud M.C., Smith D.M., Benson E.C., Gildow F.E., and Gray S.M. (2006). Genetic regulation of polerovirus and luteovirus transmission in the aphid *Schizaphis graminum*. Phytopathology **96,** 828-837.

Caplan J., Padmanabhan M., and Dinesh-Kumar S.P. (2008). Plant NB-LRR immune receptors: From recognition to transcriptional reprogramming. Cell Host Microbe **3,** 126-135.

Chakrabarty R., Banerjee R., Chung S., Farman M., Citovsky V., Hogenhout S.A., Tzfira T., and Goodin M. (2007). pSITE vectors for stable integration or transient expression of autofluorescent protein fusions in plants: Probing *Nicotiana benthamiana*-virus interactions. Mol. Plant-Microbe Interact. **20,** 740-750.

Chiemsombat P., Sharman M., Srivilai K., Campbell P., Persley D., and Attathom S. (2010). A new tospovirus species infecting *Solanum esculentum* and *Capsicum annuum* in Thailand. Australas. Plant Dis. Notes **5,** 75-78.

Cilia M., Tamborindeguy C., Fish T., Howe K., Thannhauser T.W., and Gray S. (2011a). Genetics coupled to quantitative intact proteomics links heritable aphid and endosymbiont protein expression to circulative polerovirus transmission. J. Virol. **85,** 2148-2166.

Cilia M., Howe K., Fish T., Smith D., Mahoney J., Tamborindeguy C., Burd J., Thannhauser T.W., and Gray S. (2011b). Biomarker discovery from the top down: Protein biomarkers for efficient virus transmission by insects (Homoptera: Aphididae) discovered by coupling genetics and 2-D DIGE. Proteomics **11,** 2440-2458.

Ciuffo M., Kurowski C., Vivoda E., Copes B., Masenga V., Falk B.W., and Turina M. (2009). A new *Tospovirus* sp. in cucurbit crops in Mexico. Plant Dis. **93,** 467-474.

Ciuffo M., Mautino G.C., Bosco L., Turina M., and Tavella L. (2010). Identification of *Dictyothrips betae* as the vector of Polygonum ring spot virus. Ann. Appl. Biol. **157,** 299-307.

Colpitts T.M., Cox J., Nguyen A., Feitosa F., Krishnan M.N., and Fikrig E. (2011). Use of a tandem affinity purification assay to detect interactions between West Nile and dengue viral proteins and proteins of the mosquito vector. Virology **417,** 179-187.

Cortez I., Aires A., Pereira A.M., Goldbach R., Peters D., and Kormelink R. (2002). Genetic organization of *Iris yellow spot virus* M RNA: indications for functional homology between the G_C glycoproteins of Tospoviruses and animal-infecting Bunyaviruses. Arch. Virol. **147,** 2313-2325.

Culbreath A.K., Todd J.W., and Brown S.L. (2003). Epidemiology and management of *Tomato spotted wilt virus* in peanut. Annu. Rev. Phytopathol. **41,** 53-75.

Dallai R., Del Bene G., and Marchini D. (1991). The ultrastructure of the Malpighian tubules and hindgut of *Frankliniella occidentalis* (Pergande) (Thysanoptera: Thripidae). Int. J. Insect Morphol. Embryol. **20,** 223-233.

d'Avila-Levy C.M., Dias F.C.D., de Melo A.C.N., Martins J.L., Lopes A.H.D.C., Dos Santos A.L.S., Vermelho A.B., and Branquinha M.H. (2006). Insights into the role of gp63-like proteins in lower trypanosomatids. FEMS Microbiol. Lett. **254,** 149-156.

de Assis Filho F.M., Naidu R.A., Deom C.M., and Sherwood J.L. (2002). Dynamics of *Tomato spotted wilt virus* replication in the alimentary canal of two thrips species. Phytopathology **92,** 729-733.

de Assis F.M., Stavisky J., Reitz S.R., Deom C.M., and Sherwood J.L. (2005). Midgut infection by *Tomato spotted wilt virus* and vector incompetence of *Frankliniella tritici*. J. Appl. Entomol. **129,** 548-550.

de Haan P., Wagemakers L., Peters D., and Goldbach R. (1989). Molecular cloning and terminal sequence determination of the S and M RNAs of *Tomato spotted wilt virus*. J. Gen. Virol. **70,** 3469-3473.

de Haan P., Wagemakers L., Peters D., and Goldbach P. (1990). The S RNA segment of *Tomato spotted wilt virus* has an ambisense character. J. Gen. Virol. **71,** 1001-1007.

de Haan P., de Avila A.C., Kormelink R., Westerbroek A., Gielen J.J.L., Peters D., and Goldbach R. (1992). The nucleotide sequence of the S RNA of *Impatiens necrotic spot virus*, a novel Tospovirus. FEBS Lett. **306,** 27-32.

de Haan P., Kormelink R., de Oliveira Resende R., van Poelwijk F., Peters D., and Goldbach R. (1991). *Tomato spotted wilt virus* L RNA encodes a putative RNA polymerase. J. Gen. Virol. **72,** 2207-2216.

de Oliveira A., Bertran A., Inoue-Nagata A., Nagata T., Kitajima E., and Oliveira Resende R. (2011). An RNA-dependent RNA polymerase gene of a distinct Brazilian tospovirus. Virus Genes **43,** 385-389.

Del Bene G., Dallai R., and Marchini D. (1991). Ultrastructure of the midgut and the adhering tubular salivary glands of *Frankliniella occidentalis* (Pergande) (Thysanopthera: Thripidae). Int. J. Insect Morphol. Embryol. **20,** 12-15.

Duijsings D., Kormelink R., and Goldbach R. (2001). In vivo analysis of the TSWV capsnatching mechanism: single base complementarity and primer length requirements. EMBO J. **20,** 2545-2552.

Duijsings D., Kormelink R., and Goldbach R. (1999). *Alfalfa mosaic virus* RNAs serve as cap donors for *Tomato spotted wilt virus* transcription during coinfection of *Nicotiana benthamiana*. J. Virol. **73,** 5172-5175.

Fedorowicz O., Bartoszewski G., Kaminska M., Stoeva P., and Niemirowicz-Szczytt K. (2005). Pathogen-derived resistance to *Tomato spotted wilt virus* in transgenic tomato and tobacco plants. J. Am. Soc. Hort. Sci. **130,** 218-224.

Filone C.M., Heise M., Doms R.W., and Bertolotti-Ciarlet A. (2006). Development and characterization of a Rift Valley fever virus cell-cell fusion assay using alphavirus replicon vectors. Virology **356,** 155-164.

Fontana J., Lopez-Montero N., Elliott R.M., Fernandez J.J., and Risco C. (2008). The unique architecture of Bunyamwera virus factories around the Golgi complex. Cell. Microbiol. **10,** 2012-2028.

Garcin D., Lezzi M., Dobbs M., Elliott R.M., Schmaljohn C., Kang C.Y., and Kolakofsky D. (1995). The 5'-Ends of Hantaan Virus (*Bunyaviridae*) RNAs suggest a prime-and-realign mechanism for the initiation of RNA-synthesis. J. Virol. **69,** 5754-5762.

Garry C. and Garry R. (2004). Proteomics computational analyses suggest that the carboxyl terminal glycoproteins of Bunyaviruses are class II viral fusion protein (beta-penetrenes). Theor. Biol. Med. Model. **1,** 10.

Gavrilovskaya I.N., Brown E.J., Ginsberg M.H., and Mackow E.R. (1999). Cellular entry of hantaviruses which cause hemorrhagic fever with renal syndrome is mediated by beta 3 integrins. J. Virol. **73,** 3951-3959.

Gerrard S.R. and Nichol S.T. (2007). Synthesis, proteolytic processing and complex formation of N-terminally nested precursor proteins of the Rift Valley fever virus glycoproteins. Virology **357,** 124-133.

Ghosh A.K., Ribolla P.E.M., and Jacobs-Lorena M. (2001). Targeting *Plasmodium* ligands on mosquito salivary glands and midgut with a phage display peptide library. Proc. Natl. Acad. Sci. U. S. A. **98,** 13278-13281.

Girard Y.A., Popov V., Wen J., Han V., and Higgs S. (2005). Ultrastructural study of West Nile virus pathogenesis in *Culex pipiens quinquefasciatus* (Diptera : Culicidae). J. Med. Entomol. **42,** 429-444.

Girard Y.A., Schneider B.S., McGee C.E., Wen J., Han V.C., Popov V., Mason P.W., and Higgs S. (2007). Salivary gland morphology and virus transmission during long-term cytopathologic West Nile virus infection in *Culex* mosquitoes. Am. J. Trop. Med. Hyg. **76,** 118-128.

Girard Y.A., Mayhew G.F., Fuchs J.F., Li H., Schneider B.S., McGee C.E., Rocheleau T.A., Helmy H., Christensen B.M., Higgs S., and Bartholomay L.C. (2010). Transcriptome changes in *Culex quinquefasciatus* (Diptera: Culicidae) salivary glands during West Nile virus infection. J. Med. Entomol. **47,** 421-435.

Goldbach R. and Peters D. (1994). Possible causes of the emergence of *Tospovirus* diseases. Semin. Virol. **5,** 113-120.

Gonzalez-Scarano F., Pobjecky N., and Nathanson N. (1984). La Crosse bunyavirus can mediate pH-dependent fusion from without. Virology **132,** 222-225.

Goodin M.M., Chakrabarty R., Banerjee R., Yelton S., and DeBolt S. (2007). New gateways to discovery. Plant Physiol. **145,** 1100-1109.

Gopal K., Reddy M.K., Reddy D.V.R., and Muniyappa V. (2010). Transmission of peanut yellow spot virus (PYSV) by thrips, *Scirtothrips dorsalis* Hood in groundnut. Arch. Phytopathol. Plant Protect. **43,** 421-429.

Gordillo L.F., Stevens M.R., Millard M.A., and Geary B. (2008). Screening two *Lycopersicon peruvianum* collections for resistance to *Tomato spotted wilt virus*. Plant Dis. **92,** 694-704.

Gray S. and Gildow F. (2003). *Luteovirus*-aphid interactions. Annu. Rev. Phytopathol. **41,** 539-566.

Gray S.M. and Banerjee N. (1999). Mechanisms of arthropod transmission of plant and animal viruses. Microbiol. Mol. Biol. R. **63,** 128-148.

Gubba A., Gonsalves C., Stevens M., Tricoli D., and Gonsalves D. (2002). Combining transgenic and natural resistance to obtain broad resistance to tospovirus infection in tomato (*Lycopersicon esculentum* mill). Mol. Breed. **9,** 13-23.

Harries P.A., Park J., Sasaki N., Ballard K.D., Maule A.J., and Nelson R.S. (2009). Differing requirements for actin and myosin by plant viruses for sustained intercellular movement. Proc. Natl. Acad. Sci. U. S. A. **106,** 17594-17599.

Hassani-Mehraban A., Botermans M., Verhoeven J.T.J., Meekes E., Saaijer J., Peters D., Goldbach R., and Kormelink R. (2010). A distinct tospovirus causing necrotic streak on *Alstroemeria* sp. in Colombia. Arch. Virol. **155,** 423-428.

Hepojoki J., Strandin T., Wang H., Vapalahti O., Vaheri A., and Lankinen H. (2010a). Cytoplasmic tails of hantavirus glycoproteins interact with the nucleocapsid protein. J. Gen. Virol. **91,** 2341-2350.

Hepojoki J., Strandin T., Vaheri A., and Lankinen H. (2010b). Interactions and oligomerization of Hantavirus glycoproteins. J. Virol. **84,** 227-242.

Hoffmann K., Qiu W.P., and Moyer J.W. (2001). Overcoming host- and pathogen-mediated resistance in tomato and tobacco maps to the M RNA of *Tomato spotted wilt virus*. Mol. Plant-Microbe Interact. **14,** 242-249.

Huiskonen J.T., Hepojoki J., Laurinmaki P., Vaheri A., Lankinen H., Butcher S.J., and Grunewald K. (2010). Electron cryotomography of Tula Hantavirus suggests a unique assembly paradigm for enveloped viruses. J. Virol. **84,** 4889-4897.

Hussein I.T.M., Cheng E., Ganaie S.S., Werle M.J., Sheema S., Haque A., and Mir M.A. (2012). Autophagic clearance of Sin Nombre hantavirus glycoprotein Gn promotes virus replication in cells. J. Virol. **86,** 7520-7529.

Inoue T., Sakurai T., and Murai T. (2004). Specificity of accumulation and transmission of *Tomato spotted wilt virus* (TSWV) in two genera, *Frankliniella* and *Thrips* (Thysanoptera: Thripidae). Bull. Entomol. Res. **94,** 501-507.

Inoue T. and Sakurai T. (2007). The phylogeny of thrips (Thysanoptera : Thripidae) based on partial sequences of cytochrome oxidase I, 28S ribosomal DNA and elongation factor-1 alpha and the association with vector competence of tospoviruses. Appl. Entomol. Zool. **42,** 71-81.

Ismayadi C. and Prins M. (1996). Transformation of tobacco plants with the genes NSm and Gp from tomato spotted wilt tospovirus M-RNA. Pelita Perkebunan **12,** 1-15.

Jahn M., Paran I., Hoffmann K., Radwanski E.R., Livingstone K.D., Grube R.C., Aftergoot E., Lapidot M., and Moyer J. (2000). Genetic mapping of the *Tsw* locus for resistance to the tospovirus *Tomato spotted wilt virus* in *Capsicum* spp. and its relationship to the *Sw-5* gene for resistance to the same pathogen in tomato. Mol. Plant-Microbe Interact. **13,** 673-682.

Jin M., Park J., Lee S., Park B., Shin J., Song K., Ahn T., Hwang S., Ahn B., and Ahn K. (2002). Hantaan virus enters cells by clathrin-dependent receptor-mediated endocytosis. Virology **294,** 60-69.

Kainz M., Hilson P., Sweeney L., DeRose E., and German T.L. (2004). Interaction between *Tomato spotted wilt virus* N protein monomers involves nonelectrostatic forces governed by multiple distinct regions in the primary structure. Phytopathology **94,** 759-765.

Keene K.M., Foy B.D., Sanchez-Vargas I., Beaty B.J., Blair C.D., and Olson K.E. (2004). RNA interference acts as a natural antiviral response to O'nyong-nyong virus (*Alphavirus*; Togaviridae) infection of *Anopheles gambiae*. Proc. Natl. Acad. Sci. U. S. A. **101,** 17240-17245.

Khoo C.C.H., Piper J., Sanchez-Vargas I., Olson K.E., and Franz A.W.E. (2010). The RNA interference pathway affects midgut infection- and escape barriers for Sindbis virus in *Aedes aegypti*. BMC Microbiol. **10,** 130.

Kikkert M., Meurs C., van de Wetering F., Dorfmuller S., Peters D., Kormelink R., and Goldbach R. (1998). Binding of *Tomato spotted wilt virus* to a 94-kDa thrips protein. Phytopathology **88,** 63-69.

Kikkert M., Van Lent J., Storms M., Bodegom P., Kormelink R., and Goldbach R. (1999). *Tomato spotted wilt virus* particle morphogenesis in plant cells. J. Virol. **73,** 2288-2297.

Kikkert M., Verschoor A., Kormelink R., Rottier P., and Goldbach R. (2001). *Tomato spotted wilt virus* glycoproteins exhibit trafficking and localization signals that are functional in mammalian cells. J. Virol. **75,** 1004-1012.

Kim J.W., Sun S.S.M., and German T.L. (1994). Disease resistance in tobacco and tomato plants transformed with the *Tomato spotted wilt virus* nucleocapsid gene. Plant Dis. **78,** 615-621.

Kim M., Yang M., and Kim T. (2009). Expression of Dengue Virus E glycoprotein domain III in non-nicotine transgenic tobacco plants. Biotechnol. Bioprocess Eng. **14,** 725-730.

Kitajima E.W. (1975). Peculiar type of glycocalyx on microvilli of midgut epithelial-cells of thrips *Frankliniella* sp. (Thysanoptera, Thripidae). Cytobiologie **11,** 299-303.

Kohl A., Lowen A.C., Leonard V.H.J., and Elliott R.M. (2006). Genetic elements regulating packaging of the Bunyamwera orthobunyavirus genome. J. Gen. Virol. **87,** 177-187.

Kokoza V., Ahmed A., Shin S.W., Okafor N., Zou Z., and Raikhel A.S. (2010). Blocking of *Plasmodium* transmission by cooperative action of Cecropin A and Defensin A in transgenic *Aedes aegypti* mosquitoes. Proc. Natl. Acad. Sci. U. S. A. **107,** 8111-8116.

Kormelink R., van Poelwijk F., Peters D., and Goldbach R. (1992a). Non-viral heterogeneous sequences at the 5' ends of *Tomato spotted wilt virus* mRNAs. J. Gen. Virol. **73,** 2125-2128.

Kormelink R., de Haan P., Meurs C., Peters D., and Goldbach R. (1992b). The nucleotide sequence of the M RNA segment of *Tomato spotted wilt virus*, a Bunyavirus with two ambisense RNA segments. J. Gen. Virol. **73,** 2795-2804.

Kormelink R., Storms M., Van Lent J., Peters D., and Goldbach R. (1994). Expression and subcellular location of the NSM protein of *Tomato spotted wilt virus* (TSWV), a putative viral movement protein. Virology **200,** 56-65.

Kritzman A., Gera A., Raccah B., van Lent J.W.M., and Peters D. (2002). The route of *Tomato spotted wilt virus* inside the thrips body in relation to transmission efficiency. Arch. Virol. **147,** 2143-2156.

Lewandowski D.J. and Adkins S. (2005). The tubule-forming NSm protein from *Tomato spotted wilt virus* complements cell-to-cell and long-distance movement of *Tobacco mosaic virus* hybrids. Virology **342,** 26-37.

Li W., Lewandowski D.J., Hilf M.E., and Adkins S. (2009). Identification of domains of the *Tomato spotted wilt virus* NSm protein involved in tubule formation, movement and symptomatology. Virology **390,** 110-121.

Lindbo J., Silvarosales L., Proebsting W., and Dougherty W. (1993). Induction of a highly specific antiviral state in transgenic plants - Implications for regulation of gene-expression and virus-resistance. Plant Cell **5,** 1749-1759.

Liu L., Celma C.C.P., and Roy P. (2008). Rift Valley fever virus structural proteins: expression, characterization and assembly of recombinant proteins. Virol. J. **5,** 82.

Liu S., Sivakumar S., Sparks W.O., Miller W.A., and Bonning B.C. (2010). A peptide that binds the pea aphid gut impedes entry of *Pea enation mosaic virus* into the aphid hemocoel. Virology **401,** 107-116.

Lober C., Anheier B., Lindow S., Klenk H., and Feldmann H. (2001). The Hantaan virus glycoprotein precursor is cleaved at the conserved pentapeptide WAASA. Virology **289,** 224-229.

Lokesh B., Rashmi P.R., Amruta B.S., Srisathiyanarayanan D., Murthy M.R.N., and Savithri H.S. (2010). NSs encoded by *Groundnut bud necrosis virus* is a bifunctional enzyme. Plos One **5,** e9757.

Lopez C., Aramburu J., Galipienso L., Soler S., Nuez F., and Rubio L. (2011). Evolutionary analysis of tomato *Sw-5* resistance-breaking isolates of *Tomato spotted wilt virus*. J. Gen. Virol. **92,** 210-215.

Lopez-Montero N. and Risco C. (2011). Self-protection and survival of arbovirus-infected mosquito cells. Cell. Microbiol. **13,** 300-315.

Louboutin J., Agrawal L., Reyes B.A.S., Van Bockstaele E.J., and Strayer D.S. (2010). HIV-1 gp120-induced injury to the blood-brain barrier: Role of metalloproteinases 2 and 9 and relationship to oxidative stress. J. Neuropathol. Exp. Neurol. **69,** 801-816.

Lovato F.A., Inoue-Nagata A.K., Nagata T., de Avila A.C., Pereira L.A.R., and Resende R.O. (2008). The N protein of *Tomato spotted wilt virus* (TSWV) is associated with the induction of programmed cell death (PCD) in *Capsicum chinense* plants, a hypersensitive host to TSWV infection. Virus Res. **137,** 245-252.

Lozach P., Mancini R., Bitto D., Meier R., Oestereich L., Overby A.K., Pettersson R.F., and Helenius A. (2010). Entry of bunyaviruses into mammalian cells. Cell Host Microbe **7,** 488-499.

Mandal B., Jain R.K., Krishnareddy M., Kumar N.K.K., Ravi K.S., and Pappu H.R. (2012). Emerging problems of tospoviruses (*Bunyaviridae*) and their management in the Indian subcontinent. Plant Dis. **96,** 468-479.

Margaria P., Ciuffo M., Pacifico D., and Turina M. (2007). Evidence that the nonstructural protein of *Tomato spotted wilt virus* is the avirulence determinant in the interaction with resistant pepper carrying the *Tsw* gene. Mol. Plant-Microbe Interact. **20,** 547-558.

Martin K., Kopperud K., Chakrabarty R., Banerjee R., Brooks R., and Goodin M.M. (2009). Transient expression in *Nicotiana benthamiana* fluorescent marker lines provides enhanced definition of protein localization, movement and interactions *in planta*. Plant J. **59,** 150-162.

Mazzotta S. and Kemmerling B. (2011). Pattern recognition in plant innate immunity. J. Plant Pathol. **93,** 7-17.

Means J.C. and Passarelli A.L. (2010). Viral fibroblast growth factor, matrix metalloproteases, and caspases are associated with enhancing systemic infection by baculoviruses. Proc. Natl. Acad. Sci. U. S. A. **107,** 9825-9830.

Medeiros R.B., Ullman D.E., Sherwood J.L., and German T.L. (2000). Immunoprecipitation of a 50 kDa protein: a candidate receptor component for *Tomato spotted wilt tospovirus* (*Bunyaviridae*) in its main vector, *Frankliniella occidentalis*. Virus Res. **67,** 109-118.

Millar A.H., Carrie C., Pogson B., and Whelan J. (2009). Exploring the function-location nexus: Using multiple lines of evidence in defining the subcellular location of plant proteins. Plant Cell **21,** 1625-1631.

Moritz G., Kumm S., and Mound L. (2004). Tospovirus transmission depends on thrips ontogeny. Virus Res. **100,** 143-149.

Morse J. and Hoddle M. (2006). Invasion biology of thrips. Annu. Rev. Entomol. **51,** 67-89.

Mound L.A. (2005). Thysanoptera: Diversity and interactions. Annu. Rev. Entomol. **50,** 247-269.

Nagata T., Storms M.M.H., Goldbach R., and Peters D. (1997). Multiplication of *Tomato spotted wilt virus* in primary cell cultures derived from two thrips species. Virus Res. **49,** 59-66.

Nagata T., Inoue-Nagata A.K., Smid H.M., Goldbach R., and Peters D. (1999). Tissue tropism related to vector competence of *Frankliniella occidentalis* for *Tomato spotted wilt tospovirus*. J. Gen. Virol. **80,** 507-515.

Nagata T., Nagata-Inoue A.K., Prins M., Goldbach R., and Peters D. (2000). Impeded thrips transmission of defective *Tomato spotted wilt virus* isolates. Phytopathology **90,** 454-459.

Nagata T., Inoue-Nagata A.K., van Lent J., Goldbach R., and Peters D. (2002). Factors determining vector competence and specificity for transmission of *Tomato spotted wilt virus*. J. Gen. Virol. **83,** 663-671.

Nagata T., Carvalho K.R., Sodre R.D.A., Dutra L.S., Oliveira P.A., Noronha E.F., Lovato F.A., Resende R.D.O., De Avila A.C., and Inoue-Nagata A.K. (2007). The glycoprotein gene of *Chrysanthemum stem necrosis virus* and *Zucchini lethal chlorosis virus* and molecular relationship with other tospoviruses. Virus Genes **35,** 785-793.

Naidu R.A., Sherwood J.L., and Deom C.M. (2008). Characterization of a vector-non-transmissible isolate of *Tomato spotted wilt virus*. Plant Pathol. **57,** 190-200.

Naidu R.A., Ingle C.J., Deom C.M., and Sherwood J.L. (2004). The two envelope membrane glycoproteins of *Tomato spotted wilt virus* show differences in lectin-binding properties and sensitivities to glycosidases. Virology **319,** 107-117.

Nervo G., Cirillo C., Accotto G., and Vaira A. (2003). Characterization of two tomato lines highly resistant to *Tomato spotted wilt virus* following transformation with the viral nucleoprotein gene. J. Plant Pathol. **85,** 139-144.

Ng J., Tian T., and Falk B. (2004). Quantitative parameters determining whitefly (*Bemisia tabaci*) transmission of *Lettuce infectious yellows virus* and an engineered defective RNA. J. Gen. Virol. **85,** 2697-2707.

Ohnishi J., Knight L.M., Hosokawa D., Fujisawa I., and Tsuda S. (2001). Replication of *Tomato spotted wilt virus* after ingestion by adult *Thrips setosus* is restricted to midgut epithelial cells. Phytopathology **91,** 1149-1155.

Okazaki S., Okuda M., Komi K., Yamasaki S., Okuda S., Sakurai T., and Iwanami T. (2011). The effect of virus titer on acquisition efficiency of *Tomato spotted wilt virus* by *Frankliniella occidentalis* and the effect of temperature on detectable period of the virus in dead bodies. Australas. Plant Pathol. **40,** 120-125.

Oliveira V.C., Bartasson L., Batista de Castro M.E., Correa J.R., Ribeiro B.M., and Resende R.O. (2011). A silencing suppressor protein (NSs) of a tospovirus enhances baculovirus replication in permissive and semipermissive insect cell lines. Virus Res. **155,** 259-267.

Paape M., Solovyev A.G., Erokhina T.N., Minina E.A., Schepetilnikov M.V., Lesemann D.E., Schiemann J., Morozov S.Y., and Kellmann J.W. (2006). At-4/1, an interactor of the *Tomato spotted wilt virus* movement protein, belongs to a new family of plant proteins capable of directed intra- and intercellular trafficking. Mol. Plant-Microbe Interact. **19,** 874-883.

Pang S., Jan F., Carney K., Stout J., Tricoli D., Quemada H., and Gonsalves D. (1996). Post-transcriptional transgene silencing and consequent tospovirus resistance in

transgenic lettuce are affected by transgene dosage and plant development. Plant J. **9,** 899-909.

Pappu H.R., Jones R.A.C., and Jain R.K. (2009). Global status of tospovirus epidemics in diverse cropping systems: Successes achieved and challenges ahead. Virus Res. **141,** 219-236.

Park S.H., Morris J.L., Park J.E., Hirschi K.D., and Smith R.H. (2003). Efficient and genotype-independent *Agrobacterium* - mediated tomato transformation. J. Plant Physiol. **160,** 1253-1257.

Passarelli A.L. (2011). Barriers to success: How baculoviruses establish efficient systemic infections. Virology **411,** 383-392.

Pittman H.A. (1927). Spotted wilt of tomatoes. J. Council for Sci. and Indus. Res. **1,** 74-77.

Plassmeyer M.L., Soldan S.S., Stachelek K.M., Martin-Garcia J., and Gonzalez-Scarano F. (2005). California serogroup, G_C (Gl) glycoprotein is the principal determinant of pH-dependent cell fusion and entry. Virology **338,** 121-132.

Plassmeyer M.L., Soldan S.S., Stachelek K.M., Roth S.M., Martin-Garcia J., and Gonzalez-Scarano F. (2007). Mutagenesis of the La Crosse Virus glycoprotein supports a role for Gc (1066-1087) as the fusion peptide. Virology **358,** 273-282.

Prehaud C., Lopez N., Blok M.J., Obry V., and Bouloy M. (1997). Analysis of the 3' terminal sequence recognized by the Rift Valley fever virus transcription complex in its ambisense S segment. Virology **227,** 189-197.

Premachandra W.T.S.D., Borgemeister C., Maiss E., Knierim D., and Poehling H.M. (2005). *Ceratothripoides claratris*, a new vector of a capsicum chlorosis virus isolate infecting tomato in Thailand. Phytopathology **95,** 659-663.

Reitz S.R. (2005). Biology and ecology of flower thrips in relation to *Tomato spotted wilt virus*. Acta Hort. **695,** 75-84.

Reitz S.R. (2009). Biology and ecology of the western flower thrips (Thysanoptera: Thripidae): the Making of a pest. Fla. Entomol. **92,** 7-13.

Ribeiro D., Foresti O., Denecke J., Wellink J., Goldbach R., and Kormelink R.J.M. (2008). *Tomato spotted wilt virus* glycoproteins induce the formation of endoplasmic reticulum- and Golgi-derived pleomorphic membrane structures in plant cells. J. Gen. Virol. **89,** 1811-1818.

Ribeiro D., Borst J.W., Goldbach R., and Kormelink R. (2009a). *Tomato spotted wilt virus* nucleocapsid protein interacts with both viral glycoproteins G_N and G_C *in planta*. Virology **383,** 121-130.

Ribeiro D., Goldbach R., and Kormelink R. (2009b). Requirements for ER-arrest and sequential exit to the Golgi of *Tomato spotted wilt virus glycoproteins* (report). Traffic **10,** 664(9).

Richmond K.E., Chenault K., Sherwood J.L., and German T.L. (1998). Characterization of the nucleic acid binding properties of *Tomato spotted wilt virus* nucleocapsid protein. Virology **248,** 6-11.

Rotenberg D., Kumar N.K.K., Ullman D.E., Montero-Astúa M., Willis D.K., German T.L., and Whitfield A.E. (2009). Variation in *Tomato spotted wilt virus* titer in *Frankliniella occidentalis* and is association with frequency of transmission. Phytopathology **99,** 404-410.

Rotenberg D. and Whitfield A.E. (2010). Analysis of expressed sequence tags from *Frankliniella occidentalis*, the western flower thrips. Insect Mol. Biol. **19,** 537-551.

Samuel G., Bald J.G., and Pittman H.A. (1930). Investigations on " Spotted Wilt " of Tomatoes. J. Council for Sci. and Indus. Res. **44**, 8-11.

Sanchez-Vargas I., Scott J.C., Poole-Smith B.K., Franz A.W.E., Barbosa-Solomieu V., Wilusz J., Olson K.E., and Blair C.D. (2009). Dengue Virus type 2 infections of *Aedes aegypti* are modulated by the mosquito's RNA interference pathway. **5,** e1000299.

Sanders H.R., Foy B.D., Evans A.M., Ross L.S., Beaty B.J., Olson K.E., and Gill S.S. (2005). Sindbis virus induces transport processes and alters expression of innate immunity pathway genes in the midgut of the disease vector, *Aedes aegypti*. Insect Biochem. Mol. Biol. **35,** 1293-1307.

Schnettler E., Hemmes H., Huismann R., Goldbach R., Prins M., and Kormelink R. (2010). Diverging affinity of tospovirus RNA silencing suppressor proteins, NSs, for various RNA duplex molecules. J. Virol. **84,** 11542-11554.

Scholthof K.G., Adkins S., Czosnek H., Palukaitis P., Jacquot E., Hohn T., Hohn B., Saunders K., Candresse T., Ahlquist P., Hemenway C., and Foster G.D. (2011). Top 10 plant viruses in molecular plant pathology. Mol. Plant Pathol. **12,** 938-954.

Schwach F., Adam G., and Heinze C. (2004). Expression of a modified nucleocapsid-protein of Tomato spotted wilt virus (TSWV) confers resistance against TSWV and *Groundbut ringspot virus* (GRSV) by blocking systemic spread. Mol. Plant Pathol. **5,** 309-316.

Seepiban C., Gajanandana O., Attathom T., and Attathom S. (2011). Tomato necrotic ringspot virus, a new tospovirus isolated in Thailand. Arch. Virol. **156,** 263-274.

Sevik M.A. and Arli-Sokmen M. (2012). Estimation of the effect of *Tomato spotted wilt virus* (TSWV) infection on some yield components of tomato. Phytoparasitica **40,** 87-93.

Shao C., Wu J., Zhou G., Sun G., Peng B., Lei J., Jin D., Chen S., Upadhyaya N., Waterhouse P., and Gong Z. (2003). Ectopic expression of the spike protein of Rice

Ragged Stunt Oryzavirus in transgenic rice plants inhibits transmission of the virus to insects. Mol. Breed. **11,** 295-301.

Sharga U.S. (1933). On the internal anatomy of some Thysanoptera. T. Entomol. Soc. London **81,** 185-204.

Sherman J., Moyer J., and Daub M. (1998). *Tomato spotted wilt virus* resistance in chrysanthemum expressing the viral nucleocapsid gene. Plant Dis. **82,** 407-414.

Shi X.H., van Mierlo J.T., French A., and Elliott R.M. (2010). Visualizing the replication cycle of Bunyamwera orthobunyavirus expressing fluorescent protein-tagged GC glycoprotein. J. Virol. **84,** 8460-8469.

Shi X., Kohl A., Li P., and Elliott R.M. (2007). Role of the cytoplasmic tail domains of Bunyamwera orthobunyavirus glycoproteins Gn and Gc in virus assembly and morphogenesis. J. Virol. **81,** 10151-10160.

Silva C.P., Silva J.R., Vasconcelos F.F., Petretski M.D.A., DaMatta R.A., Ribeiro A.F., and Terra W.R. (2004). Occurrence of midgut perimicrovillar membranes in paraneopteran insect orders with comments on their function and evolutionary significance. Arth. Struct. Dev. **33,** 139-148.

Sim S., Ramirez J.L., and Dimopoulos G. (2012). Dengue Virus infection of the *Aedes aegypti* salivary gland and chemosensory apparatus induces genes that modulate infection and blood-feeding behavior. PLoS Pathog. **8,** e1002631.

Simon M., Johansson C., Lundkvist A., and Mirazimi A. (2009a). Microtubule-dependent and microtubule-independent steps in Crimean-Congo hemorrhagic fever virus replication cycle. Virology **385,** 313-322.

Simon M., Johansson C., and Mirazimi A. (2009b). Crimean-Congo hemorrhagic fever virus entry and replication is clathrin-, pH- and cholesterol-dependent. J. Gen. Virol. **90,** 210-215.

Sin S., McNulty B.C., Kennedy G.G., and Moyer J.W. (2005). Viral genetic determinants for thrips transmission of *Tomato spotted wilt virus*. Proc. Natl. Acad. Sci. U. S. A. **102,** 5168-5173.

Snippe M., Borst J.W., Goldbach R., and Kormelink R. (2005). The use of fluorescence microscopy to visualize homotypic interactions of *Tomato spotted wilt virus* nucleocapsid protein in living cells. J. Virol. Methods **125,** 15-22.

Snippe M., Borst J.W., Goldbach R., and Kormelink R. (2007a). *Tomato spotted wilt virus* Gc and N proteins interact *in vivo*. Virology **357,** 115-123.

Snippe M., Smeenk L., Goldbach R., and Kormelink R. (2007b). The cytoplasmic domain of *Tomato spotted wilt virus* Gn glycoprotein is required for Golgi localization and interaction with Gc. Virology **363,** 272-279.

Soellick T.R., Uhrig J.F., Bucher G.L., Kellmann J.W., and Schreier P.H. (2000). The movement protein NSm of *Tomato spotted wilt tospovirus* (TSWV): RNA binding, interaction with the TSWV N protein, and identification of interacting plant proteins. Proc. Natl. Acad. Sci. U. S. A. **95,** 2373-2378.

Sonoda S. and Tsumuki H. (2004). Analysis of RNA-mediated virus resistance by NSs and NSm gene sequences from *Tomato spotted wilt virus*. Plant Sci. **166,** 771-778.

Sonoda S., Nishiguchi M., and Tsumuki H. (2005). Evaluation of virus resistance conferred by the NSs gene sequences from *Tomato spotted wilt virus* in transgenic plants. Breed. Sci. **55,** 27-33.

Sparks W.O., Rohlfing A., and Bonning B.C. (2011). A peptide with similarity to baculovirus ODV-E66 binds the gut epithelium of *Heliothis virescens* and impedes infection with *Autographa californica multiple nucleopolyhedrovirus*. J. Gen. Virol. **92,** 1051-1060.

Spassova M., Prins T., Folkertsma R., Klein-Lankhorst R., Hille J., Goldbach R., and Prins M. (2001). The tomato gene *Sw5* is a member of the coiled coil, nucleotide binding, leucine-rich repeat class of plant resistance genes and confers resistance to TSWV in tobacco. Mol. Breed. **7,** 151-161.

Spiropoulou C., Goldsmith C., Shoemaker T., Peters C., and Compans R. (2003). Sin Nombre virus glycoprotein trafficking. Virology **308,** 48-63.

Stafford C.A., Walker G.P., and Ullman D.E. (2011). Infection with a plant virus modifies vector feeding behavior. Proc. Natl. Acad. Sci. U. S. A. **108,** 9350-9355.

Storms M.M.H., van der Schoot C., Prins M., Kormelink R., van Lent J.W.M., Goldbach R.W., and Goldbach R.W. (1998). A comparison of two methods of microinjection for assessing altered plasmodesmal gating in tissues expressing viral movement proteins. Plant J. **13,** 131-140.

Storms M.M.H., Kormelink R., Peters D., Van Lent J.W.M., and Goldbach R.W. (1995). The nonstructural NSm protein of *Tomato spotted wilt virus* induces tubular structures in pllant and insect cells. Virology **214,** 485-493.

Sutula C.L., Gillet J.M., Morrissey S.M., and Ramsdell D.C. (1986). Interpreting Elisa Data and Establishing the Positive-Negative Threshold. Plant Dis. **70,** 722-726.

Takeda A., Sugiyama K., Nagano H., Mori M., Kaido M., Mise K., and Okuno S.T.a.T. (2002). Identification of a novel RNA silencing suppressor, NSs protein of *Tomato spotted wilt virus*. FEBS Lett. **532,** 75-79.

Torres R., Larenas J., Fribourg C., and Romero J. (2012). Pepper necrotic spot virus, a new tospovirus infecting solanaceous crops in Peru. Arch. Virol. **157,** 609-615.

Uhrig J.F., Soellick T.R., Minke C.J., Philipp C., Kellmann J.W., and Schreier P.H. (1999). Homotypic interaction and multimerization of nucleocapsid protein of *Tomato spotted*

wilt tospovirus: identification and characterization of two interacting domains. Proc. Natl. Acad. Sci. U. S. A. **96,** 55-60.

Ullman D.E., Wescot D.M., Hunter W.B., and Mau R.F.L. (1989). Internal anatomy and morphology of *Frankliniella occidentalis* (Pergande) (Thysanoptera:Thripidae) with special reference to interactions between thrips and *Tomato spotted wilt virus*. Int. J. Insect Morphol. Embryol. **18,** 289-310.

Ullman D.E., Cho J.J., Mau R.F.L., Wescot D.M., and Custer D.M. (1992). A midgut barrier to *Tomato spotted wilt virus* acquisition by adult western flower thrips. Phytopathology **82,** 1333-1342.

Ullman D.E., German T.L., Sherwood J.L., Wescot D.M., and Cantone F.A. (1993). Tospovirus replication in insect vector cells: immunocytochemical evidence that the nonstructural protein encoded by the S RNA of *Tomato spotted wilt tospovirus* is present in thrips vector cells. Phytopathology **83,** 456-463.

Ullman D.E., Westcot D.M., Chenault K.D., Sherwood J.L., German T.L., Bandla M.D., Cantone F.A., and Duer H.L. (1995). Compartmentalization, intracellular transport, and autophagy of *Tomato spotted wilt tospovirus* proteins in infected thrips cells. Phytopathology **85,** 644-654.

Ultzen T., Gielen J., Venema F., Westerbroek A., Dehaan P., Tan M.L., Schram A., Vangrinsven M., and Goldbach R. (1995). Resistance to *Tomato spotted wilt virus* in transgenic tomato hybrids. Euphytica **85,** 159-168.

van de Wetering F., Goldbach R., and Peters D. (1996). *Tomato spotted wilt tospovirus* ingestion by first instar larvae of *Frankliniella occidentalis* is a prerequisite for transmission. Phytopathology **86,** 900-905.

van de Wetering F., Hulshof J., Posthuma K., Harrewijn P., Goldbach R., and Peters D. (1998). Distinct feeding behavior between sexes of *Frankliniella occidentalis* results in higher scar production and lower tospovirus transmission by females. Entomol. Exp. Appl. **88,** 9-15.

van de Wetering F., van der Hoek M., Goldbach R., and Peters D. (1999). Differences in *Tomato spotted wilt virus* vector competency between males and females of *Frankliniella occidentalis*. Entomol. Exp. Appl. **93,** 105-112.

van Knippenberg I., Goldbach R., and Kormelink R. (2002). Purified *Tomato spotted wilt virus* particles support both genome replication and transcription *in vitro*. Virology **303,** 278-286.

van Poelwijk F., Kolkman J., and Goldbach R. (1996). Sequence analysis of the 5' ends of *Tomato spotted wilt virus* N mRNAs. Arch. Virol. **141,** 177-184.

Vandenheuvel J.F.J.M., Boerma T.M., and Peters D. (1991). Transmission of *Potato leafroll virus* from plants and artificial diets by *Myzus persicae*. Phytopathology **81,** 150-154.

Walker T., Johnson P.H., Moreira L.A., Iturbe-Ormaetxe I., Frentiu F.D., McMeniman C.J., Leong Y.S., Dong Y., Axford J., Kriesner P., Lloyd A.L., Ritchie S.A., O'Neill S.L., and Hoffmann A.A. (2011). The wMel *Wolbachia* strain blocks dengue and invades caged *Aedes aegypti* populations. Nature **476,** 450-U101.

Walter C.T. and Barr J.N. (2011). Recent advances in the molecular and cellular biology of bunyaviruses. J. Gen. Virol. **92,** 2467-2484.

Webster C.G., Reitz S.R., Perry K.L., and Adkins S. (2011). A natural M RNA reassortant arising from two species of plant- and insect-infecting bunyaviruses and comparison of its sequence and biological properties to parental species. Virology **413,** 216-225.

Whitfield A.E., Ullman D.E., and German T.L. (2005a). *Tomato spotted wilt virus* glycoprotein G_C is cleaved at acidic pH. Virus Res. **110,** 183-186.

Whitfield A.E., Ullman D.E., and German T.L. (2005b). Tospovirus-thrips interactions. Annu. Rev. Phytopathol. **43,** 459-489.

Whitfield A.E., Kumar N.K.K., Rotenberg D., Ullman D.E., Wyman E.A., Zietlow C., Willis D.K., and German T.L. (2008). A soluble form of the *Tomato spotted wilt virus* (TSWV) glycoprotein G_N (G_N-S) inhibits transmission of TSWV by *Frankliniella occidentalis*. Phytopathology **98,** 45-50.

Whitfield A.E., Ullman D.E., and German T.L. (2004). Expression and characterization of a soluble form of *Tomato spotted wilt virus* glycoprotein G_N. J. Virol. **78,** 13197-13206.

Wijkamp I., van Lent J., Kormelink R., Goldbach R., and Peters D. (1993). Multiplication of *Tomato spotted wilt virus* in its insect vector, *Frankliniella occidentalis*. J. Gen. Virol. **74,** 341-349.

Wijkamp I., Almarza N., Goldbach R., and Peters D. (1995). Distinct levels of specificity in thrips transmission of tospoviruses. Phytopathology **85,** 1069-1074.

Wijkamp I., van de Wetering F., Goldbach R., and Peters D. (1996). Transmission of *Tomato spotted wilt virus* by *Frankliniella occidentalis*; median acquisition and inoculation access period. Ann. Appl. Biol. **129,** 303-313.

Yang H., Ozias-Akins P., Culbreath A.K., Gorbet D.W., Weeks J.R., Mandal B., and Pappu H.R. (2004). Field evaluation of *Tomato spotted wilt virus* resistance in transgenic peanut (*Arachis hypogaea*). Plant Dis. **88,** 259-264.

Zhang Y., Zhang C., and Li W. (2012). The nucleocapsid protein of an enveloped plant virus, *Tomato spotted wilt virus*, facilitates long-distance movement of *Tobacco mosaic virus* hybrids. Virus Res. **163,** 246-253.

Zheng Y.X., Chen C.C., and Jan F.J. (2011). Complete nucleotide sequence of *Capsicum chlorosis virus* isolated from Phalaenopsis orchid and the prediction of the unexplored genetic information of tospoviruses. Arch. Virol. **156,** 421-432.

Zhou G.Y., Lu X.B., Lu H.J., Lei J.L., Chen S.X., and Gong Z.X. (1999). Rice Ragged Stunt Oryzavirus: role of the viral spike protein in transmission by the insect vector. Ann. Appl. Biol. **135,** 573-578.

Zhou J., Kantartzi S., Wen R.-., Newman M., Hajimorad M., Rupe J., and Tzanetakis I. (2011). Molecular characterization of a new tospovirus infecting soybean. Virus Genes **43,** 289-295.